The effect of phytonanotherapy on diabetic rats

Keletso Modise

A mini-thesis submitted in partial fulfilment of the requirements for the degree Magister Scientiae in Nanoscience

Department of Biotechnology, University of the Western Cape

Supervisor: Prof AM Madiehe

Co-supervisor: Prof M Meyer

April 2021

Abstract

The effect of phytonanotherapy on diabetic rats

K Modise

MSc. Mini Thesis, National Nanoscience Postgraduate Teaching and Training Platform, Department of Biotechnology, University of the Western Cape.

Diabetes Mellitus is a major global health issue, affecting over 463 million adults in the world. Metformin is the standard drug administered to most people suffering from diabetes; however, this medication is contraindicated in many individuals, like most of the medicines developed to combat diabetes. Many diabetic patients turn to herbal medicines due to their renowned traditional use and fewer side effects. While the beneficial effects of phytotherapy are very evident, separation of non-toxic from toxic phytochemicals is still a challenge. Phytonanotherapy is a branch in nanotechnology that seeks to find the middle ground between the fast-acting mechanism of conventional drugs which also present with long lasting or severe toxic side effects, and the slow-acting mechanism of phytotherapy which presents with less severe side effects. As such, the aim of this study was to pioneer the investigation of gold nanoparticles biosynthesized using the *Carprobrotus edulis* fruit aqueous extract (CeFe-AuNPs) as potential treatment for diabetes mellitus.

Previously optimized conditions were used to synthesize CeFe-AuNPs which were concurrently characterized using UV-Vis, dynamic light scattering, High Resolution – Transmission Electron Microscopy and Fourier Transform Infrared Spectroscopy techniques. The physichochemical stability of CeFe-AuNPs in phosphate buffer saline, 0.5 % bovine serum albumin, water and 10 % NaCl was also investigated. The effect of CeFe and CeFe-AuNPs on glucose uptake by yeast cells was investigated using 5, 10 and 25 mM glucose reactions. Acute toxicity of CeFe and CeFe-AuNPs was conducted in female Wistar rats (n = 20) and major organs were analyzed through the haematoxylin-eosin stain. The anti-diabetic effects of the CeFe (200 and 400 mg/kg) and CeFe-AuNPs (100 and 200 mg/kg) were investigated in male Wistar rats divided into seven group (n = 6). Histopathology of the pancreas, and the serum insulin were determined.

CeFe-AuNPs exhibit a Surface Plasmon Resonance of 532 nm, a hydrodynamic size of 75.30 ± 61.63 nm and a core size of 16 ± 0.31 nm. CeFe-AuNPs were spherical in shape, stable in various physiological media and exhibiting a zeta potential of – 30 mV. CeFe and CeFe-AuNPs induced 58 – 84 % and 8 – 48 % glucose uptake activity in yeast cells, respectively, thus advocating for the anti-diabetic potential. There were no signs of toxicity observed in the acute toxicity study. Furthermore, low dose CeFe-AuNPs were ineffective in treating hyperglycemia; however CeFe was observed to slow-down the progression of hyperglycemia. While further studies, such as investigation of the lipid profile, are still required, this study showed, for the first time, the *in vivo* non-toxic effects of CeFe and CeFe-AuNPs, and the anti-hyperglycemic potential thereof.

Keywords:

• *Carpobrotus edulis* fruit (sour fig)

• Phytonanotherapy

• Biogenic gold nanoparticles

• Diabetes Mellitus

• Streptozotocin

• Phytochemicals

• Green Synthesis

• Glucose uptake

Declaration

I declare that "The effect of phytonanotherapy on diabetic rats" is my own work and has not been submitted before for any degree or examination in this university or any other tertiary institustion. All the sources that I have used or quoted have been indicated and acknowledged by complete references.

Keletso Modise

Signature

April 2021

Acknowledgements

"All of us must die eventually. Our lives are like water spilled out on the ground, which cannot be gathered up again. But God does not just sweep life away; instead, He devises ways to bring us back when we have been separated from Him." 2 Samuel 14:14

I genuinely thought I would not finish this degree. Without God, and the encouragement of Holy Spirit, I don't think I would have. I am grateful that God is real, that He speaks and that He cares. This is my testimony that where I end, You truly begin. Thank You for always showing up for me.

To my grandmother, Lucy Modise, who is always so supportive and loving, I see you and you see me too. Without you, nothing would be the way it is. Everything would be bleak and heavy. Thank you for everything that you, my mom, Mapoone Martins, and my siblings, Liyema, Joseph, Sweetness, Atlehang, Sihle, Ntokozo, and Lwazi do to help pave a clear path for me. Especially the laughs, we all know I need that!

I would like to extend my gratitude to my supervisor, Prof AM Madiehe, there aren't enough words to express how much I thank God for your life. Not only are you intelligent, eager to teach and compassionate, but you stand on a league of your own. Thank you for your patience, kindness and support.

I also extend my sincerest gratitude to my co-supervisor Prof M Meyer for providing me with the reagents and infrastructure I needed to complete this degree, Dr M Goboza for her invaluable advice and support throughout the animal study, Nasr Eshibona and Maryam Hassan for their assistance with my statistical analysis, Ekeoma Festus for training me in analysis of histology slides, as well as Joritha van Heerden and Philida Beukes at the MRC for their work with the animals. Ms Valencia Jamalie, thank you for being an amazing and genuine course coordinator.

To my friends and great companions, Maryam Hassan and Tusekile Kangwa, I couldn't have chosen a better pair to take on this journey. To Koena Moabelo, Ali Ali, Toni Oliver and Riziki Martins, thank you for the great friendship and the constant reminder that nothing is impossible. To Buntu Mdodana and Tadi Chitaunike, thank you for the amazing study breaks and allowing me to vent about misbehaving rats. I love you all, plenty!

Finally, I'd like to thank the Nanoscience platform for affording me the opportunity to further my studies, as well as the Nanotechnology Innovation Centre for their immense contribution.

List of Abbreviations

α	Alpha
β	Beta
ºC	Degrees Celsius
µl	microliter
λ	Lambda
%	Percentage
ΔOD	Change in optical density
λmax	Absorbance maximum
Abs.	Absorbance
ADP	Adenosine diphosphate
AMP	Adenosine monophosphate
AMPK	5’ AMP Activate Protein Kinase
ANOVA	Analysis of Vaiance
AREC	Animal Research Ethics Committee
AuCl	Gold Chloride
AuNPs	Gold nanoparticles
AgNPs	Silver nanoparticles
BGL	Blood glucose levels
BSA	Bovine Serum Albumin
BW	Bodyweight
Ca^{2+}	Calcium ion
CeFe	*Carpobrotus edulis* Fruit extract
DC	Diabetic control
ddH_2O	Distilled deionized water
DLS	Dynamic Light Scattering
DM	Diabetes Mellitus
ECRA	Ethics Committee for Research on Animals
FPG	Fasting plasma glucose

FTIR	Fourier Transform Infrared Spectroscopy
g	Grams
G-6-P	Glucose 6 phosphate
GDM	Gestational Diabetes Mellitus
GLP-1	Glucagon-like peptide1
GLP-2	Glucagon like peptide 2
GLUT	Glucose transporter
GSV	GLUT4 Storage Vesicles
H & E	Hematoxylin and Eosin stain
HEC	Hyperinsulinemic-Euglycemic Clamp
HLA	Human Leukocyte Antigen
HR-TEM	High Resolution Transmission Electron Microscopy
IDF	International Diabetes Federation
IR	Insulin Resistance
IRAP	Insulin Regulated Aminopeptides
ip	Intraperitoneal
K_{ATP}	Potassium – Adenosine triphosphate
M	Molar
MANOVA	Multivariate Analysis of variance
MHC	Major Histocompatibility Complex
Min	Minutes
mmol/L	millimoles per liter or millimolar
ml	milliliters
Na^+	Sodium ion
NDC	Non-diabetic control
NIDDK	National Institute of Diabetes and Digestive and Kidney diseases
nm	Nanometers
NPs	Nanoparticles
OGTT	Oral Glucose Tolerance Test
PBS	Phosphate Buffer Saline

pmol/L	Picomoles per liter or picomolar
RES	Reticulo-Endothelial System
RPM	Rotations per minute
RT	Room temperature
SAMRC	South African Medical Research Council
SD	Standard drug, 250 mg/kg metformin
STZ	Streptozotocin
SLGT	Sodium-Linked Glucose Transporters
T1	200 mg/kg CeFe
T2	400 mg/kg CeFe
T3	100 mg/kg CeFe-AuNPs
T4	200 mg/kg CeFe-AuNPs
T1DM	Type 1 diabetes Mellitus
T2DM	Type 2 Diabetes Mellitus
TGN	Trans-Golgi network
TNF-α	Tumor necrosis factor-alpha
UV-Vis	Ultraviolet-visible light spectroscopy
WHO	World Health Organization

List of Figures

List of Tables

List of supplementary material

Figures

Tables

Annexure A

Table of Contents

Chapter 1: Literature Review

1.1 Introduction

Diabetes mellitus (DM) is a chronic, multifactorial and multi-hormonal disease that affects over 463 million adults in the world (IDF, 2019). It is characterized by either the lack of insulin secretion, due to autoimmune β-cell destruction, or the inability of insulin responsive cells to successfully utilize the insulin produced by the pancreas in response to high blood glucose levels (BGL) (Gyamfi et al., 2019). Physical activity and a healthy lifestyle are the main methods used to prevent or manage DM; with the progression of the disease, conventional drugs are often incorporated (White, 2014; ADA, 2017).

Anti-diabetic drugs are usually contraindicated in many individuals, and they induce undesirable side effects such as gastrointestinal issues, liver dysfunction, and hypoglycaemia (Carpio and Fonseca, 2014; White, 2014). Many diabetic patients turn to the use of herbal medications to treat this illness, or they use it in combination with their prescribed drugs (Yeh et al., 2003). The abundant diversity, and traditional knowledge, surrounding medicinal plants in continents such as Asia, Africa and South America, also encourages their use (Kasole et al., 2019). Although the success of phytotherapy is very evident, this treatment approach is limited by poor isolation of active ingredients within the medicinal plant of choice; as such, patients end up ingesting both useful and toxic phytochemicals (Ghorbani, 2013; Governa et al., 2018).

Phytonanotherapy is a fast growing branch of nanotechnology that seeks to use therapeutic phytochemicals from medicinal plants for the production of nanoparticles (NPs) (Nasrollahzadeh et al., 2019). The vantage point of phytonanotherapy is to find the middle ground between the "fast-acting and long-lasting side effect" of pharmaceutical drugs and the "slow acting but few side effects" of phytotherapy. By taking advantage of the small size and large surface area of NPs, phytonanotherapy seeks to design and develop nanomedicines that are cost effective and have high efficacy, while inducing the lowest possible side effects (Iravani, 2011). Herein, the anti-diabetic activity of gold NPs synthesised from the aqueous extract of the *Carpobrotus edulis* fruit (CeFe) were investigated in streptozotocin-induced diabetic rats.

1.2 Epidemiology of Diabetes Mellitus

There are approximately 463 million adults living with Diabetes Mellitus (DM) in the world; 19 million of these adults are found in Africa, and 4.6 million of these are found in South Africa. Of this total, about 2 million South Africans do not know that they are living with DM (IDF, 2019). In 2015, diabetes resulted in 1.5 million deaths worldwide and Africa accounted for 321 100 of these deaths. As of 2019, the mortality rate has since increased by over 14%, thereby amounting to a total of 366 200 adult deaths (Mutyambizi et al., 2018).

Rural-urban migration is the main cause of increasing diabetes cases within Sub-saharan Africa (Den Braver et al., 2018). Task-shifting among clinical stuff (Lekoubou et al., 2010), and the lack of advanced diagnostic and therapeutic techniques also play a pivotal role (Mutyambizi et al., 2018). If alternative treatment and diagnostic methods, that are effective, rapid and cost conscious, are not developed and put into effect by 2030, Africa is predicted to experience a 143% projection thus making it the world's leading diabetic outbreak (IDF, 2019).

1.3 Diabetes Mellitus and the hormones involved in glucose homeostasis

For a very long time, DM was thought to be a mono-hormonal disorder, characterized only by the complete or relative deficiency of insulin. Insulin is an anabolic peptide hormone that is produced by pancreatic β-cells in response to high BGL. Insulin mediates the storage of glucose in the muscle, liver and adipose tissues. However, the discovery of glucagon, an insulin antagonistic hormone secreted by the pancreatic α-cell, which functions to promote the production of glucose via the breakdown of glycogen, changed the definition of DM to it being a bi-hormonal disorder (Aronoff et al., 2004; Lankatillake et al., 2019).

Research in glucose homeostasis has revealed a string of different hormones that have glucoregulatory capabilities. One of these hormones is amylin, a β-cell hormone whose activity complements that of insulin. Amylin, like insulin, is known to suppress postprandial glucagon secretion, food intake, body weight gain and gastric emptying, and has been observed to be absent in diabetic patients (NIDDK, 2016). In general, DM is influenced by the amount of glucose present in one's body, this blood glucose is derived from the food an individual eats. Holistically, the definition of glucose homeostasis encompasses the interrelation of glucagon, amylin, insulin and the incretin hormones (glucagon-like peptide – 1 (GLP-1) and glucose-dependent insulinotropic

peptide), thus making it a multihormonal disorder (**Figure 1.1**). Nevertheless, insulin and glucagon are seen as the major regulators of blood glucose (Aronoff et al., 2004; Qaid and Abdelrahman, 2016).

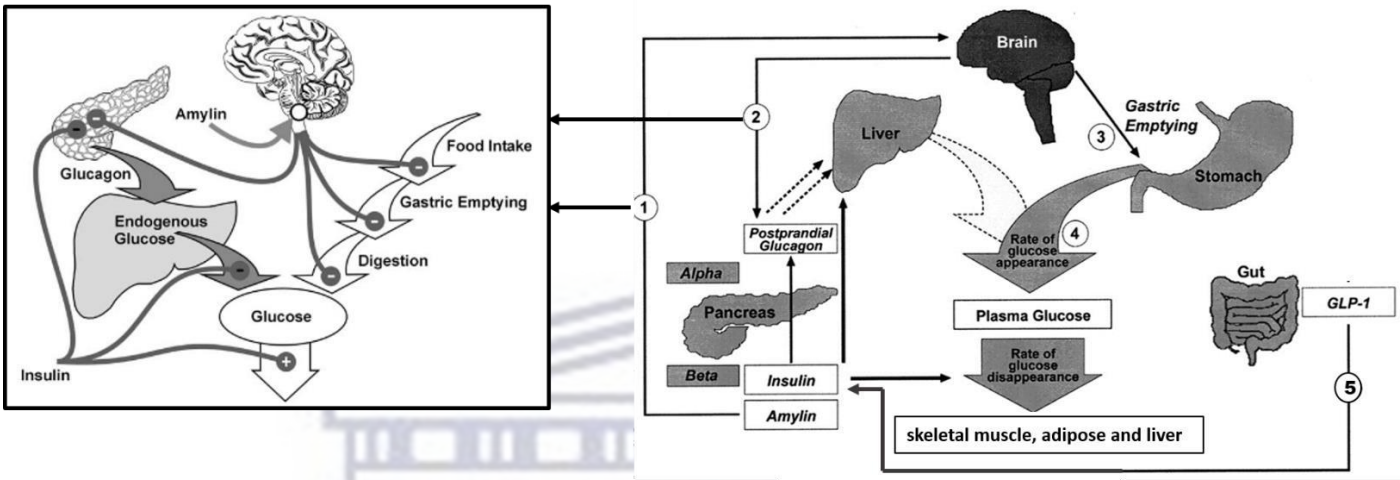

1.3.1 Insulin and insulin resistance

Insulin is a dipeptide that consists of an A (21 amino acids) and a B (30 amino acids) chain. These chains are joined via two disulphide bridges (Mann and Bellin, 2016). Insulin is a hormone that has transformed the manner in which diabetes, one of the most studied diseases in the human history, is diagnosed and treated. A variety of pathways influence its secretion but the most general alterations occur during transcription, translation and post-translational modifications (Aronoff et al., 2004). Insulin was first isolated in 1921 following an 1889 hypothesis by two German scientists, Minkowski and von Menug, who proposed that a substance secreted by the pancreas was responsible for metabolic control. It took a year for the isolated hormone to be tested in a human, and by the year 1923 insulin was commercially available in the United States (Wilcox, 2005; Vecchio et al., 2018). In 1936, long-acting insulin was commercialized and it eradicated the need for diabetic patients to wake up in the middle of the night to take injections of the former rapidly acting insulin (White, 2014).

The glucose sensory mechanism (the relationship between insulin, glucagon and the other related hormones that influence blood glucose concentrations) can be divided into the proximal entry of glucose and its metabolism, as well as the distal mechanism of insulin secretion that results from mitochondrial signal generation and electrical activity directed at the effectors responsible for the

exocytosis of insulin (MacDonald et al., 2005). That is to say, as depicted in (**Figure 1.2**), the pancreatic β-cells of the Langerhans, the potassium – ATP channel and the calcium channel are among the mechanisms that are used to regulate glucose concentration, in the body (Wilcox, 2005; Koster et al., 2005; McTaggart et al., 2010). In the event of diabetes, communication between these pathways is lost and the release of insulin becomes nullified or hindered (McTaggart et al., 2010).

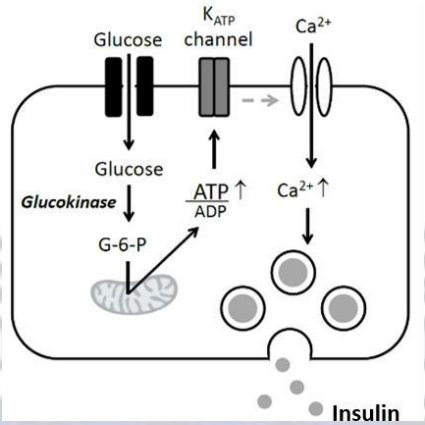

Figure 1.2: Illustration of glucose induced insulin secretion in the pancreas: Increased blood glucose results in an increased influx of glucose into the pancreas via the relevant GLUT transporters (discussed in section 1.4). Once engulfed glucose is phosphorylated into glucose-6-phosphate (G-6-P) under the facilitation of glucokinase (this is the rate limiting step for the metabolism of glucose). G-6-P enters the mitochondria and goes into the kerbs cycle where it is used for the synthesis of Adenosine Triphosphate (ATP). ATP is responsible for the closure of the K^+ATP channel. This closure leads to the depolarization of the cell membrane and subsequently triggers the voltage-gated Ca^{2+} channel, which will then prompt the secretion of insulin (Mann and Bellin, 2016).

Normal physiological conditions require that the glucose concentration be kept at a range of ≤3.3mmol/L (NIDDK, 2016). However, following the consumption of a meal, BGL will inevitably undergo a drastic increase, which then causes the body to secrete a parallel concentration of insulin; this will cause insulin to exceed its basal concentration of 18 – 90pmol/l (Wilcox, 2005). In the event that the glucoregulatory system of an individual cannot return the BGL back to the normal concentration range, the patient is said to be hyperglycaemic. This could be a result of insulin resistance, which serves as a symptom of DM. Conversely, should a diabetic patient be prescribed a treatment drug or drug dose that does not match their physiological need, they can develop hypoglycaemia, which is a condition that results from severely decreased BGL. Both occurrences can be life threatening when they go untreated (NIDDK, 2016; Lankatillake et al., 2019).

Insulin resistance (IR) is defined as an event where normal or even elevated physiological insulin secretion does not instigate the anticipated biological response from insulin sensitive cells, thus causing the pancreatic β-cells to work harder at producing insulin and, after sometime, stopping the production all together (Cerf, 2013; NIDDK, 2018). IR is the major contributor to the development and progression of the metabolic syndrome. However, it does not supersede β-cell dysfunction in its ability to induce diabetes. In fact, these two conditions are presumed to work together in intensifying diabetes (Cerf, 2013).

While the aetiology of IR is complex and controversial, in regard to it being an essential component for the development of type II diabetes mellitus (Gerich, 2000), it has been established that obesity is its most common cause in men; therefore, overfeeding leads to increased inflammation (Glass and Olefsky, 2012; Johnson and Olefsky, 2013), changes the manner in which the body utilizes lipids (Gustafson et al., 2015), and changes the composition of the gastrointestinal microbiota, consequently, the routine interaction between the microbiota and the body is changed, thus enhancing the individual's susceptibility to obesity (Johnson and Olefsky; 2013, Shen et al., 2013).

1.3.1.1 Insulin resistance, inflammation and obesity

The adipose tissue of an obese individual is characterized by the excess presence of activated macrophages that promote the secretion of the Tumour Necrosis Factor – α (TNF-α), which is directly responsible for causing IR (Glass and Olefsky, 2012). In this manner, obesity is a direct cause of IR, which is one of the key factors for the development of type II diabetes mellitus (discussed in section 1.5). In the same way that obesity has been established as a common cause for IR, it has also been recognized that the accumulation of fat in the visceral adipose tissue has the most effect in decreasing insulin sensitivity as compared to the subcutaneous fat (which, in fact, has a very restricted ability to expand in order to accommodate excess fat, but rather promotes ectopic storage of fat). Obesity is also said to cause inflammation of the hypothalamus, thus prompting the local production of cytokines that cause central leptin resistance. The occurrence of these two events is then closed in a positive feedback loop that fuels weight gain and systemic IR (Johnson and Olefsky, 2013; Gustafson et al., 2015).

Furthermore, it is often promoted that IR is a cause for type II diabetes mellitus (T2DM); however, Gerich (2000) argues that it is the impaired insulin secretion that should be credited for

this, as IR is mostly a result of obesity and that it only plays a role of propagating the disease rather than causing it, considering how weight loss is able to improve insulin sensitivity even though T2DM would still persist. This corroborates Cerf's (2013) argument on β-cell dysfunction being the majorcause of diabetes. To add on to this controversy, individuals who are non-obese but present with T2DM and IR have been identified, even though they only make up 10 – 15% of the diabetic population (Gerich, 2000; Gustafson et al., 2015).

1.3.2 Glucagon Hormone

The islet β-cells make up 10% of the pancreatic cells and only 20% of this mass is dedicated to the secretion of the α-cell hormone glucagon, the remaining 80% is dedicated to the secretion of the previously discussed (section 1.3.1) β-cell hormone insulin (Taborsky Jr, 2010). Glucagon acts as a counter-regulatory hormone whose name was established, in 1923, after a hypothesis that was framed during the isolation of insulin, it stated that "insulin was contaminated by a glucose agonist" (Godoy-Matos, 2014). Furthermore, glucagon is responsible for the stimulation of gluconeogenesis and glycogenolysis, which occur in the liver and result in formation of glucose (Mann and Bellin, 2016).

The preproglucagon gene is responsible for the expression of glucagon (Taborsky Jr, 2010). This pre-pro gene can undergo various modifications to yield either GLP-1, GLP-2 or glucagon and the end product is dictated by the tissue in which the gene is expressed. In the pancreatic islet α-cells, the GLP-1 and GLP-2 sequences are flanked out, thus resulting in glucagon being the dominant hormone; whereas in the L-cells of the small and large intestine, the glucagon sequence is the one that is flanked out, making the other two hormones dominant. Surprisingly, these two hormones have different roles: GLP-1 is reported to have a role in the stimulation of insulin release while suppressing glucagon, and GLP-2 is known to increase the proliferation of the intestinal epithelial cells (Müller et al., 2017; Hædersdal et al., 2018).

Although previously mentioned that the secretion of glucagon increases the internal production of glucose, this amount is not so significant that it can substitute the importance of exogenous glucose; instead, it acts as a backup in case of starvation, of which in the occurrence, three mechanisms will be prompted in order to notify the body that there is a need for glucagon secretion, namely: The direct effect of low blood glucose, the inhibitory effect of insulin on α-hormones, as well as triggering the autonomic input of the sympathetic nerve, the parasympathetic nerve and the

circulating hormone epinephrine towards the α-cells (Taborsky Jr, 2010). The concentration of plasma glucagon is increased in patients with diabetes. Pharmaceutical drugs that decrease the concentration of glucagon have also been of key interest in the treatment of diabetes (Hædersdal et al., 2018; Finan et al., 2020).

1.4 Glucose transporters

The movement of glucose into glucose sensitive cells is governed by specific transporter proteins that surround the cell's plasma membrane. The importance of these transporter protein's lies in the fact that glucose is a large molecule that has a polar charge, as such, it cannot simply diffuse through the cell membrane without assistance. There are two known types of transporter proteins, namely: the sodium-linked glucose transporters (SLGTs) and the diffusion glucose transporters (GLUTs). The major difference between these two types of transporters is that the SLGTs are made of 14 transmembrane helices where both the carboxyl and amine terminal groups face the extracellular space, while GLUTs are made up of 12 membrane-spanning regions that have their carboxyl and amine terminal groups located intracellularly (Mann and Bellin, 2016; Navale and Paranjape, 2016).

SLGTs are typically located in the intestines, brain and kidneys. They are also found, in a lesser percentage, in the lungs, liver, pancreas, testes and the thyroid, and they function at a lower affinity than the aforementioned locations (Navale and Paranjape, 2016). Genetic mutations in the SLGT – 1 are associated with rare conditions that results in glucose/ galactose malabsorption thus affirming their biological role (Brown, 2000). There are 14 known GLUTs and a few of these are major role players in the transportation of glucose. These GLUTs are subdivided into three classes, illustrated in **figure 1.3 E**, and are all present in different tissues, at different compositions, and all have varying sensitivities towards insulin (**Figure 1.3 A – D**) (Augustin, 2010; Mann and Bellin, 2016). The GLUT classes are determined by how identical the molecules' sequences are to each other, and although they are named GLUTs, they transport other types of monosaccharide as well (Szablewski, 2019).

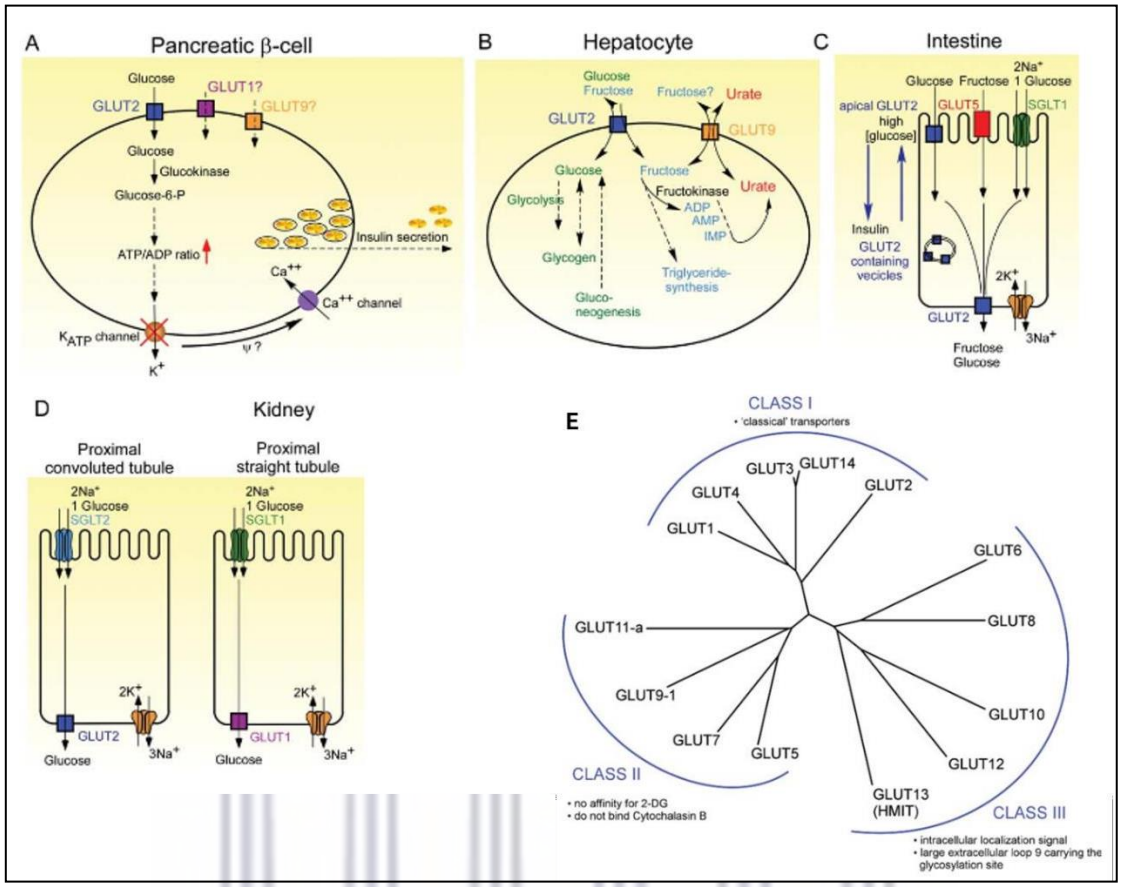

Figure 1.3: The physiological role of hexose transportation in different tissues. A: GLUT2 facilitates the uptake of glucose into the pancreatic β-cells. This uptake initiates a cascade of mechanism that stimulate the release of insulin (**figure 1.2**). B: GLUT2 mediates the endocytosis and exocytosis of glucose and the endocytosis of fructose into hepatocytes. Glucose is then converted into glycogen via glycolysis or the glycogen to glucose via gluconeogenesis. Fructose joins the mechanism that leads to triglyceride synthesis and can also be catalyzed by fructokinase for the production of uric acid. GLUT9 is known for its involvement in the transportation of urate and is suspected to also transport fructose although the idea has not been thoroughly studied. C: At the apical site of the intestines, glucose uptake, by the SLGT-1, is dependent upon the sodium-potassium pump while the uptake of fructose is conducted via GLUT5. In cases of high glucose concentration, GLUT2 undergoes translocation to the apical transmembrane of the intestines to aid in with its absorption. The translocation of GLUT2 is reversed by the presence of insulin. Exocytosis of both fructose and glucose is mediated by GLUT2. D: Transepithelial reabsorption of glucose in the kidneys is mediated by SLGT-2 on the apical site and GLUT2 in the basolateral membrane. The same is observed in the proximal straight tubule except the uptake is mediated by SLGT-1 on the apical site and GLUT1 on the basolateral membrane. E: An unrooted phylogenetic tree that illustrates the relationship between the 14 GLUTs and the classes they are divided into. The distance between the branches and the length of the lines indicates the degree of evolution that the GLUTs have underwent. Adapted from (Augustin, 2010).

Class I consists of GLUT1 - 4and GLUT14, class II consists of GLUT5,7,9,11 and class III consists of GLUT6,8,10,12,13 (Szablewski, 2019). The class I GLUTs are the classic transporters and are of great interest in understanding the pathogenesis of diabetes. GLUT1 serves a unique role in that it can transport glucose across the blood brain barrier while GLUT2, unlike most GLUTs that only serve to transport glucose to other locations, it is responsible for the reabsorption of glucose (and potentially that of galactose) from the gut and into the liver and pancreas (Brown, 2000, Augustin, 2010). Deficiency in the expression of GLUT1 and 3 is associated with Alzheimer's diseases, while deficiency in the expression of GLUT2 is associated with hyperglycaemia (Augustin, 2010). GLUT4, together with GLUT1, are said to be the most extensively studied glucose transporters, and this is because of their role in glucose homeostasis (Huang and Czech, 2007).

$GLUT_4$ is the most responsive to insulin, and it is associated with the development of type II diabetes (Olson, 2012). When insulin is secreted into the bloodstream, the GLUT4 transporters that are sequestrated within the glucose storage vesicles (GSV) are stimulated to undergo translocation from the cytoplasm of the adipose tissue cells, skeletal tissue cells and cardiomyocytes, and are taken to the respective tissues' plasma membrane. This translocation can also be prompted by exercise or by contractions. Translocation of GLUT4 occurs under a tightly regulated mechanism (**Figure 1.4**). GSVs are composed of proteins such as v-SNARE, Vamp-2 and insulin-responsive aminopeptidase (IRAP). The presence of IRAP, instead of transferrin receptors, in the GSVs is the reason they are able to respond to insulin, as opposed to acting like normal endocytic components. In the absence of insulin, GLUT4 remains intracellularly encapsulated within the GSV (Richter and Hargreaves, 2013). Although insulin sensitive tissues express other types of GLUTs, GLUT4 is the one that conducts most of the glucose uptake, and 80% of this goes to the muscle tissue (Richter and Hargreaves, 2013; Vargas et al., 2019).

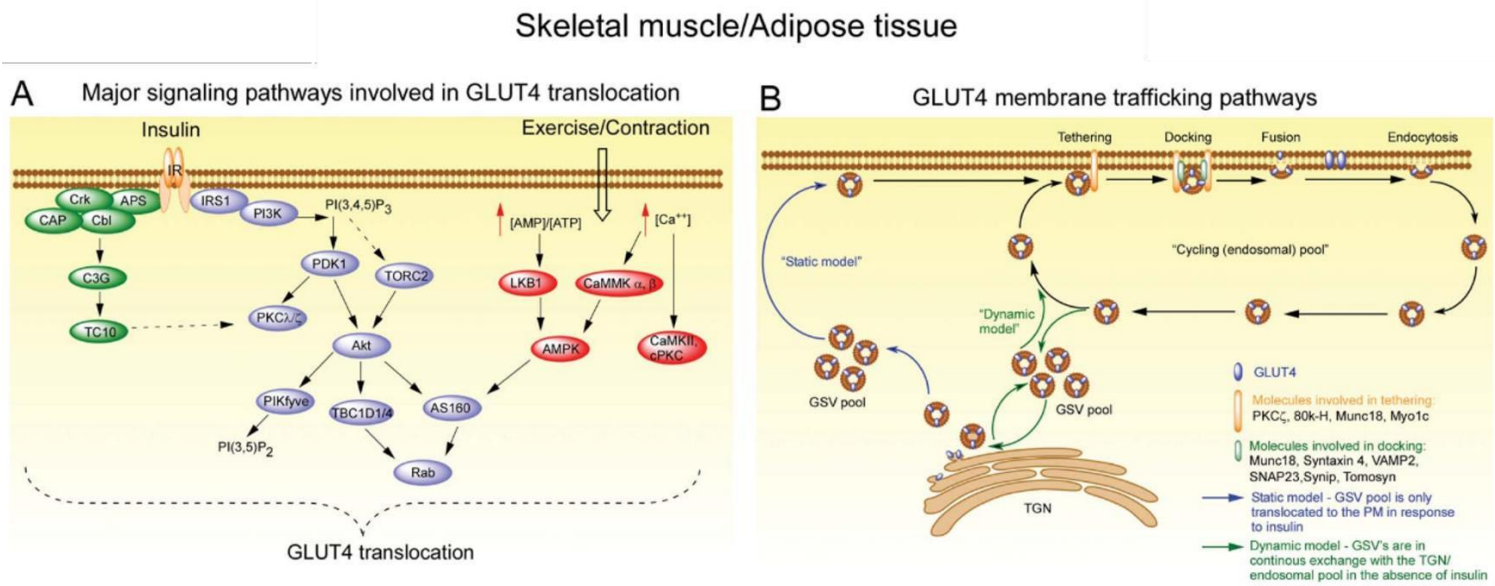

Figure 1.4: The translocation mechanism of $GLUT_4$ in the adipose tissue and skeletal muscle is divided into the signal transduction (A) and vesicular transport (B). A: Insulin receptors respond to the presence of insulin by capturing the hormone, thus triggering the cascade of the phosphoinositide-3-kinase (PI3-kinase) independent pathway (green) and PI3-kinase dependent pathway (blue). Exercise triggers the activation of the 5'AMP protein kinase (AMPK) in the skeletal muscle, due to an increased demand of energy, and also contributes to the translocation of GLUT4. B: A successful signal transduction prompts either the static model (blue arrows) or dynamic model (green arrows). The static model is observed only in the presence of insulin, while in the dynamic model the GSVs are in a constant exchange with the trans-Golgi network (TGN), thereby leading to a non-insulin related respond of glucose uptake (Augustin, 2010).

The expression of GLUT4 is changed according to the state of one's metabolic condition. A disruption in its transcription and/ or expression is associated with the pathology of impaired glucose uptake and IR, which both later become characteristics of type II diabetes and obesity (Marín-Juez et al., 2014). When the adipose tissue begins to house an abnormal amount of fat, $GLUT_4$ becomes down-regulated. This is thought to be a mechanism that protects the brain and heart from glucose deprivation since a bigger adipocyte would require a larger amount of glucose (Abel et al., 2001; Fam et al., 2012). This same behaviour is observed in diabetic patients. However, it is not seen in the skeletal muscle of either obese or diabetic individuals (Brown, 2000). Contradictory to this, skeletal muscle specific knock-out of the GLUT4 gene in mice (Zisman et al., 2000; Fam et al., 2012), as well as suppressing its translocation from the cytoplasm to the plasma membrane (Xu et al., 2015) has been found to cause severe IR and glucose intolerance.

The homologous recombination of GLUT4, in order to alter its expression, proved true to the development of T2DM, although complete knock-out of the GLUT4 did not lead to a T2DM phenotype; such mice were found to have an increased expression of insulin (Stenbit et al., 1997).

1.5 Types of Diabetes Mellitus

The failure to achieve homeostasis from pre-diabetes results in the development of diabetes; there are three main clinical forms of Diabetes Mellitus: Type I diabetes mellitus (T1DM) is characterized by the autoimmune destruction of pancreatic β-cells, which leads to an inadequate production of insulin, type II diabetes mellitus (T2DM) is a result of genetic predisposition, environmental factors and lifestyle choices, and it is characterized by an individual's resistance to insulin, and the progressive deterioration of the pancreatic β-cells, as well as gestational diabetes which is a form of diabetes that develops during pregnancy (IDF, 2019).

1.5.1 Type I Diabetes Mellitus

Formerly known as juvenile-onset diabetes (because of its commonness in children under 20 years), or insulin-dependent diabetes, T1DM currently has no known preventative measures (Todd, 2010). Since the disease thrives on the autoimmune destruction of pancreatic β-cells, thus the depletion of endogenous insulin, individuals who are diagnosed with T1DM depend on the intravenous injection of the insulin hormone for survival (Gyamfi et al., 2019). It is known that at 12 months after birth, the immune system has developed well enough to be able to support an automatic pathogenic response, and it is at this stage that the preclinical autoimmunity of T1DM is naturally and spontaneously triggered in susceptible individuals (Todd, 2010). Autoimmune destruction is marked by the presence of autoantibodies (antibodies that are produced by the immune system to target one or more of the host's own proteins) within the biological system; however, T1DM can exist in the absence of these autoantibodies, and these individuals are classified as idiopathic or type 1B patients (Gyamfi et al., 2019).

T1DM is a disease that is richly influenced by an individual's genetics (Steck and Rewers, 2011). Rat and mouse models have shown that no environmental or infectious triggers are required for the offset of T1DM (Todd, 2010); conversely, the fact that there is a positive correlation between T1DM, geographic location and seasons of the year suggests that one or more environmental factors (viruses, gut microbiota and toxins) may play a role in the onset of this disease (Gyamfi et al., 2019). Furthermore, the evolution of sedentary living, the prevalence of obesity, and other

metabolic disorders have increased the frequency of T1DM by 3% annually in children worldwide (Steck and Rewers, 2011; Gyamfi et al., 2019).

The Major Histocompatability Complex (MHC) class II, whose role is to stimulate the proliferation of T-helper cells, is the main role player when it comes to an individual's susceptibility to T1DM. Human Leukocyte Antigen (HLA) region on chromosome 6p21 is responsible for the development of approximately 50% of all T1DM that occurs within families. The strongest associations are seen in the HLA DR and DQ haplotypes. Although more than 40 non-HLA susceptibility genes have been identified and confirmed, 90% of T1DM patients carry either the DR4 – DQ8 or DR3 – DQ2 haplotype and carrying both haplotypes simultaneously presents the highest risk of developing T1DM (Todd et al., 2007; Steck and Rewers, 2011).

1.5.2 Type II Diabetes Mellitus

Accounting for 90 – 95% of all diabetic cases recorded in the world, type II diabetes mellitus (T2DM) is potentially one of the longest existing diseases known to humankind, and is currently a worldwide problem (Atkins and Zimmet, 2010; Olokoba et al., 2012). One of the major predictions for the onset of T2DM is when a whole-body insulin resistance is observed in a patient. This abnormality in glucose uptake is noted to usually start in the muscle tissue and is referred to as "the earliest detectable abnormality of T2DM" (Taylor, 2013). T2DM is characterized by relative insulin deficiency as well as insulin resistance by insulin responsive cells, which ultimately leads to chronic hyperglycemia (Olokoba et al., 2012; Gyamfi et al., 2019).

At the inception of the disease, insulin is able to successfully match the demand of the increasing BGL. However, with the progression of the disease, and the negligible response given by insulin sensitive cells, pancreatic β-cells begin to wear-out. A decrease in insulin production is soon observed, thus leading to uncontrollably high BGL even during fasting periods (Gyamfi et al., 2019). Beta-cell mass is said to decrease by approximately 50% in individuals with T2DM as compared to those with normal physiology. Their decline is observed to continue with the progression of the disease, thereby causing patients to eventually become insulin dependent (Taylor, 2013).

The increased frequency of T2DM is said to be the result of westernization, and consequently, the prevalence of obesity across all age groups (Banoo et al., 2015). Obesity is a contributing factor to T2DM in that the white adipose tissue is among the three main organs that are responsible for the

uptake of glucose. Furthermore, accumulation of excess fat in these cells tempers with their normal functioning, and they begin to release proinflammatory cytokines such as interleukin-6 and TNF-α, which are responsible for the advancement of low insulin sensitivity (Gyamfi et al., 2019). In this regard, T2DM is influenced by both genetic (McCarthy, 2010; Olokoba et al., 2012) and environmental risk factors (Zhang et al., 2017). T2DM also puts patients at a high risk of developing austere long-term comorbidities such as hypertension, cardiovascular diseases, neurocognitive impairments, kidney diseases, non-alcoholic fatty liver diseases as well as retinopathy, to mention a few (Zimmet et al., 2001; Atkins and Zimmet, 2010).

People with a familial history of T2DM are 3 times more likely to develop the disease compared to those who do not come from this background; other developmental risks are due to the use of tobacco, poor lifestyle choices such as high alcohol consumption, a lack of exercise and relaying largely on a high calorie diet (Haghvirdizadeh et al., 2015; Zhang et al., 2017). Patients with a familial background of T2DM are thought to develop the diseases earlier, and face far more complications than people who do not (Jeong et al., 2010). Environmental toxins have also been implicated as being a causative of T2DM and these include the likes of bisphenol A, a constituent of plastic that causes a decrease in insulin sensitivity, as well as arsenic, which is found in seafood, rice and mushrooms (Pizzorno, 2016; Zhang et al., 2017).

1.5.3 Gestational Diabetes Mellitus

Gestational diabetes mellitus (GDM) is a common metabolic disorder that is diagnosed during the pregnancy of a female who, prior to conceiving, was not diabetic (ADA, 2004). GDM is essentially a form of hyperglycaemia and is often detected between months 6 and 7 of the pregnancy (CDC, 2019). The increase in insulin resistance is credited to the weight gain that comes with the pregnancy as well as the hormones associated with the placenta. The implication of the placenta in GDM is supported by the fact that this condition is often reversed after birth, and there are very limited chances that the mother will develop type II diabetes later on in their lives (Buchanan and Xiang, 2005)

When GDM goes untreated, it becomes detrimental to both mother and child, and it increases the chances of a caesarean-section labour, spontaneous abortions, and nerve damage to the new-born, which is a consequences of increased bodyweight (BW) thus pressure build-up on the baby's shoulders during natural labour (ADA, 2004; Buchanan and Xiang, 2005; CDC, 2019). BW during

pregnancy, blood pressure, the age of the female at the time of conceiving the pregnancy, and a history of GDM from previous pregnancies, are some of the factors that influence the development of GDM (Buchanan and Xiang, 2005). Although GDM can later develop into type II diabetes mellitus, this outcome can often be negated by exercise and a healthy diet (ADA, 2004; Buchanan and Xiang, 2005).

1.6 Screening and diagnostic methods for insulin sensitivity and DM

1.6.1 Insulin sensitivity

Many of the methods used for the assessment of insulin sensitivity are based on the Hyperinsulinemic-Euglycaemic Clamp (HEC), as it serves as the gold standard technique. The HEC technique involves the concurrent intravenous administration of insulin and glucose at constant and at variable rates, respectively. An individual presenting with insulin sensitivity will require a higher dose of glucose to maintain euglycaemia, while one with insulin resistance (IR) will require minimal glucose for the same purpose. Nonetheless, HEC is limited by its long turnaround period, as well as its high running costs. As such, derivative methods like the glucose tolerance test, intravenous glucose tolerance test and the insulin tolerance test were developed to offer simpler technologies that are able to combat these shortcomings. A persistent challenge to these techniques is that they are all invasive, and are too complicated to perform in daily clinical work, or on large population studies (Gutch et al., 2015; Tagi et al., 2019).

To aid in simplifying the assessment of insulin sensitivity in clinical studies, surrogate indexes have been developed. These are divided into two categories: 1) Using fasting plasma concentrations of glucose, triglycerides and insulin to calculate the indices, and 2) indices are calculated based on insulin plasma concentrations, and glucose concentrations that are obtained within 2 hours of a standard oral glucose tolerance test (Gutch et al., 2015). These varying indices include the plasma fasting insulin (FPI), the quantitative insulin sensitivity check index (QUICKI) and the homeostasis model assessment insulin resistance (HOMA-IR). Different conclusions exist about the accuracy of these indices. Nonetheless, literature maintains that the clinical application of indices is limited by the absence of values that reference normal and impaired insulin sensitivity, and that they are more beneficial when being used for epidemiological studies that seek to understand the projection of diabetes in a non-diabetic population rather than as diagnostic tools (Gutch et al., 2015; Fiorentino et al., 2019; Khan et al., 2019; Muniyappa et al., 2019; Okosun et

al., 2020). Even so, the proper diagnosis of IR remains a venture of great importance, as it is a significant risk factor for the development of T2DM. When IR is detected early, it leaves room for the possible prevention and/or reversal of DM (Gutch et al., 2015; Tagi et al., 2019).

1.6.2 Diabetes Mellitus

In the case of diabetes, two screening and diagnostic approaches exist: The A1c based approach and the plasma glucose test (ADA, 2015). Glycated haemoglobin A1C (HbA1C) is a widelyused biomarker for chronic hyperglycaemia. It is used to assess the average BGL of an individualover the past 2 – 3 months. The HbA1C test plays a more valuable role in the management of diabetic patients and is often discouraged as a diagnostic tool. This is because HbA1C can be well correlated to micro- and macro- vascular complications. However, this test is considered insufficiently standardized to act as a go-to method for the diagnosis of diabetes, and only presents data that correlates to the previous 3 months (not instantaneous glucose status). Furthermore, the results obtained from individuals with sickle cell anaemia or other forms of haemoglobinopathy can lead to a misdiagnosis. As such, it is important that any HbA1C test be carried out according to the National Glycohemoglobin Standardization Programme (NGSP) guidelines, which state that a 5.7 to 6.4% result corresponds to pre-diabetes, while any percentage higher than 6.5% is a confirmation of existing diabetes (ADA, 2012; ADA, 2015).

Although the HbA1C test is much more convenient than the plasma glucose test, in that it does not require fasting, has a greater pre-analytical stability and causes less discomfort to the patient during times of illness, it is still not easily accessible in many regions within 3rd world countries, and is still relatively expensive to develop (ADA, 2012; ADA, 2015; Tomkins and Smith, 2020). In light of this, the oral glucose tolerance test (OGTT) still remains the gold standard for diagnosing DM; nevertheless, it is not without its own limitations and contradictions (Salmasi and Dancy, 2005; Tomkins and Smith, 2020).

The OGTT is conducted by first withdrawing blood from a patient who has undergone an overnight fast – this will be used to determine the fasting Plasma Glucose (FPG) levels. The patient is then provided with 75g of glucose, diluted in water, for ingestion, and this is followed by a blood withdrawal at times 60 min and 120 min. Glucose levels are then determined and compared to standard readings, and a diagnosis is made (Salmasi and Dancy, 2005). The preparations needed prior to the test, namely: high consumption of carbohydrates 3 days before the test, 10+ hours of

fasting, various blood withdrawals and various waiting times, render the OGTT method tedious and inconvenient. Regardless, the adversities associated with DM require that the screening be as accurate as possible (Tomkins and Smith, 2020).

The combined use of the FPG and the HbA1c test have been recommended as a way of reducing the misdiagnosis of possible diabetic patients. Results have shown that screening methods are largely dependent on factors such as age, ethnicity, and the risk profiles of the individuals involved. As such, a Standard Operating Protocol cannot be developed (Hu et al., 2010; Tomkins and Smith, 2020). A study carried out in 144 subjects with no known pre-existing diabetes revealed that the use of FPG alone failed to identify 62% of persons that had an abnormal OGTT result, while 83% of the HbA1c tests performed in individuals who were later found to be diabetic, had a reading that was less than 6.1% (lower than the 6.4% threshold recommended by the World Health Organization and the American Diabetes Association, refer to table 1). As a result, the OGTT is the only conclusive diagnostic tool that is currently available (Salmasi and Dancy, 2005). A different study concluded that the HbA1c threshold should be decreased to 5.9%, and that the combined use of FPG and HbA1c did indeed improve the sensitivity of the diagnosing process; additionally, the study maintained that the OGTT should still be performed prior to confirming a diabetic case (Yu et al., 2015).

Table 1: Criteria for diagnosing DM.

1. FPG ≥ 7.0 mmol/L OR
2. *OGTT with a plasma glucose level of ≥ 11.1mmol/L. OR
3. HbA1c of 6.5% or more (≥ 48 mmol/mol). OR
4. Random plasma glucose ≥ 11.1 mmol/L in patients with classic symptoms of hyperglycaemia.

*Test should be conducted according to WHO guidelines. Table adapted from (Tomkins and Smith, 2020).

1.7 Management and treatment of Diabetes Mellitus

1.7.1 Lifestyle modification in DM patients

As in many non-communicable diseases, lifestyle modification is often the first line of defense against the development or advancement of DM. It is so fundamental that even after a treatment regimen has been established, normally a pharmaceutical one, it will often include a balanced and

healthier lifestyle as its foundation Self-management of DM requires the combined efforts of the patient, the caregiver to the patient, and the clinician involved. The self-management approach is centered on the behavioural changes of the patient, which mostly entail better dietary choices and increased physical activity (ADA, 2017; Sheng et al., 2019).

Stress management, smoke cessation, physical activity, socio-environmental support systems and a nutritional diet that focuses on a high intake of fruits and vegetables, and a lower intake of saturated fats, salts and sugar, are some of the recommendations that are given by the American Diabetes Association in order to manage or prevent diabetes, along with its comorbid diseases, i.e cardiovascular disorders and hypertension (Patel et al., 2017; Sheng et al., 2019). A study conducted on a vegetarian population, residing in California, revealed that this population group was at a lower risk of developing metabolic diseases as compared to a non-vegetarian population. This finding is thought to be a result of the lower body weights that are observed in vegetarians, as well as their low blood pressure and low LDL cholesterol (Fraser, 2009).

One study showed that an improved dietary intake, physical activity, and a well-established knowledge on diabetes, could reduce the incidence of T2DM by 2-folds, within an average of 2.8 years, when compared to a population that was simply prescribed metformin with no further instruction (Diabetes Prevention Program Research Group, 2002). Another study found that weight loss intervention in individuals who are at a risk of developing DM, worked better when the individual was moderately overweight as compared to obese patients. This, however, did not mean that intensive lifestyle modifications were invaluable for the obese individual; instead it is shown to destabilize the trend towards other comorbid diseases (Lindström et al., 2005).

Although pharmaceutical interventions may be required at some point, or even prior to the illness, and especially in people who present with risk factors that are propelled by age and genetic predisposition, lifestyle modifications, as well as patient education and counselling, remain at the heart of the public health care system for the prevention and management of metabolic disorders (Lin et al., 2014; Patel et al., 2017; Patnode et al., 2017; LeBlanc et al., 2018).

1.7.2 Pharmaceutical intervention for DM

In addition to lifestyle modification (diet and exercise), oral and injectable hypoglycaemic drugs form part of the strategies that are used in DM management. Deciding which type of pharmacotherapy to use is dependent on the type of DM one has, and how each individual responds to their therapeutic targets, namely: weight, blood pressure and blood glucose control. Therapeutic targets are agreed upon by both doctor and patient. Prior to the administration of any drug, patients should be well informed about the progression of the disorder, as well as the varying forms of treatment, and their role in terms of symptom monitoring and drug dosing. Patients should be made to understand that the treatment they receive is solely catered for their needs and that they might not only improve from the disease, but there is a potential of them progressing from just one form of treatment to multiple therapies (Alwan, 1994; Domiguez-Salazar, 2017). **Figure 1.5** conceptualizes some of the criteria that can be followed in order to successfully treat a diabetic patient:

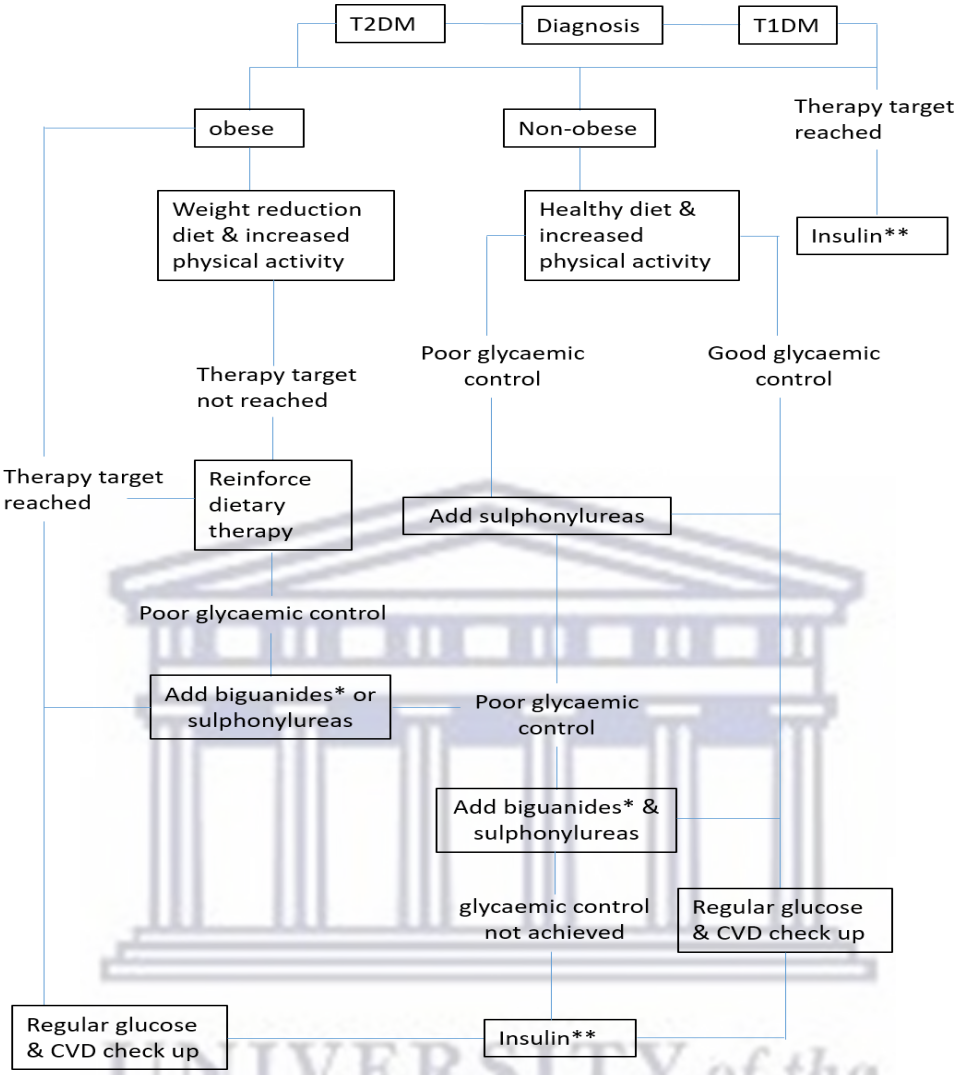

Figure 1.5: A simplified schematic representation for the treatment of diabetes mellitus. Drug can be prescribed during dietary therapy. This is done is accordance to the state of the hyperglycaemia, and if whether or not there are other comorbidities. * Biguanides should only be prescribed when there are no contraindications (Renal or hepatic failure, metabolic acidosis and/ or decreased creatinine removal) present. ** Insulin dosage should be defined for each individual. Adapted from (Alwan, 1994).

While insulin is arguably the most effective and predictable therapy, aside from its tendency to induce weight gain, chronic skin reactions, allergies, and its risk for causing hypoglycaemia, biguanides and sulphonylureas are the most prevalent forms of pharmaceutical treatments for T2DM patients. Other drug classes such as Thiazolidinedione (TZD), α-glucosidase inhibitors, DPP-4 inhibitors, SGLT-2 inhibitors, GLP-1 receptor antagonist, pramlintide, colesevelam, and bromocriptine exist, and are all said to decrease the presence of HbA1c by at least 0.5 – 1%,

except for biguanides and sulphonylureas. The two latter forms of treatment have a reduction rate of ~1.5% and 1 – 2%, respectively (DeFronzo et al., 2014; White, 2014; Thrasher, 2017).

For a time, clinicians were most sceptical about the use of biguanides to treat diabetes, and this was because of the association of phenformin and buformin with lactic acidosis. Now, metformin has become the most widely used anti-hyperglycaemic drug in the world (Engler et al., 2020). The primary mechanism of action of metformin involves the reduction of gluconeogenesis and lipogenesis, and an increase in glucose uptake and utilization via the mild improvement in insulin-sensitivity (Carpio and Fonseca, 2014; White, 2014). Metformin also promotes weight loss and/or suppresses weight gain, thus making it the ideal drug for obese T2DM individuals. However, it is known to cause gastro- related side effects such as nausea, vomiting and diarrhea, and cannot be used in individuals with contraindications (Carpio and Fonseca, 2014).

Unlike biguanides, there are several formulations of sulphonylureas that are available, namely: Glimepiride, Glipizide and Glibenclamide. This drug class' mechanism of action mainly functions through the stimulation of insulin release by the β-cells. It does this by binding to the sulphonylurea receptor located on the pancreatic β-cells. This occurrence leads to the closure of the calcium-potassium channel, cell depolarization, as well as calcium influx, thus the release of insulin. Because of their mechanism of action, sulphonylureas are well known for causing hypoglycaemia and weight gain, and are contraindicated in individuals with poor functioning livers, and those with nephropathy (Carpio and Fonseca, 2014; Thrasher, 2017).

As of 2014, there were 11 classes of drug treatments for diabetes (White, 2014). This is a considerably strenuous amount for clinicians who are trying to come up with an effective and safe treatment regimen for their patients. Many more analogues and classes are being developed, each with their own advantages and disadvantages (Thrasher, 2017).

1.8 Phytotherapy in the management Diabetes Mellitus

Many anti-diabetic pharmaceutical drugs stem from botanical sources e.g metformin is derived from the French lilac (*Galege officialis*). As such, many people feel safe to use medicinal plants as an alternative to conventional medicines or as a co-therapy (Bailey and Day, 2004; Dias et al., 2012). For many centuries, developing countries have exploited plants for their medicinal properties, and this is largely influenced by socio-cultural beliefs, especially in Africa, Asia and

South America. Over 80% of people living in third world countries depend on herbs for the treatment of ailments (Kasole et al., 2019). A study by Yeh et al. (2003) reviewed 108 clinical studies that focused on the mono or combinational use of phytotherapy for the treatment of diabetes, clearly exhibiting the large amount of literature available regarding this topic; nonetheless, there are still disputes about the effectiveness and safety of phytotherapy.

Due to the growing use of herbal medicines, the World Health Organization (WHO) developed four volumes of monographs, each detailing the safety, efficacy, quality assurance and contraindications of some of the most widely used phytotherapies. The main aim of these monographs is to enhance the scientific information that is available on these plants and to ensure human safety (WHO, 2009). *Allium cepa, Azadirachta indica, Momordica charantia, Ocimum tenuiflorum, Panax ginseng, Panax quinquefolius* and *Rehmannia glutinosa* are some of the plants that have been reported to possess hypoglycaemic properties. Their main mechanisms of action were reported to either be the inhibition of α-glucosidase, or the increase in the expression of GLUT-4 and PPARs, or the possession of phytochemicals that promote the secretion of insulin by β-cells, as well as having the ability to increase insulin sensitivity in glucose utilizing tissue (Yeh et al., 2003; Ghorbani, 2013; Governa et al., 2018).

Clinical studies using *Gymnema sylvestre* have long been carried out in both T1DM and T2DM patients. In T1DM, it was found that the administration of 200 mg of *G. sylvestre*, 2 times a day, per person, for a maximum of 30 months, along with the doctor prescribed amount of insulin injection, was able to decrease the average dose of insulin, increase serum c-peptide (thus potentially increasing β-cell function), improve glucose homeostasis, as well as reduce the activity of serum amylase (Shanmugasundaram et al., 1990). In T2DM, *G. sylvestre* (400 mg/day) was found to have the ability to regenerate pancreatic β-cells, as well as improve glycaemic control. This was postulated to be as a result of either increased insulin secretion or that the active component in *G. sylvestre*, termed GS_4, was acting on the liver and inhibiting the process by which insulin inactivation may have been occurring. Administration of *G. sylvestre* in non-diabetic individuals did not impact insulin secretion (Baskaran et al., 1990).

In addition to the pharmacokinetic and phytochemical studies of *G. sylvestre* (Sarker et al., 2019), scientist found that oral ingestion of this plant was able to decrease the desire to eat sweet foods by 21.5%, the pleasantness of sweet food by 31% and overall hunger by 21.4% (Turner et al.,

2020). *G. sylvestre* is thought to alter taste receptors to be more sensitive to the bitter taste in any given food (Hudson et al., 2018). Although *G. sylvestre* is a very promising plant for the treatment, and possible cure of diabetes, much research is still being done in trying to understand its mechanism of action, as well as the most effective way to combine its phytochemicals (since some of the active compounds are allergens or toxins, while other are therapeutic). The same dilemma is being faced by cinnamon, and much of the anti-diabetic herbal medicines (Ghorbani, 2013; Governa et al., 2018).

1.9 The role of nanotechnology in pharmaceutics

Nanotechnology, defined as the study and use of materials with a diameter of 10^{-9} m (1 billionth of a meter), is a multidisciplinary field that, in the pharmaceutical industry, is seen as a "therapeutic revolution" (Thakur and Agrawal, 2015). In this regard, nanotechnology has become one of the most exciting strategies for drug-repurposing, drug-discovery and drug development (Mizushima, 2011; Anselmo and Mitragotri, 2019). Nanoparticle formulations are desirable and promising products because of their tendency to acquire new physical and chemical properties, which are unlike their bulk counterparts. For instance, during the Roman Empire, gold nanoparticles (AuNPs) were used to manufacture a spectrum of coloured glasses, when, in fact, the colour of bulk gold is the famously known metallic yellow (Murty et al., 2013; Shah et al., 2014).

Some of the properties that are changed when transforming bulk material to NPs, or synthesising NPs using the bottom-up approach, include their thermal, optical and elastic properties, their surface area, as well as their encapsulation capacity. How these properties change is dependent upon the size and the method used to synthesize the NPs (Holister et al., 2003; Khanna, 2016). Other advantageous properties of NPs include the ability to tailor their size to match that of, or be smaller than, the molecules found within biological systems, their drug release can be easily manipulated, multiple ligands can be attached to their surface and they display an increased stability when compared to conventional drugs. Together, these characteristics enable NPs to escape the reticular-endothelial system (RES), as such, avoid setting-off the immune response; which is a problem faced by many conventional drugs (Salata, 2004). Commonly used materials for the synthesis of biomedical NPs include liposomes, dendrimers, noble metals and metal oxides. These variants can be used as drug carriers, labelling agents and imaging sensors (Anderson, 2018).

The use of NPs to treat diseases is termed nanotherapy. This approach can either be targeted or non-targeted, depending on the knowledge available about the biomarkers of the disease of interest. Nanotherapy has thus been vastly used in the treatment of cancer (Kim and Nie, 2005; Ediriwickrema and Saltzman, 2015), and in recent times has stretched its reach into the treatment of obesity (Sibuyi et al., 2019) and in ocular therapy (Kaur and Kakkar, 2014; Reimondez-Troitiño et al., 2015). Illnesses that result from the complications of diabetes have also been an area of interest for nanotechnology (Vives-Pi and Pujol-Autonell, 2015). Lipid based NPs have also been well received by the Food and Drug Administration (FDA) and many are commercially available (Anselmo and Mitragotri, 2019). Silver NPs have been mainly exploited for their antimicrobial properties (Marin et al., 2015), while AuNPs are exploited for their Surface Plasmon Resonance (SPR) that has improved bio-imaging and diagnosis (Ghosh and Pal, 2007). Other noble metals are also used in green nanotechnology [as discussed in section 1.10] (Jadoun et al., 2020).

1.10 Phytonanotherapy

Research in the use of green nanotechnology for biomedical application, also known as phytonanotherapy, is a fast growing branch in nanotechnology. Scientists all over the world have concerned themselves with the task of finding new ways to decrease the known, and unknown, toxicity of NPs. Phytonanotherapy removes the use of chemical reducing and capping agents, and replaces them with phytochemicals (flavonoids, polyphenols, tannins, carboxylic acids and amides) and antioxidants isolated from plant materials. This method alleviates cost constraints, presents a more sustainable and environmentally-friendly way of developing nanomedicines, reduces side effects that are associated with the chemical synthesis of NPs, and enhances their stability (Nasrollahzadeh et al., 2019).

Because of the large number of plant species that are available in the world, especially in Africa, Asia and South America, and the encouragement by the WHO, to use environmentally-friendly and cost effective medicines for the treatment of burden diseases, different phytonanotherapies are being actively investigated for their hypoglycemic properties and their effectiveness in treating diabetes mellitus, and other diseases that arise as its complication (Anand et al., 2017). *Cassia auriculata* is a plant that is well known for its hypoglycemic potency. Using the leaf extract of this plant, AuNPs with a size of 15 – 25 nm were successfully synthesised at room temperature (RT)

and were found to be very stable at various pH points. These NPs have not been tested for their antidiabetic activity (Kumar et al., 2011).

Furthermore, biosynthesised *Cassia fistula* stem bark AuNPs, ranging between 55.2 and 98.4 nm were used to treat streptozotocin (STZ) induced diabetic rats. The BW, serum glucose, and lipid profile of these rats were significantly improved by this treatment. *C. fistula* AuNPs were also able to decrease the amount of HbA1c present in the diabetic rats, and did not have any effect on the non-diabetic rats. The efficacy of these NPs was noted to be better than that of the aqueous extract alone (Daisy and Saipriya, 2012). *In vitro* testing of *Gymnema sylvestre* AuNPs was able to enhance the glucose uptake efficiency of 3T3-L1 adipocytes, and this suggests that the AuNPs could be as, or more, effective than the *G sylvestre* extract (Rajarajeshwari et al., 2014). Oral administration of *Gymnema sylvestre* silver NPs, in STZ-induced diabetic rats, was able to significantly decrease hyperglycemia and hyperlipidemia, as compared to the aqueous extract (Shanker et al., 2017a). While the treatment of STZ-induced diabetic mice with *Bacillus lichenformis* biomass AuNPs was able to decrease blood glucose by 75%, when compared with the diabetic control, these NPs were also able to return the lipid profile of the mice to almost normal (BarathManiKanth et al., 2010).

1.11 *Carpobrotus edulis* plant

C. edulis is a plant that is native to the coastal regions of the Eastern and Western Cape provinces of South Africa. It forms a part of the Aizoaceae plant family and is identified by its bright green foliage, yellow flowers that bloom during the summer time, and indehiscent fruits. This plant can now be found all around the world, where it is being used as a mat that holds together sand dunes, prevents soil erosion, and also for landscaping. However, due to its fast paced reproduction and its ability to survive extreme conditions, *C. edulis* is now classified as an invasive species, that also propagates the survival of other non-native plant species because of its tendency to increase the acidity of the soil, as well as change its biome (Herbarium, 1998).

Also called the Sour fig, Hottentot Fig, *Ikhambi lamabulawo* (IsiZulu) or *Igcukuma* (IsiXhosa), the fruits of the *C. edulis* plant can be eaten raw, dried, as a jam or added into curries. The leaves of this plant have been used to treat mouth sores, cuts, eczema, ringworms and insect bites due to their antiseptic properties (Richter, 2003). The leaves have also been reported in the treatment of HIV/AIDS-associated infections (Omoruyi et al., 2012), Tuberculosis and DM (Akinyede et al.,

2020). Following a water, ethanol and acetone extraction, *C. edulis* fruit peels were reported to have high antimicrobial activity, a high total phenolic, flavonoid and tannin content; however, the compositions of these phytochemicals was dependent upon the method of extraction (Castañeda-Loaiza et al., 2020). *C. edulis* leaf extracts have also been reported to have the potential to improve neurological function (Rocha et al., 2017).

Aim of study:

Much research that has been conducted on *C. edulis* has been focused on its leaves due to their numerous antiseptic properties and medicinal applications. To date, there is no known research that has been conducted to find the anti-diabetic potential of the *C. edulis* fruit extract, or its AuNPs. For this reason, and because of the intensive interest that is being received by phytonanotherapy for the treatment of various diseases, this research sought to investigate, for the first time, the anti-diabetic potential of AuNPs biosynthesised from the extract of the *Carpobrotus edulis* fruit (CeFe).

Main objectives were:

1. To synthesize of biogenic AuNPs using an aqueous extract of the *Carpobrotus edulis* fruit.
2. To characterize the biosynthesised CeFe-AuNPs.
3. To assess the effects of CeFe and CeFe-AuNPs on glucose uptake
4. To determine the toxicity of CeFe and CeFe-AuNPs in non-diabetic rats; and
5. To determine the anti-diabetic effects of CeFe and CeFe-AuNPs in rats with STZ-induced diabetes.

Null hypothesis:

CeFe-AuNPs do not possess hypoglycaemic properties, therefore they do not have a positive effect in rats with STZ-induced diabetes mellitus.

Hypothesis:

CeFe-AuNPs possess hypoglycaemic properties, therefore, these NPs have a positive effect in rats with STZ-induced diabetes mellitus.

Chapter 2: Materials and Methods

2.1 Preparation of *C. edulis* fruit extract

Dried *C. edulis* fruits were purchased from the Bellville market. In order to prepare a 0.25 g/ml extract solution, 100 g of the dried fruit was cleaned by removing the stem and manually removing off the top surface of the fruit. The fruits were then thoroughly washed with distilled water in order to remove debris, and were steeped in 400 ml of deionized water (ddH_2O) overnight. The rehydrated fruits were blended until smooth, using a blender, and the resulting homogenate was heated to 80 ºC for 10 min. The homogenate was cooled to RT and filtered with glass wool in order to remove the chunky portions. The filtrate was centrifuged at 9000 rpm, 25 ºC, 10 min, filtrated through a Whatman No.1 filter paper, and was topped up with ddH_2O to a final volume of 400 ml. The *C. edulis* fruit extract (CeFe) was then stored at -80 ºC until further use.

2.2 Green synthesis of gold NPs

The frozen (CeFe) was thawed at RT. The pH of the extract was adjusted to 8 by the addition of a 1 M NaOH solution and then centrifuged at 9000 rpm, 25 ºC, 10 min, in order to clarify the solution. A 0.5 mM gold chloride tri-anhydrous was prepared in ddH_2O, and the biogenic gold NPs were synthesised at a 1:10 ratio of extract: gold chloride. The synthesis reaction was carried out at RT, without shaking.

2.3 Determination of the absorbance Spectra

The UV-Vis spectrophotometer (PolarStar Omega microplate reader) was used to determine the absorbance spectra, as well as the SPR of the synthesized CeFe-AuNPs. A 30 µL volume of CeFe-AuNPs was diluted in 270 µL of ddH_2O, and transferred into a flat bottom Greiner 96 well plate. The UV-Vis spectrophotometer was set to a wavelength of 400 nm – 700 nm and the generated data was analysed using Microsoft excel.

2.4 Hydrodynamic size, Poly-dispersity Index and Zeta potential

Dynamic light scattering (DLS) technique was used to determine the hydrodynamic size and the poly-dispersity index (PDI) of the CeFe-AuNPs. A 1:10 ratio of CeFe-AuNPs to ddH_2O was placed into a 10 mm optic density polystyrene cuvette, and the sample was analysed using a Malvern Zetasizer Nano-ZS90 which was set to a temperature of 25 ºC. Size distribution was determined

at 90 º angle following the Strokes-Einstein relationship, and 11 experimental runs were conducted, each lasting 10 seconds. The zeta-potential was determined by adding a 1:10 ratio of CeFe-AuNPs: ddH_2O into a disposable folded capillary cell and was analysed at 25 ºC, at a 90 º angle to the light beam. The equilibration time was set to 30 seconds and the experimental runs were conducted in triplicates, at a voltage of 4 mV.

2.5 High Resolution -Transmission Electron Microscopy

To determine the core size of the synthesised CeFe-AuNPs, the sample was diluted with ddH_2O at a 1:10 ratio, drop-coated on a copper grid that is supported by a thin amorphous carbon film, and allowed to dry under a xenon lamp for 10 min. The micrographs were generated by viewing the grid under a TECNAI F20 HRTEM at an acceleration voltage of 200 kV, in a bright field mode. The micrographs were processed using the ImageJ software and the size distribution graph was obtained using the Origin8 software.

2.6 FTIR analysis

CeFe-AuNPs were pelleted using the ethanol extraction method. Briefly, a 5:1 ratio of ice cold ethanol to CeFe-AuNPs was prepared. The solution was placed at – 80 ºC for 30 min, then allowed to reach RT. It was then centrifuged at 8000 rpm, 25 ºC, 10 min, and the supernatant discarded. The CeFe-AuNPs pellet was left to air dry overnight. Potassium Bromide was crushed together with the AuNP pellet or the CeFe pellet, the resultant powder was placed in a metal disk, and analyzed using a Perkin-Elmer spectrum one FTIR spectrophotometer. The spectra range was read at 4000 – 400 cm^{-1} and a resolution of 2 cm^{-1}.

2.7 *In vitro* Stability analysis

The *in vitro* stability of CeFe-AuNPs was tested in various physiological mediums. Briefly, 1 % Bovine Serum Albumin (BSA), 10 % NaCl, phosphate buffer solution (PBS), and ddH_2O were used as the physiological media. CeFe-AuNPs were added at a 1: 5 ratio, and were incubated at 37 ºC for 24 hours. The absorbance spectra were determined using a UV-Vis spectrophotometer at an absorbance range of 350 nm to 700 nm.

2.8 Determination of gold nanoparticle concentration

A concentrated pellet of CeFe-AuNPs was obtained via centrifugation of 1 ml of the sample at 20 000 rpm, 25 ºC, 30 min. A final weight of 0.02 g of the pellet was obtained. This was placed in a clean glass vial, which was previously washed with aqua regia (3 HCl: 1 HNO_3). Two millilitres of freshly prepared aqua regia was added, and the sample was incubated at 70 ºC for 24 hours or until a 0.5 ml volume remained. The remaining solution was transferred to a 15 ml Greiner tube, and was made up to 10 ml with 2 % HCl. The samples were then sent to the Central Analytical Facilities at Stellenbosch University for Inductively Coupled Plasma – mass spectroscopy (ICP-MS) analysis.

2.9 Glucose uptake by yeast cells

Yeast cell suspension was prepared according to a published protocols (Cirillo, 1962, Bhutkar and Bhise, 2013, Saghir et al., 2020). Briefly, 1 g of commercial baker's yeast was re-suspended in 50 ml of ddH_2O and was left overnight at RT. The yeast was centrifuged at 4200 rpm, 25 ºC, 5 min, and the supernatant was discarded. The pellet was re-suspended in 50 ml ddH_2O, and centrifuged as above. This was repeated until the supernatant was clear. The pelleted yeast cells (~2 ml) were reconstituted into 18 ml of ddH_2O to make a 10 % (v/v) yeast suspension.

CeFe and CeFe-AuNPs were prepared at varying test concentrations (1.56 – 100 mg/ml). A 100 µl of each test concentration was added into an Eppendorf tube, and an equal volume of either 10 mM, 20 mM or 50 mM glucose was added. The Eppendorf tubes were incubated at 37 ºC for 10 min and then 10 µl of the yeast suspension was added. The tubes were vortexed to ensure consistent distribution of the yeast cells and was incubated at 37 ºC for a further 60 min.

The samples were centrifuged at 3800 rpm, 25 ºC, 5 min, and the supernatant was transferred to an Eppendorf tube containing 100 µl of 3,5-dinitrosalicylic acid reagent (DNS).The tubes were heated in a heating block at 100 ºC for 5 min. The samples were immediately placed in an ice water bath, and 300 µl of ice cold ddH_2O was added to stop the reaction. The absorbance was read at 540 nm using the PolarStar Omega microplate reader. The % increase in glucose uptake was calculated as follows:

$$\%\ increase\ in\ glucose\ uptake = \frac{(Abs.control - Abs.sample)}{Abs.control}\ x\ 100$$

The control of the experiment was the sample that included all the reagents except the test samples (CeFe or CeFe-AuNPs). The blanks were the varying concentrations of either CeFe or CeFe-AuNPs in water, or in water with 10 µl yeast.

2.10 Animal care

All animal experiments were carried out according to the guidelines and approval of the South African Medical Research Council (SAMRC), Ethics Committee for Research on Animals (ECRA 08/19) and the University of the Western Cape, Animal Research Ethics Committee (AR 20/1/1) (**Annexure A**). Twenty female Wistar rats and forty two male Wistar rats were sourced from the SAMRC PUDAC, and were allowed to acclimatize to the laboratory living conditions, and handling for a week (22 – 25 ºC temperature, 45 – 55 % humidity, 15 – 20 cycles/hour ventilation). Animals were subjected to 12 hours light/dark cycles, water and food were provided *ad libitum*. For socialization purposes, rats were caged in pairs, and were provided with nesting materials for enrichment. Housing tubes were also added for sleeping and hiding purposes. Rats were introduced to the jelly cubes during the week of acclimatization.

2.11 Gummy bear preparation

Jelly cubes were prepared by first thoroughly mixing 9.25 g unflavoured gelatine with 85 g of cherry/strawberry/raspberry flavoured jelly powder in 62.5 ml of ddH_2O maintained at 80 ºC, on a magnetic stirrer hot plate. It was ensured that the mixture did not boil, so as to preserve the integrity of the gelatine. Once the jelly was melted, 62.5 ml of RT ddH_2O was added. The mixture was allowed to mix for a further 1 min. To prevent the jelly from solidifying before time, the jelly mixture was kept at 20 ºC before transferring it, by weight, into silicon moulding trays using a dropper. The jelly cubes were left to set for at least 1 hour, removed from the moulds, and kept at 4 ºC until use (**Figure S1**). These jelly cubes were used during the acclimatization stage.

2.12 Acute toxicity Gummy bear preparation

A stock of the jelly mixture was prepared as in point 2.11. Prior to placing the jelly into the silicon tray, CeFe, CeFe-AgNPs or CeFe-AuNPs was added into the jelly stock, all to a final concentration of 2000 mg/kg. The CeFe-AgNPs were a gift from Prof AM Madiehe. This mixture was then transferred into the silicon tray moulds, left to set for at least 1 hour and kept at 4 ºC until use.

2.13 Acute toxicity study

Twenty female Wistar rats, aged 8 weeks, were sourced from the SAMRC PUDAC. The rats were acclimatized for a week and later randomized, by weight, into four groups (n = 5), namely: Group I: Control group, Group II: CeFe treated group, Group III: AuNPs treated group and Group IV: AgNPs treated group. The lethal dose test was performed according to the OECD guidelines and at a dose of 2000 mg/kg. Briefly, one animal in each group was fasted overnight and water was provided *ad libitum*. The fasted rats were each provided with a jelly cube containing either CeFE, CeFe-AuNPS, CeFe-AgNPs or no treatment, as a single dose, and were only allowed to eat after 1 hour of treatment administration.

The treated rats were closely observed for any signs of toxicity for 30 min and then after 4 hours. In the absence of any death or toxic effects, the remaining 16 rats were fasted overnight, with water provided *ad libitum*. Each of the animals were given jelly cubes containing 2000 mg/kg of either CeFe, CeFe-AuNPs, CeFe-AgNPs or no treatment, according to the group they belonged to. The rats were observed as above and thereafter daily, for a further 14 days. BWs were measured once a week, and on the day of necropsy. At the end of the study, blood was collected by exsanguination via the vena cava, under isoflurane anaesthesia and organs of interest were collected and placed in 10 % formalin in preparation for histology.

2.14 Anti-diabetic study gummy bear preparation

To avoid the presence of excess sugar, only gelatine was used in the preparation of these jelly cubes. Briefly, 75 ml of ddH_2O was brought to a temperature of 80 ºC, 2 ml of red food colouring was added and the two were thoroughly mixed. Following this, 47 g of unflavoured gelatine powder was added. Once evenly mixed, 75 ml of RT ddH_2O was added. The mixture was transferred to silicon moulds and allowed to set for at least 1 hour, then kept at 4 ºC until use. For the experimental animals the jelly mixture was combined with either metformin (250 mg/kg), CeFe (200 mg/kg and 400 mg/kg) or CeFe-AuNPs (100 mg/kg and 200 mg/kg), and were allowed to set for at least 1 hour in the fridge, and kept at 4 ºC until further use.

2.15 Anti-diabetic study

Forty-two male Wistar rats were sourced from the SAMRC PUDAC and were acclimatized for a week. The rats were randomized, by weight, into seven groups (n = 6), namely: Group I: non-

diabetic control, Group II: Diabetic control, Group III: Diabetic metformin treated (250 mg/kg), Group IV: Diabetic extract treated (200 mg/kg), Group V: Diabetic extract treated (400 mg/kg), Group VI: Diabetic CeFe-AuNPs treated (100 mg/kg) and Group VII: CeFe-AuNPs treated (200 mg/kg).

Rats were fasted for 6 - 8 hours, in preparation for the STZ injection. In order to avoid sudden death due to hypoglycaemia, animals were provided with 10% sucrose water *ad libitum*. STZ was freshly prepared (40 mg/kg in 0.1 M citrate buffer, pH 4.5) and intraperitoneally (IP) injected, within 5 minutes of dissolving, into Group II – VII rats (n = 38). Group I rats (n = 6) were injected with 0.1M citrate buffer at pH 4.5. Animals were kept on 10% sucrose water for 3 days and then it was changed to regular water. After 48 hours since diabetes induction, a glucometer and tail prick method was used to determine the blood glucose levels of the rats. This also served as the first day of treatment. Each group was administered a single oral dose of the appropriate treatment, daily, for 25 days. The rats were observed daily for any signs of toxicity, and their BWs were recorded weekly.

A day before necropsy, rats were fasted for 12 hours (21h00 – 09h00). On the day of necropsy, the rats were weighed and fasting blood glucose was measured using the tail prick method. The rats were anaesthetized by isoflurane inhalation and euthanized by exsanguination. Blood samples were collected via the vena cava, and various organs were collected (brain, heart, kidney, liver, spleen, pancreas, adipose tissue, lungs and testicles), weighed and placed in 10% formalin in preparation for histology.

2.16 Histopathology analysis

The livers, kidneys, spleens, pancreata and hearts of the animals used in the acute toxicity study, and the pancreases of the anti-diabetic study, were collected and fixed in 10% neutral buffered formalin. The morphological changes induced by the CeFe-AgNPs, CeFe-AuNPs and CeFe were analyzed at the National Health Laboratory Services, Department of pathology, University of Cape Town via a haematoxylin and eosin (H and E) staining procedure. Briefly, the organs were placed in cassettes and embedded in paraffin. After the embedding process, the organs were cut into sections of 2 µm and floated in 35 – 40% alcohol. The tissues were then floated into a 45 ºC water bath in order to remove creasing from the tissue, then floated onto their respective slides, and

allowed to dry at 55 ºC overnight. Finally, the sections were stained with H and E, and were viewed with a light microscope at different magnifications (10x, 40x and 200x).

2.17 Hematology analysis

Blood was collected in serum separating tubes and was centrifuged at 3500 rpm, 4 ºC, 20 min, in order to separate between serum and blood cells. The serum was aliquoted into cryovial tubes and stored at – 80 ºC until further use.

2.17.1 Serum insulin determination

The insulin assay was carried out according to the manufacturer's protocol (Erins, Rat Insulin ELISA Kit, Thermo Scientific). Briefly, all working reagent were brought to RT prior to using. The insulin standard was prepared by adding 400 µl of assay diluent C into the lyophilized insulin vial. In a separate eppendorf tube, 440 µl of diluent C was added, along with 120 µl of the insulin standard; of this solution, 300 µl were aliquoted into a new tube. A serial dilution was carried out in tubes containing 250 µl of diluent C (150, 75, 37.5, 18.75, 9.38, and 4.69 µlU/ml). Standard zero was composed only of 250 µl of diluent C.

Into the anti-rat insulin pre-coated 96-well strip plate, a 100 µl of the standard and samples was added (all reaction were carried out in duplicates). The plate was incubated at RT for 2.5 hours with gentle shaking. The samples were then discarded, the plate washed 4 times with 300 µl of 1x wash buffer, and inverted on a clean paper towel to dry. A 100 µl of biotinylated antibodies was added to each well and incubated for 1hr at RT with gentle shaking. After incubation, the solution was discarded, and was washed and dried as described previously. A 100 µl of streptavidin-HRP was added into each well, and the plate was incubated for 45 min at RT with gentle shaking. The solution was discarded, and washed and dried as before. Finally, a 100 µl of TMB substrate was added to each well and incubated for 30 min at RT with gentle shaking. A 50 µl volume of stop solution was added immediately after and the absorbance was determined at 450nm and 550nm. For all the incubation steps, a new cover slip was used and the plate was covered with foil. To account for optical imperfections, the formula Abs at 550nm minus Abs at 450nm was used.

2.18 Statistical analysis

All experiments were carried out in triplicates and analyzed using the student t-test on Microsoft excel 2013, unless stated otherwise. The statistical analysis for the anti-diabetic animal study was conducted via a one-way multivariate analysis of variance (MANOVA) on R, followed by the one-way analysis of variance (ANOVA) and TukeyHSD post hoc analysis on python (**Table S2; Table S3**). Values were considered significant at $p < 0.05$.

Chapter 3: Results and Discussion

3.1 Synthesis and characterization of CeFe-AuNPs

3.1.1 Introduction

Biogenic NPs are rapidly gaining recognition owing to their relatively easy synthesis and up-scale methods. These NPs are considered to be both eco-friendly and biocompatible, thus making them desirable for biomedical applications (Elbagory et al., 2016; Nasrollahzadeh et al., 2019). Gold NPs are amongst the most widely used biomedical NPs, and they present with valuable characteristics such as biocompatibility, high surface reactivity, as well as a high resistance to oxidation (Guo et al., 2005; Nasrollahzadeh et al., 2019). To broaden the body of knowledge already available on phytonanotherapy for the treatment of diseases, this study sought to pioneer the investigation of AuNPs biosynthesized with *Carpobrotus edulis* fruit extract as potential treatment for Diabetes Mellitus.

This chapter discusses the synthesis method and characterization of CeFe-AuNPs using techniques such as the UV-Vis spectrophotometer, Dynamic Light Spectroscopy (DLS), High-Resolution Transmission Electron Microscopy (HR-TEM) and Fourier Transform Infrared spectroscopy (FTIR).

3.1.2 Synthesis of CeFe-AuNPs

The UV-vis absorption spectrophotometer is one of the most commonly used techniques for assessing the formation of NPs. This technique takes advantage of the electron cloud oscillation that occurs around the surface of NPs (> 2 nm), and correlates it to their diameter (Philip, 2008). In this study, the biogenic synthesis of CeFe-AuNPs was conducted through the direct interaction of CeFe and $AuCl_4 \cdot 3H_2O$. The control of parameters such as pH, temperature, gold salt concentration and extract concentration are pivotal for the successful synthesis of AuNPs, as they influence their size, shape and charge; which are all important components for decision making in terms of their downstream applications (Elbagory et al., 2016). The parameters of the CeFe-AuNPs used in this study were optimized by Prof AM Madiehe (manuscript in progress); as such, these details will notbe included in this thesis.

In order to determine the rate of reaction for the formation of CeFe-AuNPs, the absorbance spectra of the NPs was measured at time intervals (in minutes) of: 1; 2.5; 5; 10; 15; 20; 30; 60; 120 and 1440 (**Figure 3.1 A and B**). The reaction was observed to reach saturation at 20 minutes (**Figure 3.1 B**). Equation 1 demonstrates the latter point and shows how the change in absorbance between these two time points is 0.0136 Abs. min^{-1}.

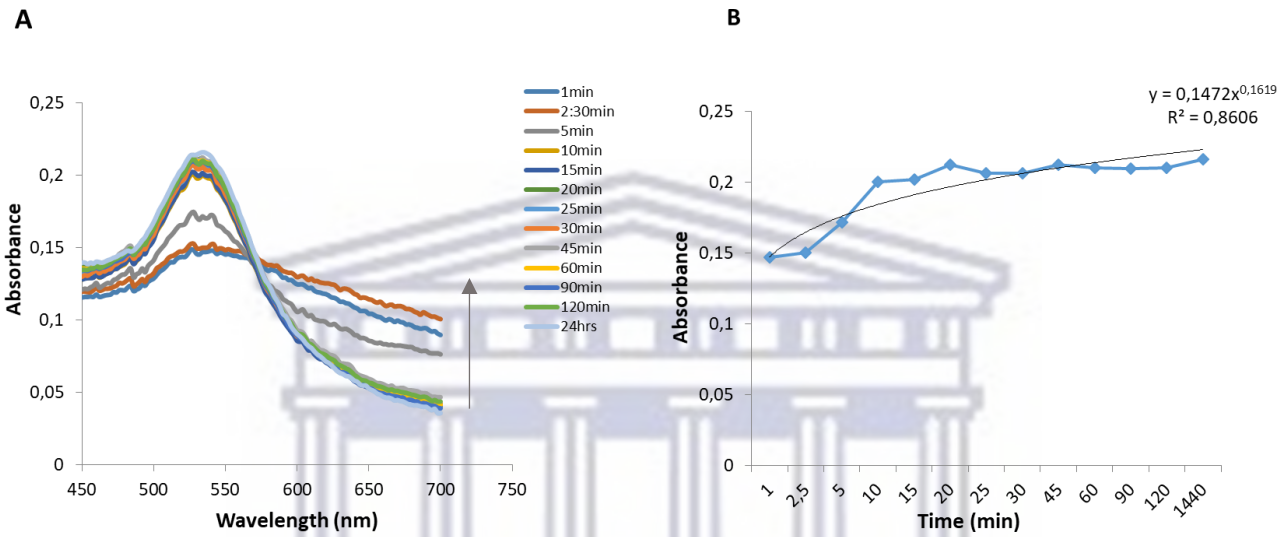

Figure 3.1: A) The absorbance spectra of CeFe-AuNPs as a function of time and B) The absorbance of CeFe-AuNPs at 532 nm as a function of time. Experiments were conducted in triplicates, and R^2 = 0.8606.

$$Eq.\ 1;\ Rate\ of\ reaction_{(t=20\text{min})} = \frac{\Delta OD\ value\ at\ \lambda\text{max}}{\Delta time} = \frac{0.212}{20\ min} = 1.1\ x\ 10^{-2} Abs.\ min^{-1}$$

$$Rate\ of\ reaction_{(t=1440\ min)} = \frac{\Delta OD\ value\ at\ \lambda\text{max}}{\Delta time} = \frac{0.216}{1440\ min} = 1.5\ x\ 10^{-4} Abs.\ min^{-1}$$

$$Change\ in\ Abs. = Rate\ of\ reactio_{(t=1440\text{min})} - Rate\ of\ reaction_{(t=20\text{min})}$$

$$= 1.5\ x\ 10^{-4} Abs.\ min^{-1} - 1.1\ x\ 10^{-2} Abs.\ min^{-1}$$

$$\underline{= 0.0136\ Abs.\ min^{-1}}$$

Amongst the many available characterization techniques of AuNPs, observing their change in visible colour is also one way in which preliminary confirmation of the successful formation of AuNPs can be done. This colour change is due to the local surface plasmon resonance and often

ranges between ruby red to purple-blue, depending on the shape of the AuNPs (colloids, cubes, rods, stars or triangles) and/or their aggregation state (Philip, 2008). The colour change from yellow to ruby red, was observed to begin between 2 and 3min, and it indicated the formation of CeFe-AuNPs. **Figure 3.2** illustrates the absorbance spectra of CeFe-AuNPs at 24 hours, as well as the collaborating colour change of the CeFe-AuNPs (**insert**). The maximum absorbance (λ_{max}) of the SPR band of these NPs was observed at 532 nm (**Figure 3.1: A**), which is in alignment with the notion that clinically applicable gold NPs will generally exhibit a SPR maxima in the range of 517 nm and 575 nm (Azzazy et al., 2012).

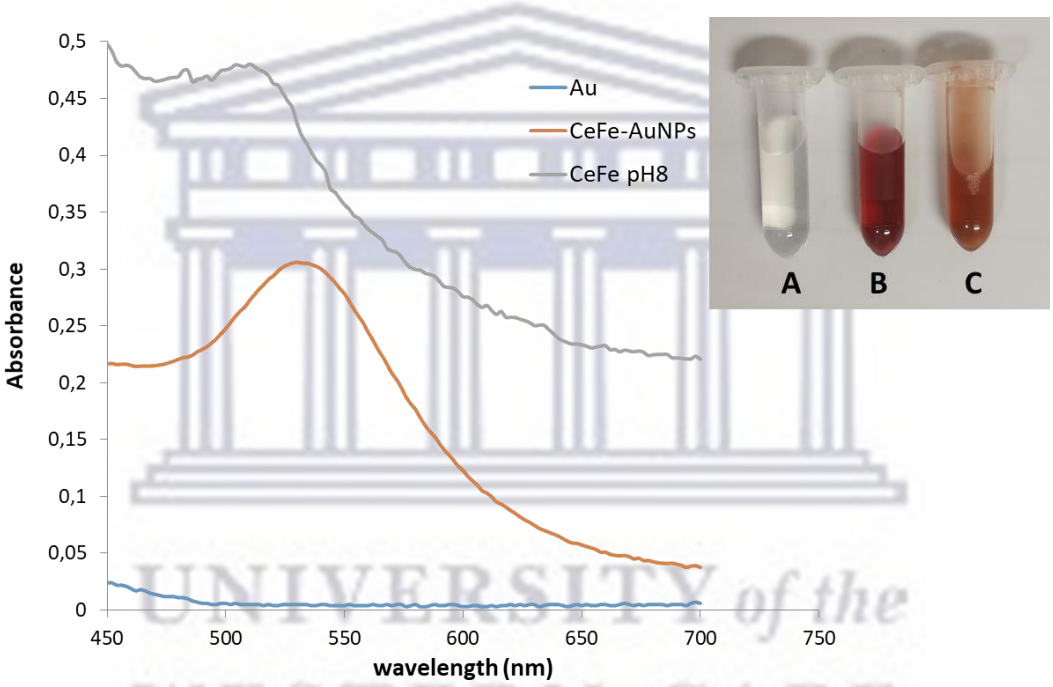

Figure 3.2: Absorbance spectras of Au, CeFe and CeFe-AuNPs. CeFe-AuNPs were observed to display a Surface Plasmon Resonance maxima at 532 nm. The insert indicates that CeFe-AuNPs display a characteristic ruby red colour compared to the unreacted ligiht yellow $AuCl_4 \cdot 3H_2O$ solution and the brownish colour of CeFe at pH 8.

3.1.3 Characterization of nanoparticle morphology, size and size distribution

3.1.3.1 Dynamic light scattering and zeta-potential analysis

The dynamic light scattering (DLS) procedure is a technique used to measure the Brownian motion of particles in solution. This measurement is then correlated to the size of the particle on the basis that larger particles will have a slower movement compared to smaller ones. For a long time this

technique was used to determine the particle size distribution of polymer latex products (Vega et al., 2003), and is now also being used for the characterization of NPs, especially those that display surface plasmon resonance (Khlebtsov and Khlebtsov, 2011). Because DLS measures the hydrodynamic size of the nanoparticle, it is recommended that it be accompanied by HR-TEM, which will reveal the particle's core size (Alexander and Dalgleish, 2006; Khlebtsov and Khlebtsov, 2011).

As shown in **figure 3.3 A**, CeFe-AuNPs synthesised in this study had an average hydrodynamic size of 75,30 ± 61,63 nm and a polydispersity index of 0.435, the zeta potential was – 30.9 mV (**Figure 3.3 B**). Literature states that a polydispersity index that is less than 0.5 is representative of NPs that are mono-dispersed, and that a zeta potential that is less than – 30 mV is indicative of NPs that have an excellent stability, due to the repulsive electrostatic forces that exist between them. These features are especially important in NPs that have biomedical applications in that their behaviour can be easily predicted, as compared to unstable and polydispersed NPs (Rajarajeshwari et al., 2014; Omran et al., 2018).

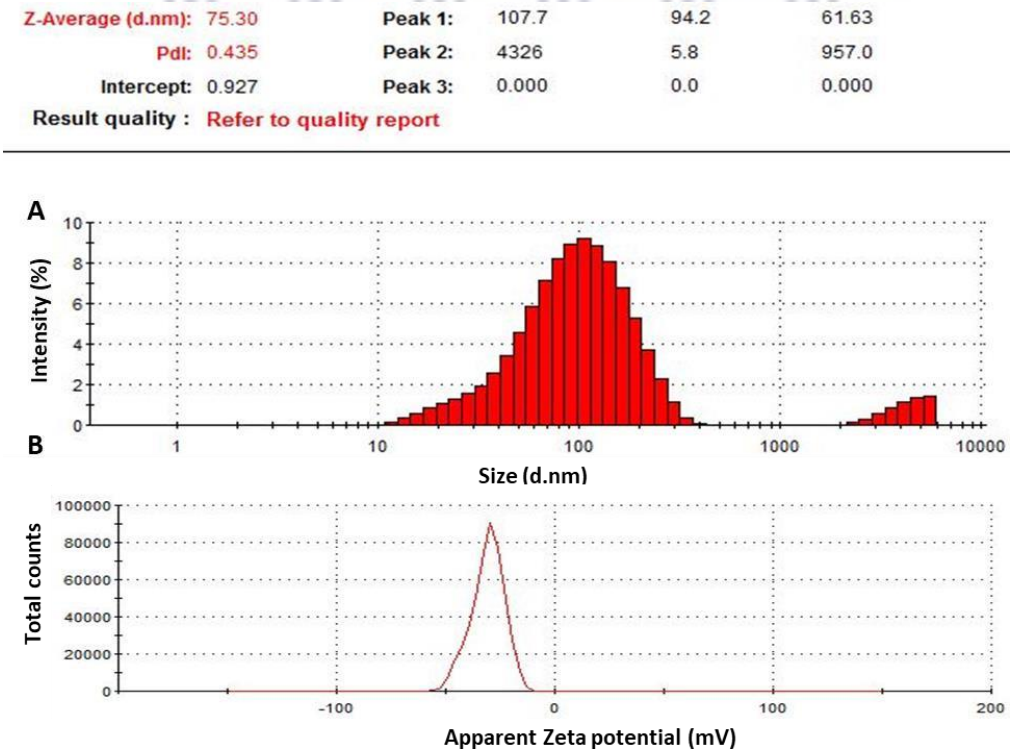

Figure 3.3: Characterization of CeFe-AuNPs using the dynamic light scattering technique. A: The hydrodynamic size distribution of aqueous CeFe-AuNPs (peak 1 = 94.2% and peak 2 = 5.8%). B: The zeta potential spectrum of CeFe-AuNPs.

3.1.3.2 High Resolution – Transmission Electron Spectroscopy

HR-TEM analysis revealed that the synthesised NPs have a spherical shape, and that they are mono-dispersed (**Figure 3.4**). These findings support the previously stated notion that a PDI value that is < 0.5 represents a sample that is homogenously dispersed. According to literature, the size and shape of the NPs is influenced by the plant and gold salt concentrations, as well as other variables such as temperature, pH, rotation per minute during mixing, and the reaction time (Sun and Xia, 2002). In order to determine the particle size distribution of the sample by HR-TEM, 50 CeFe-AuNPs were individually measured using the Image J software. The core diameter was calculated to be 16 ± 0.31 nm. Determination of the nanoparticle frequency in relation to their size, showed that the most occurring CeFe-AuNPs had a core size between 16 nm and 17 nm. DLS and HR-TEM are known to give varying results on the size of the same NPs. While HR-TEM measures the "true" core size of the AuNPs, DLS measure the hydrodynamic size which includes the metal core size, the organic molecules that may be present on the surface of the NP and any molecules present in the solvent which may have a tight association with the surface coating (Lim et al., 2013).

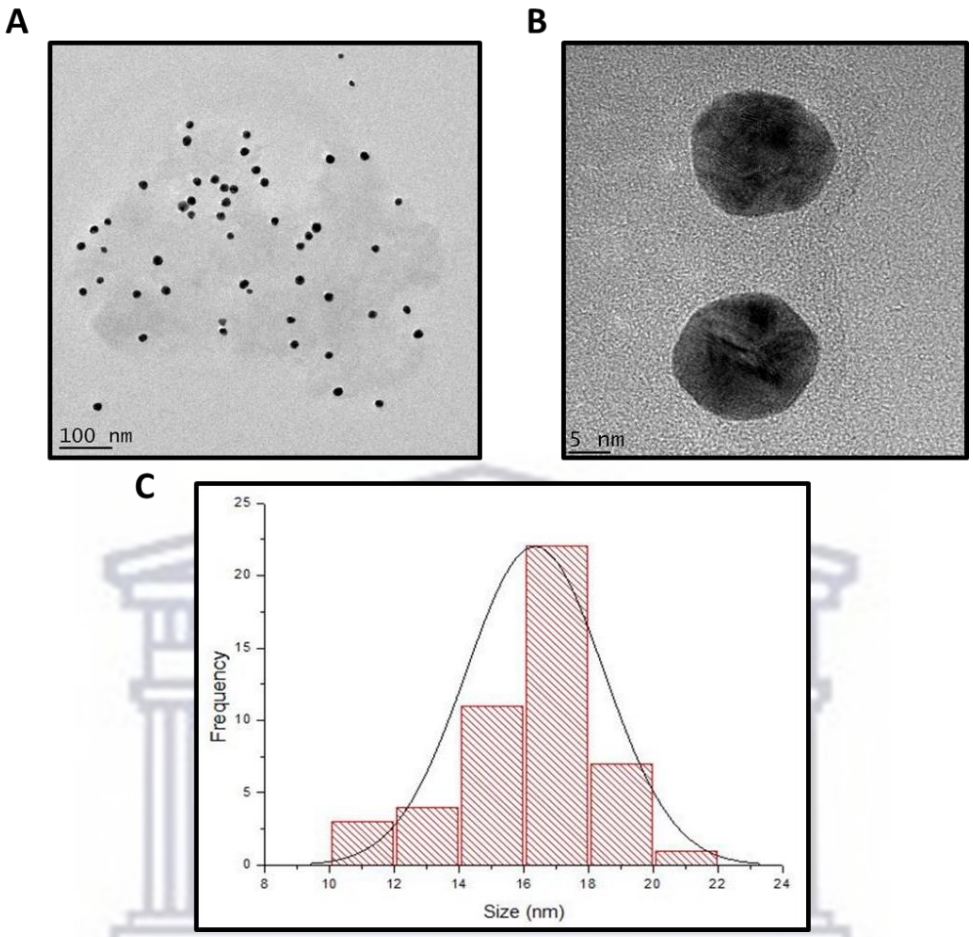

Figure 3.4: HR-TEM images showing the size and morphology of CeFe-AuNPs. A and B: Morphology of CeFe-AuNPs at a 100 nm and 5 nm scale. C: Histogram showing size distribution of CeFe-AuNPs, as determined by ImageJ software.

3.1.3.3 Identification of functional groups involved in the formation of CeFe-AuNPs

Fourier Transform Infrared (FTIR) spectroscopy is used to generate data concerning the local molecular environment on the surface area of NPs. Generally, FTIR is used to analyse the chemical composition of organic, inorganic or biological samples, minerals, polymers and paints (Devaraj et al., 2013). The FTIR spectra is divided into two sections, namely: the functional group region (4000 cm^{-1} – 1500 cm^{-1}) and the fingerprint region (1500 cm^{-1} to 400 cm^{-1}). While the functional group region remains relatively the same in many samples, the fingerprint region contains functional groups that are unique to each sample, and is thus used in the identification and/or verification of substances (Coates, 2006).

In this study, FTIR was conducted as a way of identifying biomolecules that may have been involved in the capping and reducing of Au^{3+} to Au^{0}, during the biosynthesis of CeFe-AuNPs. A variety of functional groups can be identified according their characteristic infrared absorption. As indicated in **figure 3.5**, CeFe displayed characteristic peaks at 1260.11, 864.16, 816.46, and 750.59 cm^{-1}; while CeFe-AuNPs showed characteristic peaks in the range of 2159.53, 1522.82, 1369.82 and 1146.55 cm^{-1}. The 1260.11 cm^{-1} peak could be representative of a C-N stretch, C-O stretch or a C-H wag. Due to its weak intensity, the peak could be more related to the C-H wag rather than the C-N or C-O stretch functional groups, which are often observed to display strong intensities. The peak at 864.16 cm^{-1} could be a result of the presence of the =C-H functional group, while the 816.46 and 750.59 cm^{-1} could be representative of the C-Cl functional group, which is assigned to alkyl halides. The characteristic peaks in CeFe-AuNPs: 2159.53, 1522.82, 1369.82 and 1146.55 cm^{-1}, are associated with C≡C alkynes, NO_2 stretch and C=C aromatic compounds, and the aliphatic amines C-N stretch, respectively (Coates, 2006, UCSC, 2006).

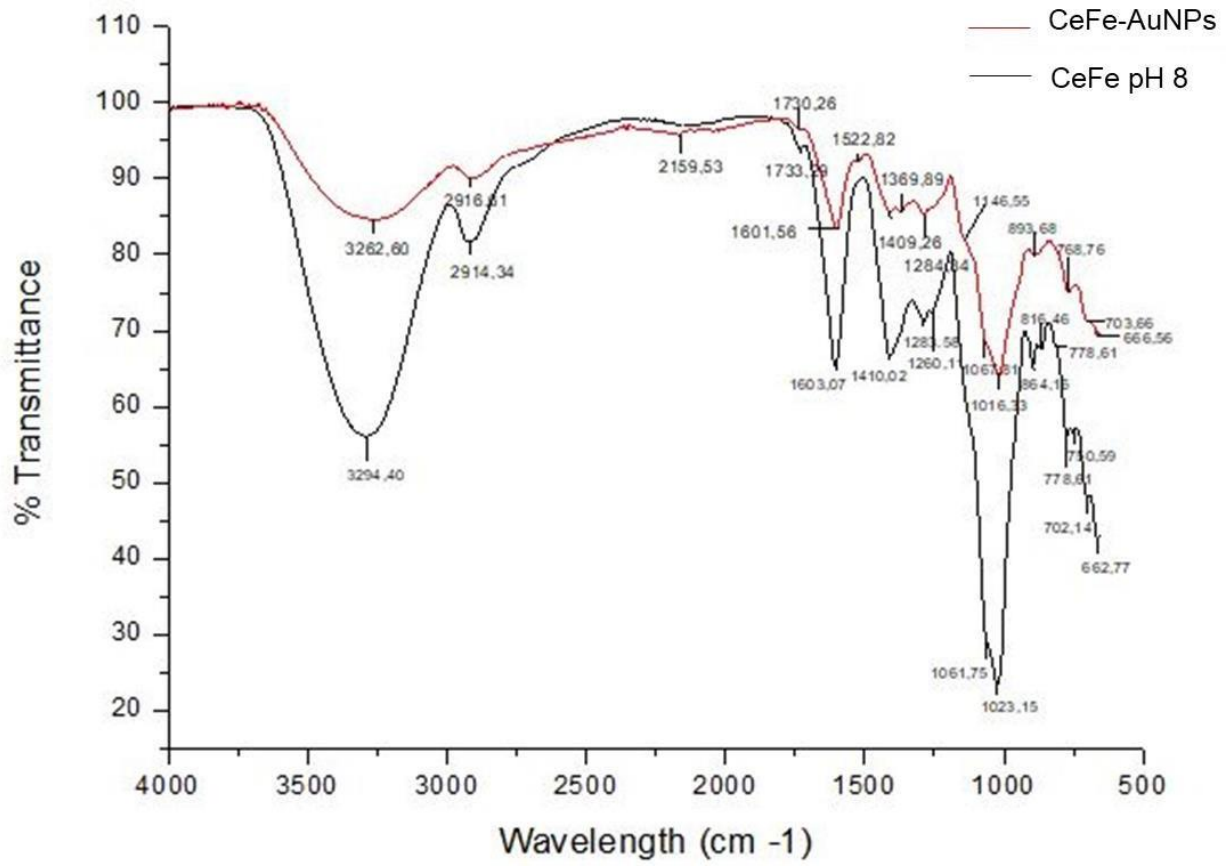

Figure 3.5: The FTIR spectrum of CeFe at pH 8 and CeFe-AuNPs.

Due to the numerous peaks that were visible in the fingerprint region, CeFe was noted to be a complex extract (**Figure 3.5**) (Coates, 2006). Fruits are generally known to contain a great variety of phenolic compounds that are associated with many health benefits, some of which are water soluble, and can be found in aqueous extracts (Haminiuk et al., 2012). It has been previously reported that the appearance of the same intensity peaks, representing the same functional groups, in both the extract and AuNPs, is an indication that the phytochemicals present in the extract may be responsible for the reduction and stabilization of the formed colloidal AuNPs (Das and Velusamy, 2014). Therefore, comparison of the functional group of CeFe and CeFe-AuNPs was performed.

Table 3.1 shows the functional groups that are shared by CeFe and CeFe-AuNPs. While FTIR cannot be used to provide definitive organic molecules that are involved in the formation of AuNPs, the technique can give an idea as to which functional groups partake in the biosynthesis. Analysis of the CeFe-AuNPs spectra revealed that alkyl and aryl halides, alcohols, ethers, carboxylic acids, aliphatic amines, primary and secondary amines, alkenes, alkynes and aromatics may have been involved in this biosynthesis. Major and minor shifts in the position of the absorption peak are said to be a result of the interaction between the phytochemicals and the present metal (Elia et al., 2014), which clearly indicates that there is an interaction between Au^{3+} and the phytochemicals present in CeFe, in order to form CeFe-AuNPs.

Table 3.1: Shift in the position of major CeFe peaks that are involved in the capping or reducing of CeFe-AuNPs

CeFe pH 8	CeFe-AuNPs	Shift in position (cm^{-1})	Peak range (cm^{-1})	Functional group
3294.40	3262.60	+31.8	3500 - 3200	O-H Stretch (Alcohols and phenols)
2914.34	2916.61	-2.27	2990 – 2850	C-H stretch (Alkanes)
1733.29	1730.26	+3.03	1740 – 1720	C=O stretch (Aldehydes)
			1750 – 1705	Ketones
1603.07	1601.58	+1.49	1650 – 1600	C=C (Alkenes)
			1625 - 1440	C=C (Aromatic compound)
1410.02	1409.26	+0.76	1000 - 1400	C-F stretch (Alkyl & Aryl halides)
1283.58	1284.34	-0.76	1335 -1250	C-N stretch (aromatic amines)
			1320 – 1000	C-O stretch (Alcohols, esters, ethers, Carboxylic
			1300 - 1150	acids)C-H wag (Alkyl halides)
1061.75	1067.81	-6.06	1320 – 1000	C-O stretch (Alcohols, esters, ethers, Carboxylic acids)
			1250 - 1020	C-N stretch (Aliphatic amines)
1023.15	1016.33	+6.82	1320 – 1000	C-O stretch (Alcohols, esters, ethers, Carboxylic acids)
896.71	893.68	+3.03	1000 – 650	=C-H bend (Alkenes)
			910 – 665	N-H wag (1º, 2º amines)
			900 - 675	C-H “oop” (Aromatics)
778.61	768.76	+9.85	1000 – 650	=C-H bend (Alkenes)
			910 – 665	N-H wag (1º, 2º amines)
			900 - 675	C-H “oop” (Aromatics)
702.14	703.66	-1.52	1000 – 650	=C-H bend (Alkenes)
			910 – 665	N-H wag (1º, 2º amines)
			900 - 675	C-H “oop” (Aromatics)
			700 – 610	-C≡C-H: C-H bend (Alkynes)
662.77	666.56	-3.79	1000 – 650	=C-H bend (Alkenes)
			910 – 665	N-H wag (1º, 2º amines)
			690 - 515	C-Br stretch (Alkyl halides)

3.1.3.4 Effect of various physiological media on the stability of CeFe-AuNPs

Good physicochemical stability is one of the most important features for NPs that are designed to have a biomedical application. Good physicochemical stability refers to the ability of NPs to preserve their composition, surface chemistry, size and shape, under various physiological conditions. Furthermore, these qualities are what define the effectiveness of the NPs, their shelf-life, and resistance to aggregation as a function of time (Phan and Haes, 2019). Since the biological impact of metal NPs is influenced by their oxidation state and the ligands attached to their surface, NPs that are prone to oxidation, or speciation, take on an unpredictable behaviour, and are thus known to induce cytotoxicity and/or genotoxicity in the experimental model (Auffan et al., 2009).

The physicochemical stability of CeFe-AuNPs was examined by incubating the NPs at 37 ºC in either 0.5 % BSA, 10 % NaCl, PBS or ddH_2O, over a 24 hours period (**Figure 3.6: A - D**). The samples were monitored for a blue colour change, as well as changes in their absorbance spectrum using UV-Vis spectrophotometry (PolarStar Omega microplate reader). CeFe-AuNPs that were incubated in 0.5% BSA were found to be stable and maintained a λ_{max} of 532 nm. CeFe-AuNPs incubated in PBS and those incubated in ddH_2O were also found to be stable and also maintained a λ_{max} of 532 nm, although a slight increase in absorbance was observed in the PBS experiment. CeFe-AuNPs incubated in 10 % NaCl were observed to undergo a blue-shift 24 hours after incubation.

Aggregation of NPs, in the presence of high ionic strength media, is associated with red-shifting (denoted by a colour change from ruby-red to blue NPs). A red-shift represents a lack of protection by the capping and stabilizing agents involved, thereby leading to particle size enlargement and precipitation due to the interaction between the NP surface area and the ions present in the solution. Analysis of this aggregated state, on a UV-Vis spectrophotometer, reveals an absorption spectra with longer wavelengths (Barreto et al., 2015). Contrary, when noble metal NPs experience a blue-shift, dipole coupling is said to have occurred (Jenkins et al., 2014). This phenomena results in the dispersion of NPs in alkali solutions, thus decreasing their wavelength (Tseng et al., 2015), as seen in the CeFe-AuNPs incubated in 10 % NaCl.

The stability or instability of NPs influences their proneness to aggregation, their bio-distribution, pharmacokinetic properties, and their degree of systemic toxicity. NPs that undergo aggregation are also inclined to being cleared by the RES, thus hindering their ability to reach their therapeutic

target, in so doing reduces their efficacy (Moore et al., 2015). Therefore, the relative stability of CeFe-AuNPs shows that the phytochemicals involved in their capping and stabilization fully protects their surface area, thus leaving no area for additional ligands to bind and disrupt their composition. This lack of aggregation also suggests that CeFe-AuNPs are good candidates for *in vitro* and *in vivo* experiments.

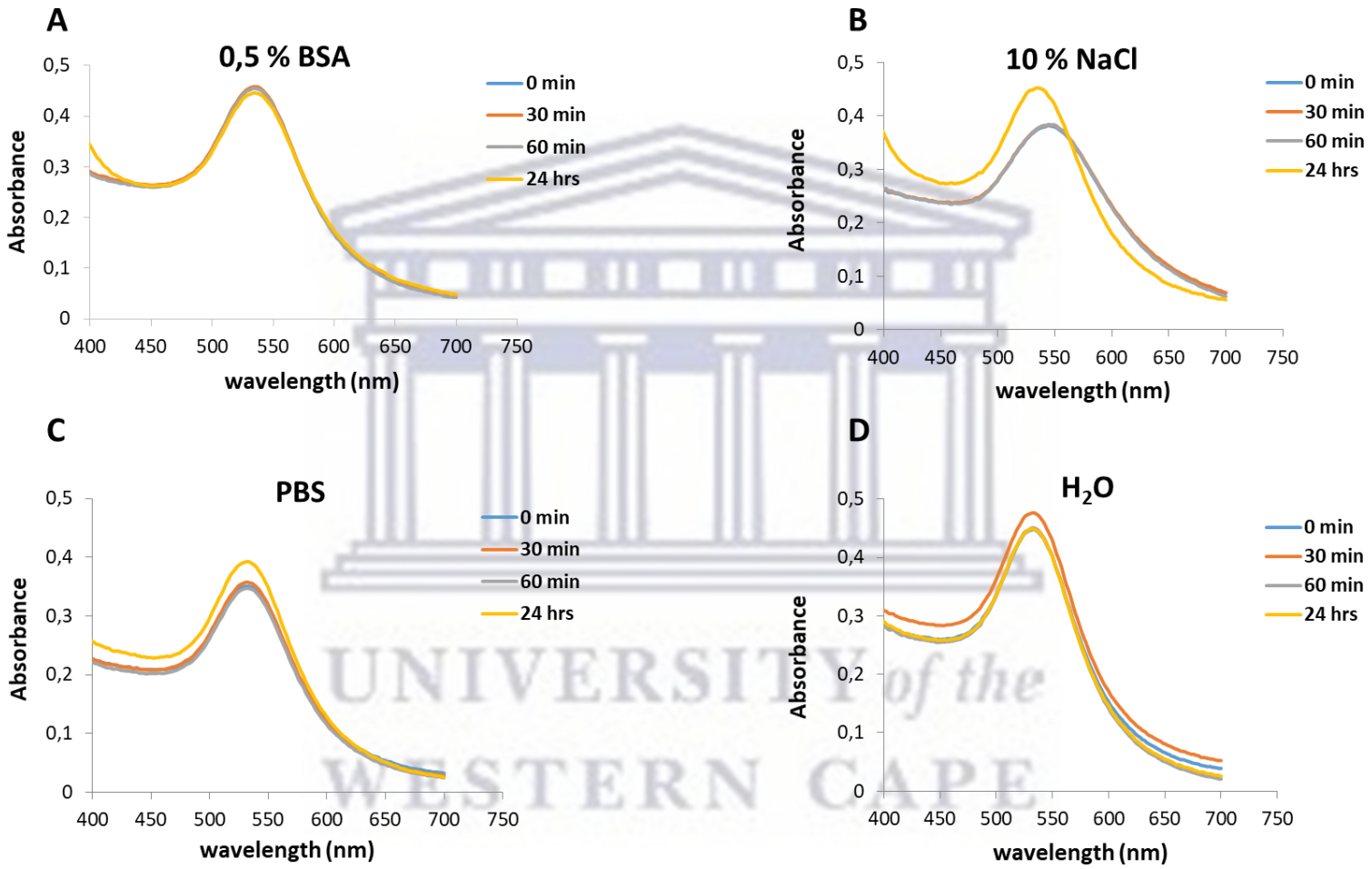

Figure 3.6: Stability of CeFe-AuNPs in various physiological media over 24 hours: A) Absorbance spectra of CeFe-AuNPs incubated in 0.5 % BSA, B) Absorbance spectra of CeFe-AuNPs incubated in 10 % NaCl, C) Absorbance spectra of CeFe-AuNPs incubated in PBS, and D) Absorbance spectra of CeFe-AuNPs incubated in H_2O.

3.2 Biomedical application of CeFe and CeFe-AuNPs

3.2.1 Introduction

Opposed to the non-diabetic population, diabetic people have a 3-fold likelihood of being hospitalized. Furthermore, hyperglycemia is reported in 22 – 46% of non-critically ill patients. Inpatients that develop hyperglycemia are at an increased risk for complications, ICU admission, home-nursing, and mortality. Experiencing hyperglycemia can also increase the chances of developing diabetes later on in life (Corsino et al., 2017). Accordingly, the successful management of BGL is of utmost importance, in both diabetic and non-diabetic patients. The combined efforts of a healthy diet, regular exercise and pharmaceutical drugs are the major role players in the management of BGL in diabetic patients (White, 2014). Available pharmaceutical drugs are known to cause serious side effects, and as such, create an urgent need for the discovery and development of non-toxic and efficient alternative medicines (Saghir et al., 2020).

Due to its abundant availability, easy accessibility, and prominent use in many regions of the world, phytotherapy has been identified as an effective treatment method that displays less toxicity compared to conventional drugs, and also bridges the financial gap that is imposed by these drugs. Conventional drugs go through vigorous manufacturing processes which later render them expensive; while medicinal plants are often home-grown and normally require boiling in water in order to extract the phytocompounds (Governa et al., 2018; Kasole et al., 2019). Nonetheless, the effectiveness of phytotherapy is still limited by the inadequate separation of therapeutic and toxic phytocompounds during the extraction process. Moreover, the self-dosing approach of this therapy may lead to liver toxicity (Del Prete et al., 2012; Laccourreye et al., 2017).

To develop safer dosage regimens, much research is being conducted in phytotherapy for DM treatment. *Capparis spinosa* leaf extract has been previously described as a phytotherapy that has the ability to significantly lower serum glucose and normalize the lipid profile of STZ-induced diabetic rats after 28 days of treatment. However, this extract was unable to increase insulin levels (Kazemian et al., 2015). *Afzelia africana* stem extract was found to decrease serum glucose in STZ-induced rats, as well as improve their hematological parameters after 10 days of treatment (Oyedemi et al., 2011). Most promising is the *Gymnema sylvestre* plant which has been studied for many years, however has been hindered by insufficient understanding on how to best combine its therapeutic phytochemicals (Ghorbani, 2013; Governa et al., 2018; Sarker et al., 2019).

The incorporation of nanotechnology into plant-based medicines is believed to improve the efficacy of phytotherapy. It does this by decreasing the required dose, overall toxicity and increasing the bioavailability of the active compounds (Gunasekaran et al., 2014). This improved performance is attributed to the large surface area to volume ratio of the NPs, which allows for the binding of different functional groups, and their small size, which allows them to withstand degradation and escape phagocytosis by the RES (Bonifácio et al., 2014).

In this chapter, the *in vitro* and *in vivo* anti-hyperglycemic effects of CeFe-AuNPs are described. In order to predict the response of a therapeutic drug in a human system, pre-clinical experiments must be conducted. The aim of this is to determine the ideal dosing concentration of the drug, its toxicity, and how it compares to drugs that are already in use. In this study two models viz., *Saccharomyces cerevisiae* and *Rattus Novergicus*, Wistar strain, were used as experimental organisms for *in vitro* and *in vivo* studies, respectively.

3.2.2 Effects of CeFe and CeFe-AuNPs on the glucose uptake by yeast cells

The use of *Saccharomyces cerevisiae* as a model for testing the anti-hyperglycemic effects of various phytocompounds is progressively becoming an accepted technique (Cirillo, 1962; Sairam and Urooj, 2012; Bhutkar and Bhise, 2013; Saghir et al., 2020). Therefore, in this study, yeast cells were used as a model to determine the effects of CeFe-AuNPs on the uptake of glucose. The experiment was carried out by subjecting yeast cells to varying concentrations of glucose (5 mM, 10 mM and 25 mM), together with varying concentrations of CeFe or CeFe-AuNPs (1.56 mg/ml – 100 mg/ml), and glucose uptake was determined using the DNS method.

Although *S. cerevisiae* transports glucose via a complex mechanism, it is generally stated that the mode of glucose transportation is through a facilitated diffusion mechanism. Because of this, the amount of glucose that is present in the media, after a period of time, is said to be representative of the glucose taken up by the yeast cell (Smits et al., 1996; Sairam and Urooj, 2012). Facilitated carriers enforce a system in which solutes are transported through a concentration gradient, thus emphasizing that an effective glucose utilization process is one where intracellular glucose is effectively reduced (Teusink et al., 1998; Pitchaipillai and Ponniah, 2016).

Treatment of yeast cells with CeFe increased glucose uptake activity by 58 – 84 %, 58 – 64 %, and 0.2 – 55 %, in the 5, 10, and 25 mM glucose reactions, respectively. High CeFe concentrations

were observed to induce a statistically significant decrease in glucose uptake activity. Even with the decrease, glucose uptake activity still ranged above 50 % (**Figure 3.7: A - C**). Plants naturally contain toxic secondary metabolites, which they use as phytoprotectants (Ifeoma and Oluwakanyinsola, 2013); therefore, the observed decrease in activity could be alluded to a potential increase in the response triggered by these phytoprotectants, such that they begin to overshadow the effects of the therapeutic compounds (Kumari et al., 2012).

The best results were observed in the 5 mM glucose reaction, where three CeFe concentrations (1.56 mg/ml, 3.125 mg/ml and 6.125 mg/ml) were able to prompt a significantly high glucose uptake activity in the yeast cells (**Figure 3.7: A**). Considering the lack of statistical significance between 1.56 mg/ml, 3.125 mg/ml and 6.125 mg/ml concentrations, it can be assumed that CeFe may have the same effect when administered at these concentrations. In the 10 mM glucose reaction, CeFe was observed to be most active between 1.56 mg/ml and 12.5 mg/ml (**Figure 3.7: B**). While both CeFe and CeFe- AuNPs seemed to induce a linear increase in glucose uptake in the 25 mM glucose reaction, the results were not statistically different from each other (**Figure 3.7: C**). It has been reported that, at this glucose concentration, uptake activity decreases due to glucose transporters being saturated, and as such a drive to establish equilibrium between intracellular and extracellular glucose is experienced (Saghir et al., 2020).

Treatment of yeast cells with CeFe-AuNPs increased the glucose uptake by 7 – 43 %, 8 – 48 %, and 4 – 62 % in the 5, 10, and 25 mM glucose reactions, respectively (**Figure 3.7: A - C**). The lowest concentration of CeFe-AuNPs, 1.56 mg/ml, did not exhibit any activity in all 3 glucose concentrations, and 6.125 mg/ml of CeFe-AuNPs also did not demonstrate any activity in 5 mM glucose reaction (**Figure 3.7: A – C**). There was no statistical significance observed between the glucose uptake responses induced by CeFe-AuNPs at concentrations 1.56 mg/ml – 12.5 mg/ml, in both the 5 mM and 10 mM glucose reactions (**Figure 3.7: A; Figure 3.7: B**). This suggested that CeFe-AuNPs may only be able to improve glucose uptake at higher concentrations (> 12.5 mg/ml). Conversely, 100 mg/ml CeFe-AuNPs did not increase glucose uptake activity in the 5 mM glucose reaction (**Figure 3.7: A**). It is possible that a statistically significant increase in glucose uptake activity may only be induced every 3-fold increase in CeFe-AuNPs concentration, considering that there was also no statistical significance observed in both the 1.56 mg/ml – 12.5 mg/ml and 25 mg/ml – 100 mg/ml concentration ranges (**Figure 3.7: A; Figure 3.7: B**). Additionally, at 50

mg/ml, CeFe-AuNPs may begin to cause saturation of the yeast cell receptors that they interact with, such that an increase in CeFe-AuNPs does not have an effect on glucose uptake activity. At this concentration, CeFe-AuNPs may also be displaying toxicity towards the yeast cells, e.g.: hindering growth of the yeast cells or inducing death. To better understand these response variabilities, further experimentations need to be conducted. Nevertheless, zinc oxide (Shwetha et al., 2020) and silver (Yakoob et al., 2016) biogenic NPs have been reported to induce a linear glucose uptake that is comparable to that of a standard drug.

Like CeFe, CeFe-AuNPs were observed to induce the most activity in the 5 mM glucose reaction; however, CeFe induced the highest glucose uptake activity, (**Figure 3.7: A**). Increase in glucose concentration (5 mM, 10 mM and 25 mM) was observed to cause a decrease in glucose uptake activity in both CeFe and CeFe-AuNPs treated yeast cells. Both these trends have been reported before (Sairam and Urooj, 2012; Bhutkar and Bhise, 2013). Additionally, it was suggested that the successful mediation of glucose uptake in yeast cells could be due to both facilitated diffusion and elevated glucose metabolism (Rehman et al., 2018). This could further imply that CeFe and CeFe-AuNPs could possibly enhance glucose uptake in the muscle cells and adipose tissue, which may result in anti-hyperglycemic properties.

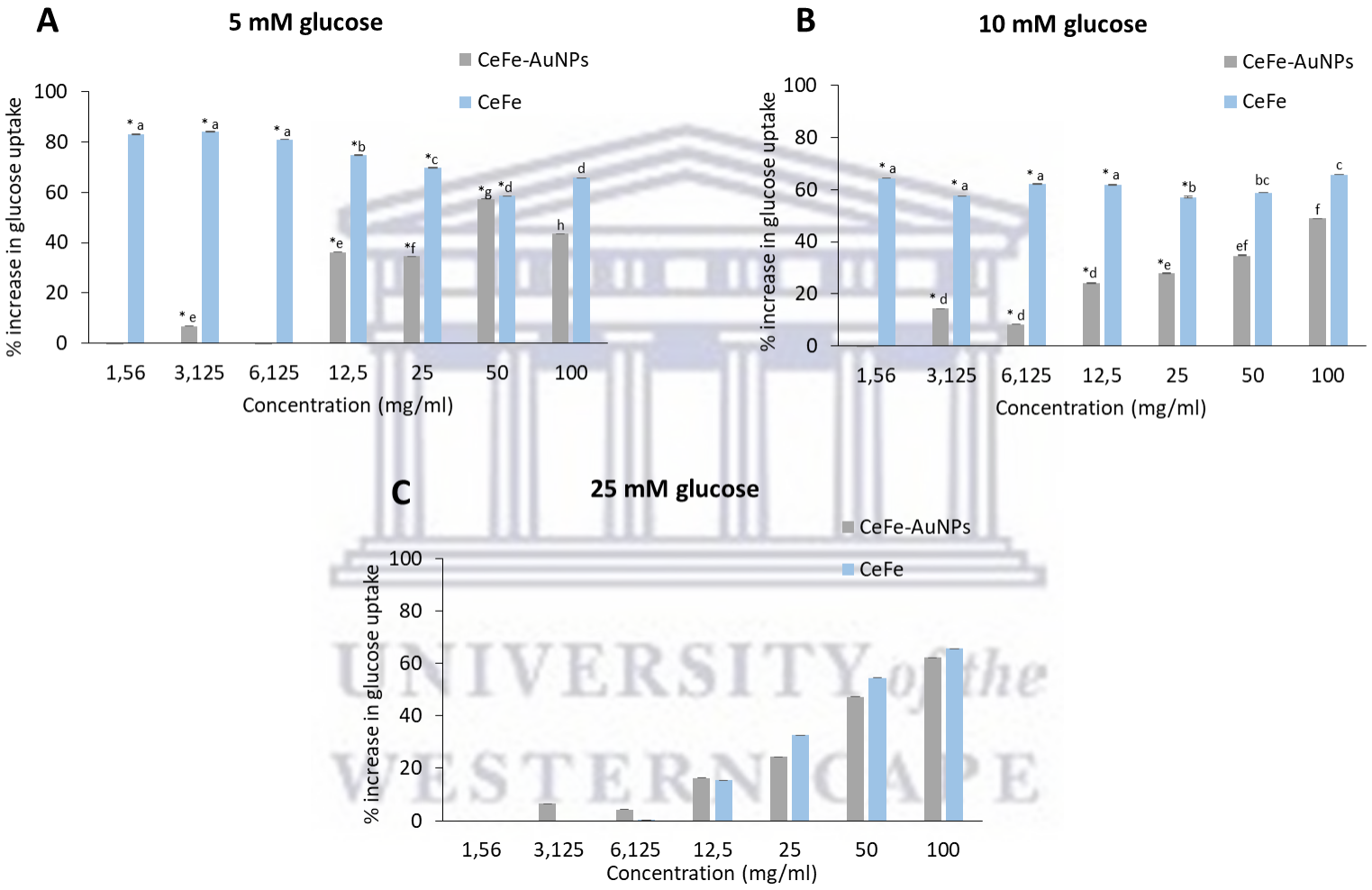

Figure 3.7: The effect of CeFe and CeFe-AuNPs on the glucose uptake by yeast cells. The concentrations that were investigated ranged from 1.56 mg/ml to 100 mg/ml. Experiments were carried out in triplicates and error bars are represented as mean ± SEM. Bars with different letters are statistically different to each other at $p < 0.05$. Asterisk (*) represents statistical difference between CeFe and CeFe-AuNPs at $p < 0.05$.

3.2.3 *In vivo* acute toxicity effects of CeFe and CeFe-AuNPs

Medicinal plants are known to house a variety of therapeutic phytochemicals, namely: flavonoids, alkaloids, steroids, terpenoids, glycosides and quinones. Because medicinal plants are naturally occurring, they are generally deemed safe for consumption. However, this is not always guaranteed, since plants exhibit a duality of both toxic and non-toxic phytochemicals (Mlozi et al., 2020). *Tephrosia vogeli* is one such plant, it is used to treat skin diseases, constipation and as a purgative. Similarly, this plant is used as an insecticide and in the making of poison-arrows used in fishing and hunting (Orwa C et al., 2009). Due to genetic conservation between taxa, phytochemicals that are designed to protect plants from herbivorous predators can cause neurological damage in humans, and these include some of the therapeutic compounds (Ifeoma and Oluwakanyinsola, 2013). Nonetheless, some phytotoxicities have been reported as being reversible, while other phytotherapies did not display any organ toxicity (Tchuente, 2018).

AuNPs form a part of the most used NPs in biomedical sciences. This is owed to their reigning stability and biocompatibility. Nevertheless, it is important to have a knowledge of their toxicity as this could assist in the development of better dosage strategies, and in avoiding the use of therapeutics that may have lethal effects (Bahamonde et al., 2018; Singh et al., 2019). The *in vivo* investigation of nanotoxicity enables researchers to monitor the long-term effects of NPs within the experiment model, their tissue localization, biodistribution, and their retention and excretion. *In vivo* tests mainly focus on blood serum chemistry, cell populations, histopathological changes in the tissues, and nanoparticle biodistributions (Marquis et al., 2009; Kaufmann and Jacobsen, 2020). Herein, focus is drawn to the changes in BWs, tissue weights and tissue histopathology.

One of the key interests of this study was not only to develop a drug that has a high efficacy and is highly effective, but also one that would also increase patient compliance. As such, an oral route of administration was selected. Acute oral toxicity was determined via the up and down procedure, as detailed in the 425 OECD guidelines (OECD, 2008). After a single-dose administration of jelly cubes containing 2000 mg/kg, the rats were observed daily for a period of 14 days, for signs of toxicity, namely: loss of appetite, change in fur colour, fatigue, weight loss, or death (BarathManiKanth et al., 2010). No signs of toxicity, abnormal behaviour or mortality were observed throughout the study. This served as preliminary evidence that a single oral dose of 2000 mg/kg CeFe, CeFe-AuNPs and CeFe-AgNPs was safe to administer (Umrani and Paknikar, 2014).

The organs of interest were selected on the basis of them either being major organs, being the target site for DM, or their involvement in NP clearance; these include the heart, pancreas, spleen, liver and kidney. As shown in **figure 3.8**, CeFe, CeFe-AuNPs and CeFe-AgNPs had no effect on the BWs of the animals, as they remained comparable between the treatment groups. **Table 3.2** shows that the organ weights were comparable to those of the control group, except for the pancreas in the CeFe-AuNPs group. A close inspection of this data revealed that two animals in this group had pancreas weighing 0.7 g, while others weighed 1 g. This may have been an error that resulted during dissection, or the natural weights of the pancreas, considering how their histology did not show any signs of pathology (**Table S1; Figure S6**), and there was no statistical significance when compared to the control ($p = 0.07$). Histopathology analysis the treatment groups did not display any signs of toxicity and were comparable to those of the control group (**Figure 3.9**).

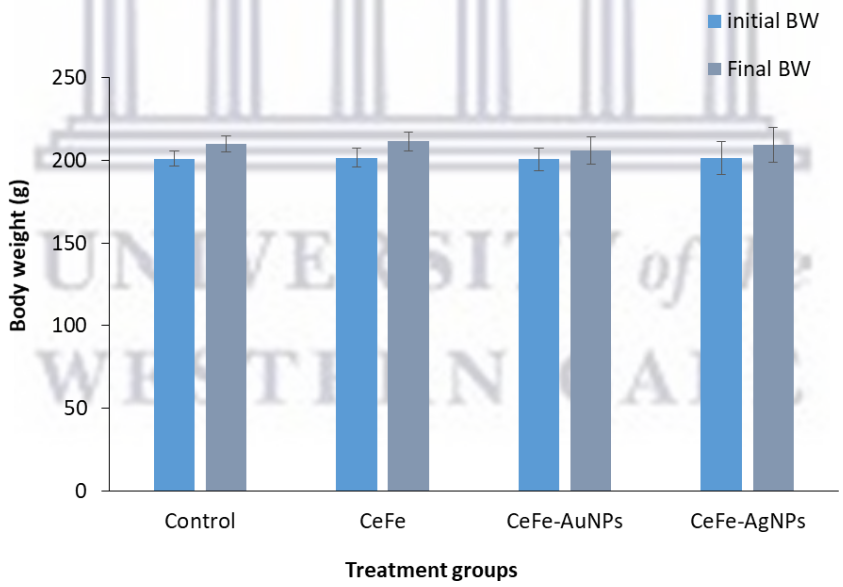

Figure 3.8: Effect of CeFe, CeFe-AuNPs and CeFe-AgNPs on the BW of female Wistar rats after 14 days. The data is expressed as mean ± SEM (n = 6).

Table 3.2: Tissue weights of the rats 14 days after administration of treatments.

Organ	Control	CeFe	CeFe-AuNPs	CeFe-AgNPs
Liver	5,975 ± 1,195	5,6852 ± 1,137	5,9286 ± 1,186	5,909 ± 1,182
Kidney	1,512 ± 0,302	1,4278 ± 0,286	1,4818 ± 0,296	1,4982 ± 0,230
Spleen	0,4846 ± 0,097	0,5066 ± 0,101	0,48 ± 0,096	0,5142 ± 0,103
Pancreas	1,1142 ± 0,222	1,107 ± 0,221	0,8928 ± 0,179	1,2318 ± 0,246
Heart	0,6498 ± 0,129	0,6038 ± 0,121	0,6314 ± 0,126	0,6058 ± 0,121

Data is presented as mean ± SEM (n = 6).

While chemically synthesised AuNPs have been reported to damage cardiac tissue, depending on their size (10, 20 or 50 nm) and duration of exposure (3 or 7 days) (Abdelhalim, 2011), another study reported their accumulation in various major organs, and causing death in rats (Bahamonde et al., 2018). However, analysis of the histology sections from the latter study did not reveal any signs of pathology, namely: fibrosis, which is characterized by an increased presence of connective tissue; inflammation, which is characterized by an influx in macrophages; and dilated or constricted blood vessels, which are characterized by red blood cell congestion, or the lack thereof (Shanker et al., 2017b).

Instead, the heart muscles cells (myocardium) were seen to display a characteristic long and flat shape with a defined parallel direction (Abdelhalim, 2011). The islets of Langerhans, in the pancreas, were intact and well granulated (Liggitt and Dintzis, 2018). The white and red pulp of the spleen where clearly distinguishable and were not invaded by erythrocytes (Abbott et al., 2004; Suttie, 2006). The liver was observed to have central veins with consistent sinusoids, healthy hepatocytes and intact portal tracts (Cardona, 2011; Krishna, 2013). The glomerulus capsule in the kidney was also found to be intact, and its tubules exhibited a normal architecture (Bachmann et al., 1986; Sangle, 2012; Madrazo-Ibarra and Vaitla, 2020) (**Figure 3.9; Figure S2 – S6**). The findings of this study corroborated those of another investigation that applied *Chamaecostus cuspidatus* biogenic AuNPS for the treatment of T2DM and wound healing (Ponnanikajamideen et al., 2019). Furthermore, the lack of significant pathological effects in these tissues shows that these NPs are coated by non-toxic phytochemicals, thus demonstrating their overall safety (Shanker et al., 2017b). Nonetheless, further investigations need to be carried out to determine their biodistribution and excretion.

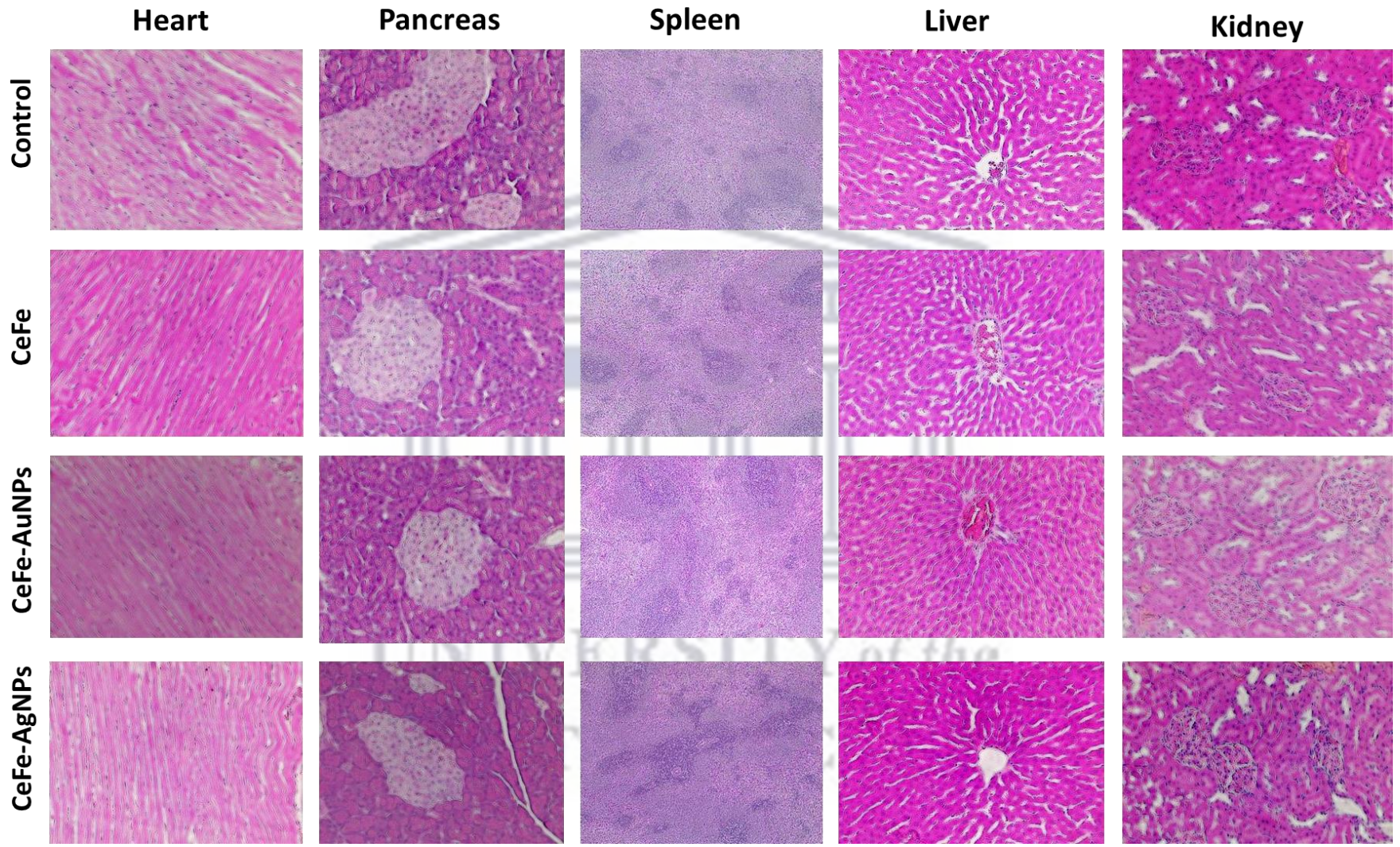

Figure 3.9: Histopathological examination of female Wistar rats' heart, pancreas, spleen, liver and kidney of the control group, CeFe, CeFe-AuNPs and CeFe-AgNPs treatment groups, after 14 days of observation following the administration of jelly cubes containing 2000mg/kg of the various treatments.

3.2.4 *In vivo* anti-diabetic effect of CeFe and CeFe-AuNPs

Streptozotocin (STZ) is a chemical predominantly used to study *in vivo* induction of diabetes when seeking to study the disease's mechanism or screen novel drugs for their anti-diabetic potential. This method is frequently used because it produces a diabetic model that is clinically similar to human diabetes (Furman, 2015). Although STZ damages numerous organs that express GLUT2, its bioaccumulation is mainly in the pancreas. This accumulation of STZ leads to the destruction of β-cells, which in turn cause a severe decrease in insulin production, hence increased BGL (Goyal et al., 2016). In this study, 60 mg/kg of freshly prepared STZ was used to ablate pancreatic β-cells thereby inducing hyperglycemia. Thereafter, the effects of CeFe and CeFe-AuNPs on BGL (**Figure 3.10**), BWs (**Figure 3.11**), relative progress in hyperglycemia (**Figure 3.12**), tissue weights (**Table 3.3**), pancreatic islet cells (**Figure 3.13**), and serum insulin (**Figure 3.14**) was analyzed. Since female rats are less sensitive to STZ, male rats were used for this section of the study (Furman, 2015).

3.2.4.1 Effects of CeFe and CeFe-AuNPs on blood glucose and bodyweight

Single high-dose STZ diabetic models are commonly characterized by hyperglycemia (high BGL) and rapid weight loss (low BW), which result from insulin deficiency and muscle-wasting elicited by the chemical (Guo et al., 2020). In this study, all animal groups that were injected with STZ were found to display some degree of hyperglycemia (17.2 ± 0.83 mmol/L) when compared to the non-diabetic control (NDC) (**Figure 3.10; Figure S7**). A progressive decline in BWs was also observed (**Figure 3.11; Figure S8**). Conversely, not all animals followed the "high-BGL, low-BW" trend often seen in a STZ diabetic model (Deeds et al., 2011; Gupta and Saxena, 2011; Furman, 2015; Shanker et al., 2017a; Shanker et al., 2017b).

Seven (7) days after STZ injection, 4 of the animals in the diabetic control (DC) group were observed to experience a spontaneous decrease in their hyperglycemic status; the 2 remaining animals maintained a severe hyperglycemic condition for the rest of the study (**Figure S7**). This outcome was problematic in that experimental controls are used to set a benchmark in which to compare the results of the primary experiment (Johnson and Besselsen, 2002). While NDC animals were observed to behave like normal and healthy Wistar rats, maintaining a constant BGL throughout the study (**Figure 3.10**), and displaying a linear increase in BW, which was due to their natural growth (**Figure 3.11**), as previously stated, much of the DC animals did not develop a

severe hyperglycemia, thus this group could not be considered a good benchmark for STZ-induced diabetes. The DC animals were also observed to gain as much weight as the NDC, further reiterating that the DC was indeed a weak control, and did not display the natural progression of STZ induced DM (**Figure 3.11; Figure S8**).

Due to the random ablation of β-cells by STZ, lower doses (40 – 75 mg/kg) have been implicated in inducing the most varied degrees of hyperglycemia, while higher doses (> 75 mg/kg) are most likely to cause animal mortality (Goyal et al., 2016). STZ has also been reported to induce varying degrees of hyperglycemia in rodents that were age or gender matched, regardless of them being an inbred or outsourced strain. These challenges present difficulties with reproducibility, thus leading to the variations observed in this study (Deeds et al., 2011).

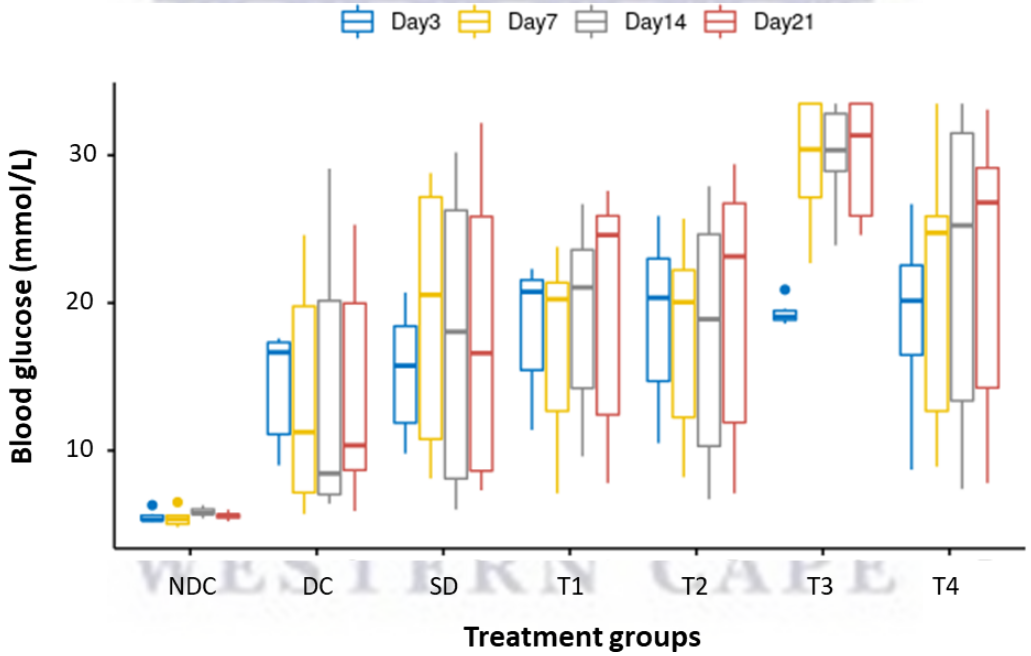

Figure 3.10: Effect of CeFe and CeFe-AuNPs on the blood glucose of male Wistar rats (n = 6). NDC: non-diabetic control, DC: Diabetic control, SD: 250 mg/kg metformin standard drug, T1: 200 mg/kg CeFe, T2: 400 mg/kg CeFe, T3: 100 mg/kg CeFe-AuNPs and T4: 200 mg/kg CeFe-AuNPs. Day 3: 3 days after STZ administration and day 1 of treatment with either T1, T2, T3 or T4. Day 7, 14 and 21: 7, 14 and 21 days after treatment.

Between day 3 and day 7 after STZ-injection, 4 of the 6 animals in the 250 mg/kg metformin standard drug (SD) treatment group maintained severe hyperglycemia while the remaining 2 experienced a mild hyperglycemia. In the 200 mg/kg CeFe (T1), 400 mg/kg CeFe (T2) and 200

mg/kg CeFe-AuNPs (T4), 5 of the 6 animals maintained severe hyperglycemia between day 3 and day 7, and the remaining animals experienced a mild hyperglycemia which is postulated to be caused by a natural recovery from severe hyperglycemia. All the animals in the 100 mg/kg CeFe-AuNPs (T3) maintained severe hyperglycemia throughout the study (**Figure 3.10; Figure S7**).

Administration of the metformin standard drug also proved challenging in that the rats would not completely consume the jelly cubes, due to the bitter taste of the metformin, thus ingesting a lower dose than intended. Considering that metformin is the go-to drug for the treatment of DM, it is safe to assume that the BGL and BWs of SD could have resembled those of the NDC (**Figure 3.11; Figure S8**). Observations of a mild and consistent decrease in BGL, as well as a mild increase in BW, between days 14 and 21, also support this hypothesis (**Figure 3.10; Figure 3.11**). Similar studies using either metformin (Shanker et al., 2017a; Shanker et al., 2017b) or glibenclamide (Ponnanikajamideen et al., 2019) as a standard drug have reported increase in BWs and normalization of blood glucose to a level that resembles that of their NDC groups.

Furthermore, for successful induction of diabetes, using 40 – 65 mg/kg STZ dosage, the preferred bodyweight of Wistar rats is between 150 g and 200 g (Cunha et al., 2009; Furman, 2015; Goyal et al., 2016; Shanker et al., 2017a; Shanker et al., 2017b; Ponnanikajamideen et al., 2019). While the initial proposal was to use animals weighing 150 g – 180 g, all rats weighed between 260 g and 390 g by the time they reached the recommended minimum experimental age of 8 weeks (Furman, 2015). The larger BWs could have influenced the bioavailability of STZ, thereby influencing the degree of hyperglycemia obtained (since larger organs are more likely to express more of the GLUT2 compared to smaller organs). Intravenous injection of STZ has been reported to give a more reproducible STZ model compared to i.p injection (Deeds et al., 2011).

In addition to exhibiting the highest BGL, T3 animals also experienced the most severe weight loss (**Figure 3.11**). Two animals (rat 32 and 33) in this group experienced a mild weight gain (4.5 g and 6.5 g) (**Figure S8**); however, judging from their hyperglycemic status (25.83 ± 3.63 mmol/L and 28.05 ± 2.97 mmol/L, respectively), this weight gain was attributed to their natural growth and not the effects of the treatment. The continuous weight loss and severe hyperglycemia (**Figure 3.10; Figure 3.11**), in T3 animals, indicated that 100 mg/kg CeFe-AuNPs do not induce any therapeutic effects on STZ-induced diabetic rats. A previous study reported that the lack of BGL normalization and increase in BW, was an indication that the *Chamaecostus cuspidatus* plant

extract had no therapeutic effects on STZ-induced diabetic albino rats (Ponnanikajamideen et al., 2019).

T4 animals followed a trend similar to T3 animals; however, 2 of the rats in this group (40 and 42) were observed to experience considerable weight gain (23 g and 45 g, respectively) (**Figure S8**). Similarly, each animal's weight gain was attributed to their low hyperglycemic state (rat 42; 9.50 ± 0.46) or potential natural recovery (rat 40; 9.98 ± 1.97). Between day 3 and 7, rat 40 was observed to move from a BGL of 16 mmol/L to 9 mmol/L, which is a change that was not observed in any of the other animals (**Figure S7**). Rats that develop mild hyperglycemia, induced by STZ, have been reported to experience β-cell regeneration. The β-cells of rats with severe hyperglycemia, were observed to continue deteriorating (Cheng et al., 2017). As such, the low hyperglycemic status of these rats may have influenced their weight gain.

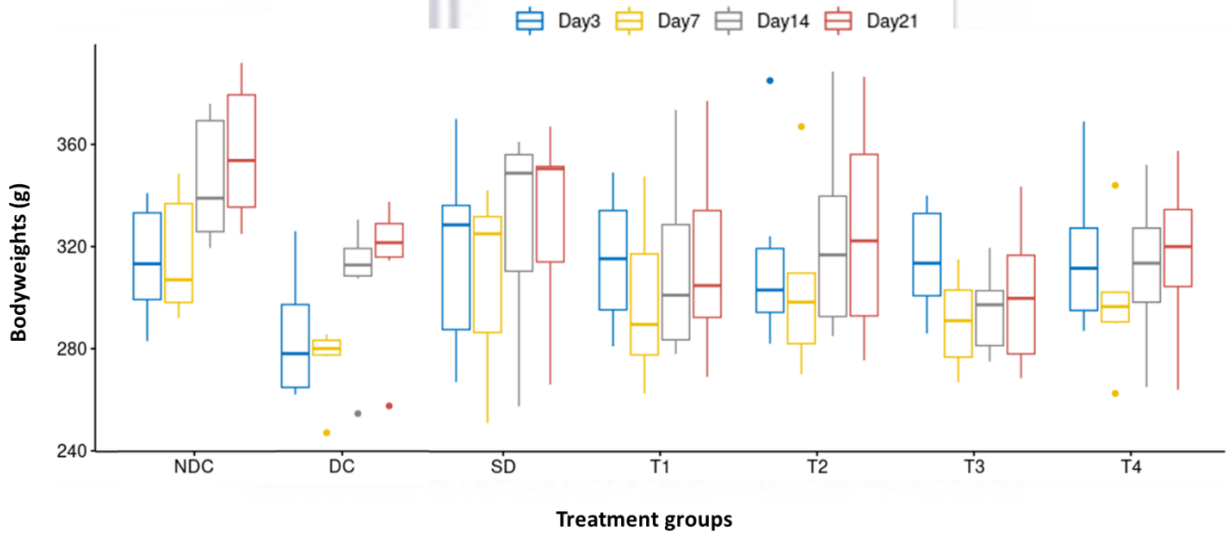

Figure 3.11: Effects of CeFe and CeFe-AuNPs on the bodyweights of male Wistar rats (n = 6). NDC: non-diabetic control, DC: Diabetic control, SD: 250 mg/kg metformin standard drug, T1: 200 mg/kg CeFe, T2: 400 mg/kg CeFe, T3: 100 mg/kg CeFe-AuNPs and T4: 200 mg/kg CeFe-AuNPs. Day 3: 3 days after STZ administration and day 1 of treatment with either T1, T2, T3 or T4. Day 7, 14 and 21: 7, 14 and 21 days after treatment.

T1 animals displayed a spectrum of responses: 2 of the animals (rat 23 and 24) experienced mild weight gain (6 g and 9 g, respectively) (**Figure S8**); of these, rat 23 experienced a severe hyperglycemia (22.33 ± 1.76 mmol/L), while rat 24 experienced a mild hyperglycemia (10.95 ±

1.27 mmol/L). Conversely, the decline in BGL of rat 24 was thought to be a result of the treatment since the decrease in BGL was steady and not as abrupt as the one observed in the DC group, or in rat 19 (48 g weight gain, 9.20 ± 0.9 mmol/L hyperglycemic status) of the same group. Rat 21 presented as an outlier in that it was both very hyperglycemic (21.9 ± 0.6 mmol/L) yet still experienced a relatively large weight gain (14 g) (**Figure S8**). This could have been a result of the animal's natural growth, since NDC animals gained an average weight of 42.83 ± 2.70 g. This weight gain could have also been a result of CeFe, considering that MANOVA analysis revealed that the various treatments used in this study could have had independent influences BGL and BW (Wilk's $\lambda = 0.198$, $p = 0.0132$). However, further investigations would have to be performed to confirm this hypothesis.

T2 animals were observed to follow a similar trend as T1 animals, where 2 rats (rat 25 and 30) were observed to experience a mild weight gain (1.5 g and 9.5 g, respectively), which was attributed to their natural growth since these rats remained hyperglycemic throughout the study (20.95 ± 0.76 mmol/L and 24.73 ± 0.78 mmol/L, respectively). Furthermore, 2 rats (27 and 29) were observed to experience and immense weight gain (23.5 g and 67 g, respectively). As in rat 19 in T1, the weight gain experienced by rat 27 was thought to be a result of it mild hyperglycemia (9.25 ± 1.41 mmol/L) and not the effects of the treatment. However, the steady decline in the BGL of rat 29 lead to the assumption that the weight gain observed may have been a result of the treatment (**Figure S7; Figure S8**). Progressive weight gain of STZ-induced diabetic Wistar rats, due to plant extract and biogenic AuNPs administration, has been associated with signs of animal recovery from DM. It is postulated that this weight gain results from improved glucose uptake by the body thus replenishing of tissue proteins that were lost due to dehydration (Sengani, 2017). Noteworthy, is that rat 29 experienced a weight gain (67 g) that greatly surpasses the average weight gain of NDC animals (42.83 ± 2.70 g), thus rendering it overweight and an outlier.

Taken together, this experiment revealed that 100 mg/kg CeFe-AuNPs were not effective at treating STZ-induced diabetes. However, while it cannot be concluded that the treatments being investigated in this animal study possess the ability to improve hyperglycemic status, comparing the BGL at the beginning (day 3) and end (day 21) of the experiment showed that 200 mg/kg CeFe, 400 mg/kg CeFe and 200 mg/kg CeFe-AuNPs had varying abilities in delaying the progression of the diabetes, thus emphasizing its anti-diabetic potential. **Figure 3.12** shows how there was no hyperglycemic progression observed in the NDC group. Furthermore, DC animals were observed

to display a negative relative progression in hyperglycemia, clearly demonstrating what is postulated to be a spontaneous decrease in hyperglycemia (resulting from the β-cell regeneration previously reported in mildly hyperglycemic animals) (Cheng et al., 2017). Due to the difficulties faced during metformin administration, the relative progression in SD animals was observed to be higher than the NDC, as well as the T1 and T2 groups. Interesting to note, was the very low progression in T1 and T2 animals. This observation clearly indicates that although CeFe does not seem to restore BGL to normal, it does indeed delay the progression of hyperglycemia. While T4 animals surpass CeFe treated animals in their relative progression of hyperglycemia, comparing T4 results to T3 result allows for the hypothesis that CeFe-AuNPs could perform better at higher concentrations. Carrying out the experiment for a longer duration could potentially provide further insight into how well CeFe and high dose concentration CeFe-AuNPs can delay the progression of hyperglycemia, and if this delay could eventually promote normoglycemia. Studying the lipid profile of these animals could also provide useful information on other parameters that these treatments could influence.

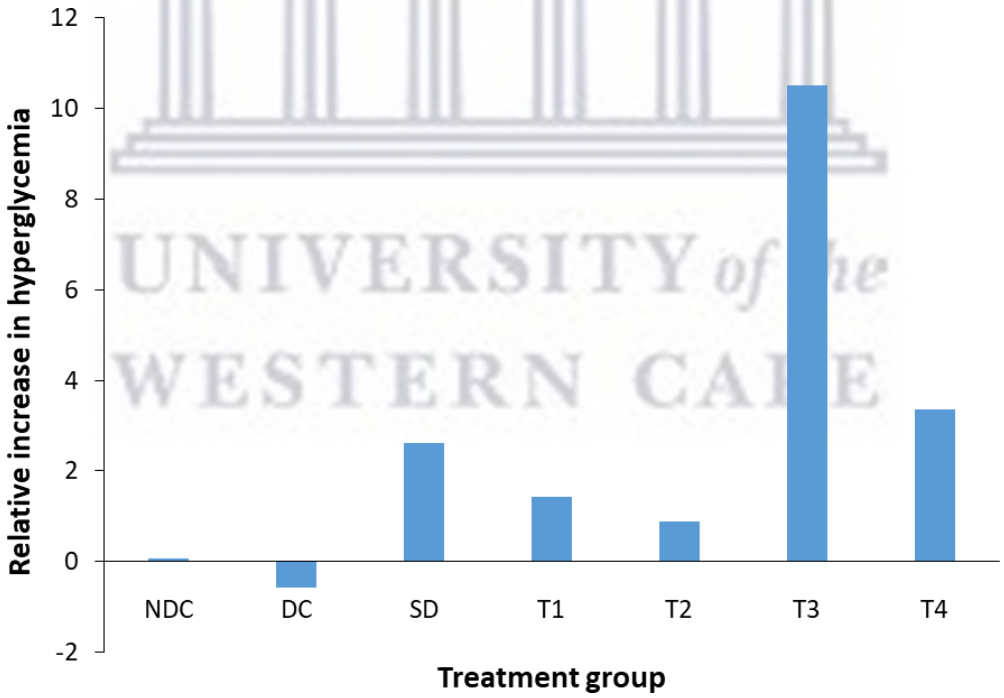

Figure 3.12: Effects of treatment on the progression of hyperglycemia. Data is represented as the difference in means of day 3 and day 21.

3.2.4.2 Effects of CeFe and CeFe-AuNPs on tissue weights

In this study, the spleens and hearts of diabetic animals were observed to experience a decrease in weight, while the livers and kidneys were observed to be slightly enlarged when compared to the NDC (**Table 3.3**). Although no statistical significance was found across all treatment groups, DM has been reported to decrease the immune capacity, and cause atrophy of immune organs via the suppression of immune cell function (Ebaid et al., 2015). As such, the decrease in spleen weight that was seen in this experiment could be a result of this common trait. Furthermore, diabetic toxicity has also been reported to cause lymphocyte stress, white pulp depletion, and depletion in the erythrocytes found in the red pulp of the spleen (Ebaid et al., 2015). Loss of heart mass may be due to the previously mentioned muscle wastage that occurs due to insulin deficiency, and also relates to the fact that cardiovascular diseases are among the most occurring comorbidities of DM (Leon and Maddox, 2015). Increase in liver weights is normally attributed to the liver specific fat accumulation that usually accompanies DM (Zafar and Naeem-ul-Hassan Naqvi, 2010), while enlargement of the kidney is often a result of vascular damage and often serves as one of the earliest signs of diabetes (Hostetter, 2001).

The white adipose tissue (WATs) weights corroborate the low BWs observed in the diabetic animals. There was no statistical significance observed between the WATs of NDC and DC, further supporting that DC animals gained as much weight as the. Furthermore, no statistical significance was observed between SD and DC. T3 animals, as previously mentioned had the lowest BWs, and their WATs were also observed to be the smallest. The white adipose tissues of CeFe treated animals (T1 and T2) were found to be larger than those of the CeFE-AuNPs treated groups (T3 and T4).

Table 3.3: Effect of CeFe and CeFe-AuNPs on the tissue weights (g) of diabetic male Wistar rats 21 days after administration of treatments.

Organ	NDC	DC	SD	T1	T2	T3	T4
Initial BW	314,17 ± 9,38	316,17 ± 16,60	317,75 ± 16,10	314,92 ± 10,97	314,83 ± 15,16	314,83 ± 8,9	316,83 ± 12,49
Final BW	357 ± 11,30	339,17 ± 15,09	331,25 ± 15,86	314,58 ± 15,91	326,17 ± 18,07	300,75 ± 11,78	316,67 ± 13,24
Liver	10,394 ± 0,257	10,196 ± 0,626	11,117 ± 0,786	10,422 ± 0,441	11,267 ± 0,359	11,352 ± 0,518	11,006 ± 0,491
Kidney	2,390 ± 0,072	2,446 ± 0,116	2,628 ± 0,143	2,654 ± 0,107	2,705 ± 0,09	2,863 ± 0,126	2,639 ± 0,123
Spleen	0,666 ± 0,017	0,578 ± 0,034	0,617 ± 0,023	0,565 ± 0,046	0,581 ± 0,047	0,550 ± 0,026	0,596 ± 0,05
Pancreas	1,376 ± 0,059	1,315 ± 0,144	1,357 ± 0,088	1,232 ± 0,043	1,314 ± 0,058	1,254 ± 0,065	1,344 ± 0,064
Heart	1,084 ± 0,023	0,969 ± 0,055	1,006 ± 0,035	1,02 ± 0,042	0,984 ± 0,068	0,98 ± 0,028	0,981 ± 0,037
Lungs	1,564 ± 0,036	1,404 ± 0,052	1,431 ± 0,063	1,376 ± 0,048	1,487 ± 0,09	1,314 ± 0,049	1,412 ± 0,055
Brain	1,997 ± 0,016	1,995 ± 0,043	1,973 ± 0,037	1,969 ± 0,031	1,944 ± 0,042	1,942 ± 0,029	1,932 ± 0,052
Testes	2,927 ± 0,087	2,910 ± 0,158	2,889 ± 0,125	2,841 ± 0,12	2,819 ± 0,132	2,826 ± 0,078	2,878 ± 0,073
Epididymal	6,308 ± 0,865	4,507 ± 1,143	4,384 ± 0,867	4,871 ± 1,32	4,568 ± 0,554	2,231 ± 0,290	3,06 ± 0,822
Subcutaneous	3,690 ± 0,395	2,824 ± 0,754	2,312 ± 0,505	2,041 ± 0,512	2,157 ± 0,357	1,023 ± 0,155	1,429 ± 0,312
Retroperitoneal	5,935 ± 0,914	4,100 ± 1,308	3,929 ± 1,013	3,499 ± 1,386	3,842 ± 0,863	1,176 ± 0,205	2,497 ± 0,6
Omental	3,751 ± 0,521	3,071 ± 0,791	2,41 ± 0,407	2,237 ± 0,799	2,239 ± 0,405	0,974 ± 0,180	1,904 ± 0,437
WATs	19,684 ± 2,695	14,503 ± 3,996	13,035 ± 2,792	12,647 ± 4,017^{c}	12,805 ± 2,180^{b}	5,404 ± 0,830^{ab}	8,889 ± 2,172^{a}

Data is presented as mean ± SEM (n = 6). White Adipose tissues (WATs) is represented as mean ± SEM of epididymal, subcutaneous, retroperitoneal and omental tissues (n = 4). a < 0.05 when compared to NDC. b < 0.05 when compared to DC. c < 0.05 when compared to SD.

3.2.4.3 Effect of CeFe and CeFe-AuNPs on pancreatic islet morphology and serum insulin

As previously mentioned, the administration of STZ leads to varying degrees of β-cell ablation, with varying severities of hyperglycemia. Administration of varying treatments, in this study, showed different capacities in their ability to delay the progression of hyperglycemia (**Figure 3.12**). Consequently, analysis of the pancreatic islets showed that CeFe treated animals (T1 and T2) had a more regular shape compared to those of the DC group. The state of T1 and T2 pancreatic islets could imply that CeFe delays the progression of hyperglycemia by decreasing the potency of STZ and as a result, preserving undamaged β-cells (**Figure 3.13**) (Ghorbani et al., 2019). This hypothesis could be corroborated by the fact that pancreatic islets in the extract treated T1 and T2 groups still maintained a similar size and shape seen in the NDC, although they were fewer in numbers. Pancreatic islets of the DC had highly irregular shapes, and were relatively hard to find (**Figure 3.13**). While the mechanism by which CeFe operates is unknown, it is understood that conventional drugs involved in the treatment of DM do so by improving insulin sensitivity of the muscle cells and adipose tissue, inhibiting gluconeogenesis, reducing glucose absorption by the gut or increasing overall insulin production (Santos et al., 2012).

Due to the high BGL in T1, T2 and T3, which served as evidence that STZ indeed ablated the β-cells, insulin production was expected be low, however this was not the case. Instead, the DC was found to have the lowest serum insulin. However, this insulin concentration was not statistically significant to either the SD or T2 (**Figure 3.14**). Metformin has been long reported to manage DM through a decrease in glucose production by the liver, an increase in insulin sensitivity of insulin responsive cells, and the reduction of calorie intake through the gut. Though the mechanism of metformin is complex, insulin production has not been implicated as one of them; therefore, the moderate insulin production in SD came as no surprise (Rena et al., 2017). Furthermore, T3 and T4 groups were observed to have a significantly higher serum insulin concentration ($p < 0.01$) (**Figure 3.14**).

The insulin concentrations of individual animals corroborated those of the mean (**Table 3.4; Figure 3.14**). Unlike the BW and BGL, there was not much variation within the serum insulin concentrations of the animals in each group. Considering how there were no outliers in any of the groups, it was surprising to see that the DC animals had the lowest serum insulin concentration even though STZ injection failed to produce severe hyperglycemia in most of the animals.

Flavonoids have been previously implicated as being able to preserve pancreatic islets, and in the potentiation of β-cells in diabetic rat models (Ghorbani et al., 2019). Flavonoids are one of the phytochemicals involved in the bio-reduction of Au^{3+} to form AuNPs, which have also been implicated in the regeneration of pancreatic islet cells and potentiation of β-cells (Shanker et al., 2017b; Guo et al., 2020). Therefore, there is reason to suspect that a similar observation was made in this study, and that this may be the reason behind the relatively higher insulin concentrations in the CeFe and CeFe-AuNPs treated groups compared to the DC.

Additionally, the microscopic anatomy of the T4 pancreas revealed architectural structures that were suspected to be immature pancreatic islets were observed (**Figure S9 – S13**); however, an insulin immunohistochemical stain would have to be performed in order to confirm this postulation. As stated before, increasing the duration of this study may allow for more in-depth knowledge, and this includes these structures; perhaps an increase in CeFe-AuNP dosage may result in the islets maturing faster and could stand to support the previously formulated hypothesis that the effect of CeFe-AuNPs could be increased with increasing dosage (**Section 4.2**). Transplantation of pancreatic islets has been, for a very long time, viewed as the only real hope that would effectively normalize BGL in T2DM patients, without running the risk of developing conventional drug-associated hypoglycemia (Bottino et al., 2018). If it is true that CeFe-AuNPs have the ability to cause regeneration of islets, then these AuNPs would present a far less tedious and invasive technique, which would not require donor organs.

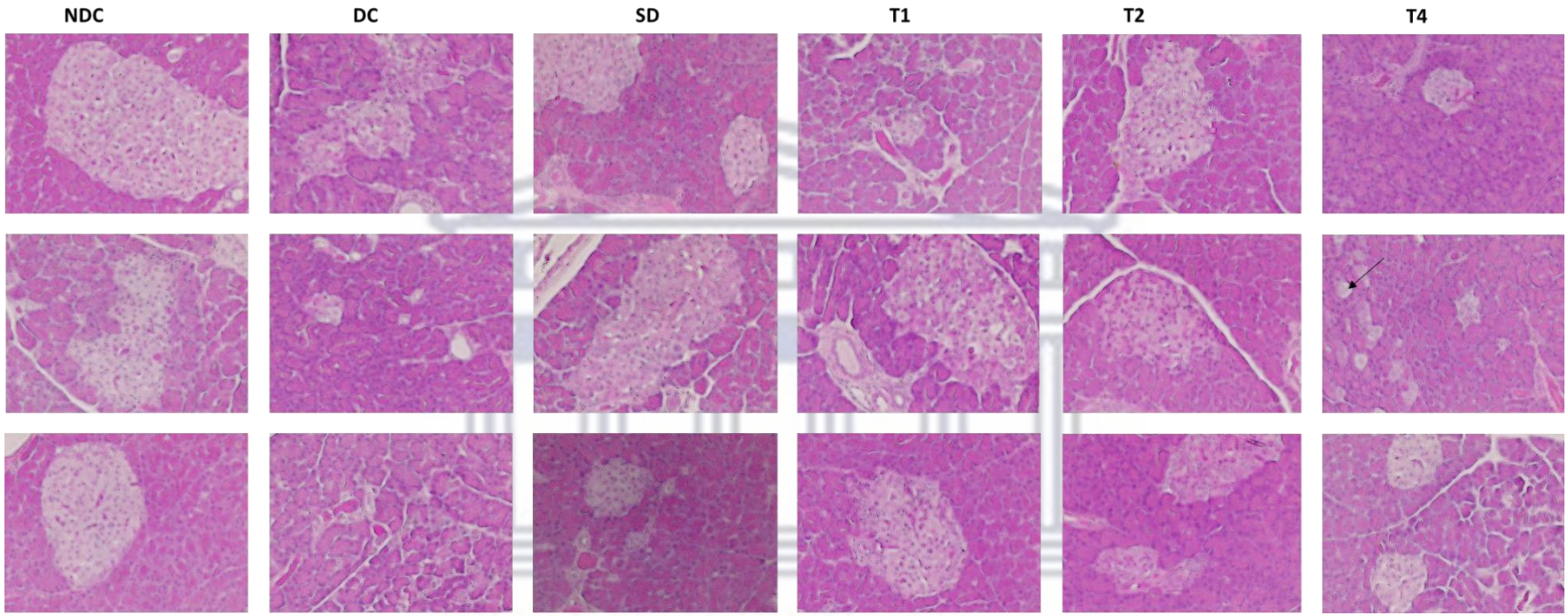

Figure 3.13: Effects of CeFe and CeFe-AuNPs on pancreatic islets. NDC: non-diabetic control, DC: Diabetic control, SD: 250mg/kg metformin standard drug, T1: 200mg/kg CeFe, T2: 400mg/kg CeFe, T3: 100mg/kg CeFe-AuNPs and T4: 200mg/kg CeFe-AuNPs. Due to their severe hyperglycemia, T3 animals a similar morphology to the DC group. Note: Structures postulated to be immature pancreatic islets are indicated with a black arrow.

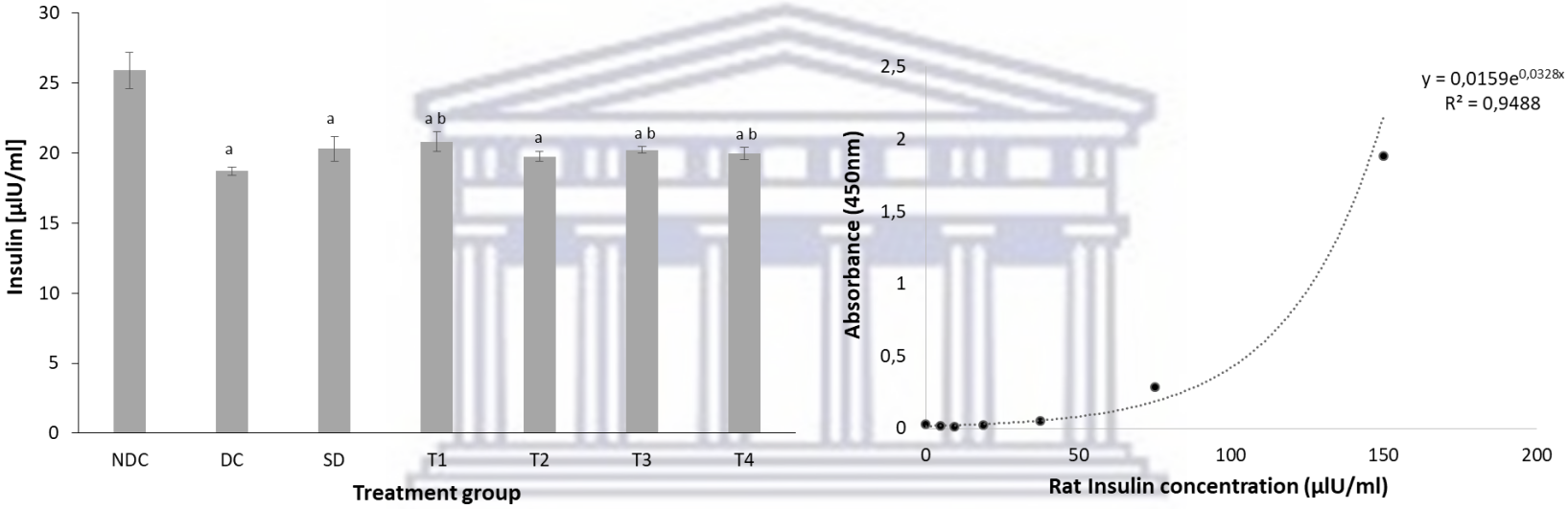

Figure 3.14: Effect of CeFe and CeFe-AuNPs on serum insulin. a < 0.05 when compared to NDC. b < 0.05 when compared to DC. NDC: non-diabetic control, DC: Diabetic control, SD: 250 mg/kg metformin standard drug, T1: 200 mg/kg CeFe, T2: 400 mg/kg CeFe, T3: 100 mg/kg CeFe-AuNPs and T4: 200 mg/kg CeFe-AuNPs**.**

Table 3.4: Effect of CeFe and CeFe-AuNPs on serum insulin levels in individual rats.

	NDC	DC	SD	T1	T2	T3	T4
	25,943	18,811	19,066	22,814	18,702	19,829	20,303
	28,127	17,956	22,814	20,266	20,194	20,849	18,738
	23,614	19,320	19,029	19,357	20,357	19,975	20,885
		19,266	23,359	19,648	19,029	20,303	22,159
		16,409	18,702	18,847	20,0298	20,084	20,485
		19,484	21,067	21,777	20,485	21,249	22,649
Average	25,895 ± 1,303	18,696 ± 0,282	20,303 ± 0,888	20,812 ± 0,732	19,751 ± 0,372	20,218 ± 0,225	19,975 ±0,453

NDC: Non-diabetic control, DC: Diabetic control, SD: 250 mg/kg metformin standard drug, T1: 200 mg/kg CeFE, T2: 400 mg/kg CeFe, T3: 100 mg/kg CeFe-AuNPs and T4: 200 mg/kg CeFe-AuNPs.
Average is represented as mean ± SEM (n = 6)

Chapter 4: Conclusion

4.1 Conclusion

The aim of the present study was to synthesize and characterize biogenic CeFe-AuNPs, and further investigate their anti-diabetic potential in STZ-induced diabetic rats. CeFe-AuNPs were successfully synthesized and characterized using various microscopic and spectroscopic techniques. The average size of the CeFe-AuNPs was found to be 16 ± 0.31 nm, with a λmax of 532 nm. The PDI was 0.435 and the zeta-potential was -30 mV, thus illustrating the desirable monodispersity and high stability required of NPs with a biomedical application. Furthermore, HR-TEM analysis revealed that CeFe-AuNPs were spherical in shape and corroborated the monodispersity observed in DLS. CeFe-AuNPs were stable in 0.5% BSA, PBS and ddH_2O; however, after 24 hours of incubation in 10 % NaCl, CeFe-AuNPs began to experience a blue shift.

CeFe and CeFe-AuNPs successfully induced glucose uptake in yeast cells. The best activity was observed in the 5 mM glucose reaction, where CeFe and CeFe-AuNPs caused uptake of 58 – 84 % and 8 – 48%, respectively. These findings demonstrated that CeFe and CeFe-AuNPs indeed have anti-diabetic properties and could potentially increase glucose uptake in *in vivo* models. A high single oral dose of CeFe and CeFe-AuNPs (2000 mg/kg) did not induce any toxic effects *in vivo*. The latter finding showed that the lethal dose of both CeFe and CeFe-AuNPs was above 2000 mg/kg and that at dosage concentrations lower than 2000 mg/kg, these treatments were safe to administer to rats.

The results for anti-diabetic effects of CeFe and CeFe-AuNPs were inconclusive. While it was clear that 100 mg/kg CeFe-AuNPs had no therapeutic effects on STZ-induced diabetic rats, the remaining three treatments (200 mg/kg and 400 mg/kg CeFe, and 200 mg/kg CeFe-AuNPs) were observed to slow down the progression of hyperglycemia or to reverse the STZ-induced hyperglycaemia. It is postulated that this delay is achieved through the preservation of pancreatic islet cells that were not damaged by STZ. Moreover, animals treated with 200 mg/kg CeFe-AuNPs were observed to display structures that were postulated to be immature pancreatic islets. However, future studies, such as immunohistochemical analysis using insulin antibodies, would have to be conducted to confirm this observation.

This study has successfully pioneered the demonstration of the *in vitro* and *in vivo* anti-hyperglycaemic potential of CeFe and CeFe-AuNPs. Nonetheless, further optimization, in terms of dosage concentration of the treatments, duration of the study and refinement of STZ injection protocol, need to be conducted in order to obtain more clinically-relevant information about the anti-hyperglycemic properties of CeFe and CeFe-AuNPs.

4.2 Limitations of the study

The development of a severely hyperglycaemic STZ model proved challenging in this study. The obtained results could have been influenced by the random nature in which STZ ablates β-cells, and the use of larger bodied animals (which may have influenced STZ bioavailability and susceptibility). Furthermore, administration of metformin using jelly cubes presented some challenges that need to be addressed in future studies. Although the rats were eating the jelly cubes, they were not ingesting all of them, thus all rats ultimately received different doses of the standard drug.

4.3 Recommendations and future work

STZ-induced diabetic models are relatively unstable models which are obtained by chance (8 out 10). In future studies it would be recommended that larger sample size of animals be used. Intravenous injection of STZ has been reported to yield more reproducible results compared to intraperitoneal injection. Therefore, to avoid variation within the animals, it would be recommended to use this route of administration. While STZ models develop hyperglycemia within 48 – 72 hours, it would be recommended that at least a week be allowed prior to administration of treatment. This is due to the reversal of hyperglycaemia that was observed in some STZ-injected rats in this study. Grouping the animals by hyperglycemic status instead of bodyweight could also decrease the variation that was observed in this study.

Further studies would include immunohistochemistry of the pancreas to assess pancreatic islets regeneration. Determining the biodistribution of CeFe-AuNPs is also a vital procedure that can help assess the bioavailability and excretion of the NPs. Analysis of the lipid profile can also provide more in depth information about the effects of CeFe and CeFe-AuNPs.

References

ABBOTT, R. M., LEVY, A. D., AGUILERA, N. S., GOROSPE, L. & THOMPSON, W. M. 2004. From the archives of the AFIP: primary vascular neoplasms of the spleen: radiologic-pathologic correlation. *Radiographics,* 24**,** 1137-1163.

ABDELHALIM, M. A. K. 2011. Exposure to gold nanoparticles produces cardiac tissue damage that depends on the size and duration of exposure. *Lipids in health and disease,* 10**,** 1-9.

ABEL, E. D., PERONI, O., KIM, J. K., KIM, Y.-B., BOSS, O., HADRO, E., MINNEMANN, T., SHULMAN, G. I. & KAHN, B. B. 2001. Adipose-selective targeting of the GLUT4 gene impairs insulin action in muscle and liver. *Nature,* 409**,** 729-733.

ADA 2004. American Diabetes Association: Gestational diabetes mellitus. *Diabetes care,* 27**,** S88. ADA 2012. Diagnosis and Classification of Diabetes Mellitus-Position Statement. *Diabetes Care,* 35**,** S64-S71.

ADA. 2015. 2. Classification and diagnosis of diabetes. *Diabetes care,* 38**,** S8-S16.

ADA 2017. 4. Lifestyle management. *Diabetes Care,* 40**,** S33-S43.

AKINYEDE, K. A., EKPO, O. E. & OGUNTIBEJU, O. O. 2020. Ethnopharmacology, therapeutic properties and nutritional potentials of Carpobrotus edulis: A comprehensive review. *Scientia Pharmaceutica,* 88**,** 39.

ALEXANDER, M. & DALGLEISH, D. G. 2006. Dynamic light scattering techniques and their applications in food science. *Food Biophysics,* 1**,** 2-13.

ALWAN, A. A. S. 1994. Management of Diabetes Mellitus Standards of Care ad Clinical Practice Guidelines. *In:* ALWAN, A. A. S. (ed.) *diabetes prevention and control.* Alexandria, Egypt: World Health Organizationn for the Eastern Mediterranean.

ANAND, K., TILOKE, C., NAIDOO, P. & CHUTURGOON, A. 2017. Phytonanotherapy for management of diabetes using green synthesis nanoparticles. *Journal of Photochemistry and Photobiology B: Biology,* 173**,** 626-639.

ANDERSON, H. 2018. *Nanotherapy: nanoparticles, research, advantages and challenges.* [Online]. microscopemaster. Available: https://www.microscopemaster.com/nanotherapy.html [Accessed 18 January 2021].

ANSELMO, A. C. & MITRAGOTRI, S. 2019. Nanoparticles in the clinic: An update. *Bioengineering & Translational Medicine,* 4**,** e10143.

ARONOFF, S. L., BERKOWITZ, K., SHREINER, B. & WANT, L. 2004. Glucose metabolism and regulation: beyond insulin and glucagon. *Diabetes spectrum,* 17**,** 183-190.

ATKINS, R. C. & ZIMMET, P. 2010. Diabetic kidney disease: act now or pay later. *Nephrology Dialysis Transplantation,* 25**,** 331-333.

AUFFAN, M., ROSE, J., WIESNER, M. R. & BOTTERO, J.-Y. 2009. Chemical stability of metallic nanoparticles: a parameter controlling their potential cellular toxicity in vitro. *Environmental Pollution,* 157**,** 1127-1133.

AUGUSTIN, R. 2010. The protein family of glucose transport facilitators: It's not only about glucose after all. *IUBMB life,* 62**,** 315-333.

AZZAZY, H. M., MANSOUR, M. M., SAMIR, T. M. & FRANCO, R. 2012. Gold nanoparticles in the clinical laboratory: principles of preparation and applications. *Clinical chemistry and laboratory medicine,* 50**,** 193-209.

BACHMANN, S., SAKAI, T. & KRIZ, W. 1986. Nephron and collecting duct structure in the kidney, rat. *Urinary system.* Springer.

BAHAMONDE, J., BRENSEKE, B., CHAN, M. Y., KENT, R. D., VIKESLAND, P. J. & PRATER, M. R. 2018. Gold nanoparticle toxicity in mice and rats: species differences. *Toxicologic pathology,* 46**,** 431-443.

BAILEY, C. J. & DAY, C. 2004. Metformin: its botanical background. *Practical Diabetes International,* 21**,** 115-117.

BANOO, H., NUSRAT, N. & NASIR, N. 2015. Type2 diabetes mellitus: a review of current trends. *RAMA Univ J Med Sci,* 1**,** 50-57.

BARATHMANIKANTH, S., KALISHWARALAL, K., SRIRAM, M., PANDIAN, S. R. K., YOUN, H.-S., EOM, S. & GURUNATHAN, S. 2010. Anti-oxidant effect of gold nanoparticles restrains hyperglycemic conditions in diabetic mice. *Journal of nanobiotechnology,* 8**,** 1-15.

BARRETO, A., LUIS, L. G., GIRÃO, A. V., TRINDADE, T., SOARES, A. M. & OLIVEIRA, M. 2015. Behavior of colloidal gold nanoparticles in different ionic strength media. *Journal of Nanoparticle Research,* 17**,** 493.

BASKARAN, K., AHAMATH, B. K., SHANMUGASUNDARAM, K. R. & SHANMUGASUNDARAM, E. 1990. Antidiabetic effect of a leaf extract from Gymnema sylvestre in non-insulin-dependent diabetes mellitus patients. *Journal of ethnopharmacology,* 30**,** 295-305.

BHUTKAR, M. & BHISE, S. 2013. In vitro hypoglycemic effects of Albizzia lebbeck and Mucuna pruriens. *Asian Pacific Journal of Tropical Biomedicine,* 3**,** 866-870.

BONIFÁCIO, B. V., DA SILVA, P. B., DOS SANTOS RAMOS, M. A., NEGRI, K. M. S., BAUAB, T. M. & CHORILLI, M. 2014. Nanotechnology-based drug delivery systems and herbal medicines: a review. *International journal of nanomedicine,* 9**,** 1.

BOTTINO, R., KNOLL, M. F., KNOLL, C. A., BERTERA, S. & TRUCCO, M. M. 2018. The future of islet transplantation is now. *Frontiers in medicine,* 5**,** 202.

BROWN, G. 2000. Glucose transporters: structure, function and consequences of deficiency. *Journal of inherited metabolic disease,* 23**,** 237-246.

BUCHANAN, T. A. & XIANG, A. H. 2005. Gestational diabetes mellitus. *The Journal of clinical investigation,* 115**,** 485-491.

CARDONA, D. 2011. Fundamental liver pathology part 1. Durham: Duke University.

CARPIO, G. R. A. & FONSECA, V. A. 2014. Update on safety issues related to antihyperglycemic therapy. *Diabetes Spectrum,* 27**,** 92-100.

CASTAÑEDA-LOAIZA, V., PLACINES, C., RODRIGUES, M. J., PEREIRA, C., ZENGIN, G., UYSAL, A., JEKO, J., CZIÁKY, Z., REIS, C. P. & GASPAR, M. M. 2020. If you cannot beat them, join them: Exploring the fruits of the invasive species Carpobrotus edulis (L.) NE Br as a source of bioactive products. *Industrial Crops and Products,* 144**,** 112005.

CDC. 2019. *Centers for Disease Control and Prevention: Gestational Diabetes and Pregnancy* [Online]. Available: https://www.cdc.gov/pregnancy/diabetes-gestational.html [Accessed 28 February 2020].

CERF, M. E. 2013. Beta cell dysfunction and insulin resistance. *Frontiers in endocrinology,* 4**,** 37.

CHENG, Y., SHEN, J., REN, W., HAO, H., XIE, Z., LIU, J., MU, Y. & HAN, W. 2017. Mild hyperglycemia triggered islet function recovery in streptozotocin-induced insulin-deficient diabetic rats. *Journal of diabetes investigation,* 8**,** 44-55.

CIRILLO, V. P. 1962. Mechanism of glucose transport across the yeast cell membrane. *Journal of bacteriology,* 84**,** 485-491.

COATES, J. 2006. Interpretation of infrared spectra, a practical approach. *Encyclopedia of analytical chemistry: applications, theory and instrumentation*.

CORSINO, L., DHATARIYA, K. & UMPIERREZ, G. 2017. Management of diabetes and hyperglycemia in hospitalized patients. *Endotext [Internet].* MDText. com, Inc.

CUNHA, J. M. D., FUNEZ, M. I., CUNHA, F. D. Q., PARADA, C. A. & FERREIRA, S. H. 2009. Streptozotocin-induced mechanical hypernociception is not dependent on hyperglycemia. *Brazilian Journal of Medical and Biological Research,* 42**,** 197-206.

DAISY, P. & SAIPRIYA, K. 2012. Biochemical analysis of Cassia fistula aqueous extract and phytochemically synthesized gold nanoparticles as hypoglycemic treatment for diabetes mellitus. *International journal of nanomedicine,* 7**,** 1189.

DAS, J. & VELUSAMY, P. 2014. Catalytic reduction of methylene blue using biogenic gold nanoparticles from Sesbania grandiflora L. *Journal of the Taiwan Institute of Chemical Engineers,* 45**,** 2280-2285.

DEEDS, M., ANDERSON, J., ARMSTRONG, A., GASTINEAU, D., HIDDINGA, H., JAHANGIR, A., EBERHARDT, N. & KUDVA, Y. C. 2011. Single dose streptozotocin-induced diabetes: considerations for study design in islet transplantation models. *Laboratory animals,* 45**,** 131-140.

DEFRONZO, R. A., TRIPLITT, C. L., ABDUL-GHANI, M. & CERSOSIMO, E. 2014. Novel agents for the treatment of type 2 diabetes. *Diabetes Spectrum,* 27**,** 100-112.

DEL PRETE, A., SCALERA, A., IADEVAIA, M. D., MIRANDA, A., ZULLI, C., GAETA, L., TUCCILLO, C., FEDERICO, A. & LOGUERCIO, C. 2012. Herbal products: benefits, limits, and applications in chronic liver disease. *Evidence-Based Complementary and Alternative Medicine,* 2012.

DEN BRAVER, N., LAKERVELD, J., RUTTERS, F., SCHOONMADE, L., BRUG, J. & BEULENS, J. 2018. Built environmental characteristics and diabetes: a systematic review and meta-analysis. *BMC medicine,* 16**,** 12.

DEVARAJ, P., KUMARI, P., AARTI, C. & RENGANATHAN, A. 2013. Synthesis and characterization of silver nanoparticles using cannonball leaves and their cytotoxic activity against MCF-7 cell line. *Journal of nanotechnology,* 2013.

DIABETES PREVENTION PROGRAM RESEARCH GROUP, D. 2002. Reduction in the incidence of type 2 diabetes with lifestyle intervention or metformin. *New England journal of medicine,* 346**,** 393-403.

DIAS, D. A., URBAN, S. & ROESSNER, U. 2012. A historical overview of natural products in drug discovery. *Metabolites,* 2**,** 303-336.

DOMIGUEZ-SALAZAR, K. 2017. Pharmacology of Diabetes Mellitus medication. *New Mexico Nurse Practitioner council spring conference.* New Mexico: New Mexico Nurse Practitioner council.

EBAID, H., AL-TAMIMI, J., METWALLI, A., ALLAM, A., ZOHIR, K., AJAREM, J., RADY, A., ALHAZZA, I. M. & IBRAHIM, K. E. 2015. Effect of STZ-induced diabetes on spleen of rats: improvement by camel whey proteins. *Pakistan J. Zool,* 47**,** 1109-1116.

EDIRIWICKREMA, A. & SALTZMAN, W. M. 2015. Nanotherapy for cancer: targeting and multifunctionality in the future of cancer therapies. *ACS biomaterials science & engineering,* 1**,** 64-78.

ELBAGORY, A. M., CUPIDO, C. N., MEYER, M. & HUSSEIN, A. A. 2016. Large scale screening of Southern African plant extracts for the green synthesis of gold nanoparticles using microtitre-plate method. *Molecules,* 21**,** 1498.

ELIA, P., ZACH, R., HAZAN, S., KOLUSHEVA, S., PORAT, Z. E. & ZEIRI, Y. 2014. Green synthesis of gold nanoparticles using plant extracts as reducing agents. *International journal of nanomedicine,* 9**,** 4007.

ENGLER, C., LEO, M., PFEIFER, B., JUCHUM, M., CHEN-KOENIG, D., POELZL, K., SCHOENHERR, H., VILL, D., OBERDANNER, J. & EISENDLE, E. 2020. Long-term trends in the prescription of antidiabetic drugs: real-world evidence from the Diabetes Registry Tyrol 2012–2018. *BMJ Open Diabetes Research and Care,* 8**,** e001279.

FAM, B. C., ROSE, L. J., SGAMBELLONE, R., RUAN, Z., PROIETTO, J. & ANDRIKOPOULOS, S. 2012. Normal muscle glucose uptake in mice deficient in muscle GLUT4. *Journal of endocrinology,* 214**,** 313.

FINAN, B., CAPOZZI, M. E. & CAMPBELL, J. E. 2020. Repositioning glucagon action in the physiology and pharmacology of diabetes. *Diabetes,* 69**,** 532-541.

FIORENTINO, T. V., MARINI, M. A., SUCCURRO, E., ANDREOZZI, F. & SESTI, G. 2019. Relationships of surrogate indexes of insulin resistance with insulin sensitivity assessed by euglycemic hyperinsulinemic clamp and subclinical vascular damage. *BMJ Open Diabetes Research and Care,* 7.

FRASER, G. E. 2009. Vegetarian diets: what do we know of their effects on common chronic diseases? *The American journal of clinical nutrition,* 89**,** 1607S-1612S.

FURMAN, B. L. 2015. Streptozotocin-induced diabetic models in mice and rats. *Current protocols in pharmacology,* 70**,** 5.47. 1-5.47. 20.

GERICH, J. E. 2000. Insulin resistance is not necessarily an essential component of type 2 diabetes. *The Journal of Clinical Endocrinology & Metabolism,* 85**,** 2113-2115.

GHORBANI, A. 2013. Best herbs for managing diabetes: a review of clinical studies. *Brazilian Journal of Pharmaceutical Sciences,* 49**,** 413-422.

GHORBANI, A., RASHIDI, R. & SHAFIEE-NICK, R. 2019. Flavonoids for preserving pancreatic beta cell survival and function: A mechanistic review. *Biomedicine & Pharmacotherapy,* 111**,** 947-957.

GHOSH, S. K. & PAL, T. 2007. Interparticle coupling effect on the surface plasmon resonance of gold nanoparticles: from theory to applications. *Chemical reviews,* 107**,** 4797-4862.

GLASS, C. K. & OLEFSKY, J. M. 2012. Inflammation and lipid signaling in the etiology of insulin resistance. *Cell metabolism,* 15**,** 635-645.

GODOY-MATOS, A. F. 2014. The role of glucagon on type 2 diabetes at a glance. *Diabetology & metabolic syndrome,* 6**,** 91.

GOVERNA, P., BAINI, G., BORGONETTI, V., CETTOLIN, G., GIACHETTI, D., MAGNANO, A. R., MIRALDI, E. & BIAGI, M. 2018. Phytotherapy in the management of diabetes: a review. *Molecules,* 23**,** 105.

GOYAL, S. N., REDDY, N. M., PATIL, K. R., NAKHATE, K. T., OJHA, S., PATIL, C. R. & AGRAWAL, Y. O. 2016. Challenges and issues with streptozotocin-induced diabetes–A clinically relevant animal model to understand the diabetes pathogenesis and evaluate therapeutics. *Chemico-biological interactions,* 244**,** 49-63.

GUNASEKARAN, T., HAILE, T., NIGUSSE, T. & DHANARAJU, M. D. 2014. Nanotechnology: an effective tool for enhancing bioavailability and bioactivity of phytomedicine. *Asian Pacific journal of tropical biomedicine,* 4**,** S1-S7.

GUO, R., SONG, Y., WANG, G. & MURRAY, R. W. 2005. Does core size matter in the kinetics of ligand exchanges of monolayer-protected Au clusters? *Journal of the American Chemical Society,* 127**,** 2752-2757.

GUO, Y., JIANG, N., ZHANG, L. & YIN, M. 2020. Green synthesis of gold nanoparticles from Fritillaria cirrhosa and its anti-diabetic activity on Streptozotocin induced rats. *Arabian Journal of Chemistry,* 13**,** 5096-5106.

GUPTA, R. & SAXENA, A. 2011. Hypoglycemic and anti-hyperglycemic activities of Syzygium cumini (Linn.) skeels whole fruit, in normal and streptozotocin-induced diabetic rats. *Asian J Pharm Biol Res Jul-Sep,* 1.

GUSTAFSON, B., HEDJAZIFAR, S., GOGG, S., HAMMARSTEDT, A. & SMITH, U. 2015. Insulin resistance and impaired adipogenesis. *Trends in Endocrinology & Metabolism,* 26**,** 193-200.

GUTCH, M., KUMAR, S., RAZI, S. M., GUPTA, K. K. & GUPTA, A. 2015. Assessment of insulin sensitivity/resistance. *Indian journal of endocrinology and metabolism,* 19**,** 160.

GYAMFI, D., AWUAH, E. O. & OWUSU, S. 2019. Molecular aspects and biochemical regulation of diabetes mellitus. *Molecular Nutrition: Carbohydrates.* Elsevier.

HÆDERSDAL, S., LUND, A., KNOP, F. K. & VILSBØLL, T. The role of glucagon in the pathophysiology and treatment of type 2 diabetes. Mayo Clinic Proceedings, 2018. Elsevier, 217-239.

HAGHVIRDIZADEH, P., MOHAMED, Z., ABDULLAH, N. A., HAGHVIRDIZADEH, P., HAERIAN, M. S. & HAERIAN, B. S. 2015. KCNJ11: genetic polymorphisms and risk of diabetes mellitus. *Journal of diabetes research,* 2015.

HAMINIUK, C. W., MACIEL, G. M., PLATA-OVIEDO, M. S. & PERALTA, R. M. 2012. Phenolic compounds in fruits–an overview. *International Journal of Food Science & Technology,* 47**,** 2023-2044.

HERBARIUM, W. A. 1998. FloraBase–the Western Australian Flora. *Department of Parks and Wildlife*.

HOLISTER, P., WEENER, J.-W., ROMAN, C. & HARPER, T. 2003. Nanoparticles. *Technology white papers,* 3**,** 1-11.

HOSTETTER, T. 2001. Hypertrophy and hyperfunction of the diabetic kidney. *The Journal of clinical investigation,* 107**,** 161-162.

HU, Y., LIU, W., CHEN, Y., ZHANG, M., WANG, L., ZHOU, H., WU, P., TENG, X., DONG, Y. & WEN ZHOU, J. 2010. Combined use of fasting plasma glucose and glycated hemoglobin A1c in the screening of diabetes and impaired glucose tolerance. *Acta diabetologica,* 47**,** 231-236.

HUANG, S. & CZECH, M. P. 2007. The GLUT4 glucose transporter. *Cell metabolism,* 5**,** 237-252.

HUDSON, S. D., SIMS, C. A., ODABASI, A. Z., COLQUHOUN, T. A., SNYDER, D. J., STAMPS, J. J., DOTSON, S. C., PUENTES, L. & BARTOSHUK, L. M. 2018. Flavor alterations associated with miracle fruit and gymnema sylvestre. *Chemical senses,* 43**,** 481-488.

IDF. 2019. *International Diabetes Federation: Diabetes Atlas* [Online]. Brussels, Belgium. Available: http://www.diabetesatlas.org [Accessed 02 December 2019].

IFEOMA, O. & OLUWAKANYINSOLA, S. 2013. Screening of herbal medicines for potential toxicities. *New insights into toxicity and drug testing,* 244**,** 63-88.

IRAVANI, S. 2011. Green synthesis of metal nanoparticles using plants. *Green Chemistry,* 13**,** 2638-2650.

JADOUN, S., ARIF, R., JANGID, N. K. & MEENA, R. K. 2020. Green synthesis of nanoparticles using plant extracts: a review. *Environmental Chemistry Letters***,** 1-20.

JENKINS, J. A., ZHOU, Y., THOTA, S., TIAN, X., ZHAO, X., ZOU, S. & ZHAO, J. 2014. Blue-shifted narrow localized surface plasmon resonance from dipole coupling in gold nanoparticle random arrays. *The Journal of Physical Chemistry C,* 118**,** 26276-26283.

JEONG, S. U., KANG, D. G., LEE, D. H., LEE, K. W., LIM, D.-M., KIM, B. J., PARK, K.-Y., CHIN, H.-J. & KOH, G. 2010. Clinical characteristics of type 2 diabetes patients according to family history of diabetes. *Korean diabetes journal,* 34**,** 222-228.

JOHNSON, A. M. & OLEFSKY, J. M. 2013. The origins and drivers of insulin resistance. *Cell,* 152**,** 673-684.

JOHNSON, P. D. & BESSELSEN, D. G. 2002. Practical aspects of experimental design in animal research. *ILAR journal,* 43**,** 202-206.

KASOLE, R., MARTIN, H. D. & KIMIYWE, J. 2019. Traditional medicine and its role in the management of diabetes mellitus:"patients' and herbalists' perspectives". *Evidence-Based Complementary and Alternative Medicine,* 2019.

KAUFMANN, W. & JACOBSEN, M. C. 2020. Examination of Organ Toxicity. *Regulatory Toxicology***,** 1-11.

KAUR, I. P. & KAKKAR, S. 2014. Nanotherapy for posterior eye diseases. *Journal of Controlled Release,* 193**,** 100-112.

KAZEMIAN, M., ABAD, M., REZA HAERI, M., EBRAHIMI, M. & HEIDARI, R. 2015. Anti-diabetic effect of Capparis spinosa L. root extract in diabetic rats. *Avicenna journal of phytomedicine,* 5**,** 325.

KHAN, S. H., KHAN, A. N., CHAUDHRY, N., ANWAR, R., FAZAL, N. & TARIQ, M. 2019. Comparison of various steady state surrogate insulin resistance indices in diagnosing metabolic syndrome. *Diabetology & metabolic syndrome,* 11**,** 1-9.

KHANNA, V. K. 2016. Nanomaterials and their Properties. *Integrated Nanoelectronics.* Springer.

KHLEBTSOV, B. & KHLEBTSOV, N. 2011. On the measurement of gold nanoparticle sizes by the dynamic light scattering method. *Colloid Journal,* 73**,** 118-127.

KIM, G. J. & NIE, S. 2005. Targeted cancer nanotherapy. *Materials Today,* 8**,** 28-33.

KOSTER, J. C., PERMUTT, M. A. & NICHOLS, C. G. 2005. Diabetes and insulin secretion: the ATP-sensitive K+ channel (KATP) connection. *Diabetes,* 54**,** 3065-3072.

KRISHNA, M. 2013. Microscopic anatomy of the liver. *Clinical Liver Disease,* 2**,** S4.

KUMAR, V. G., GOKAVARAPU, S. D., RAJESWARI, A., DHAS, T. S., KARTHICK, V., KAPADIA, Z., SHRESTHA, T., BARATHY, I., ROY, A. & SINHA, S. 2011. Facile green synthesis of gold nanoparticles using leaf extract of antidiabetic potent Cassia auriculata. *Colloids and Surfaces B: Biointerfaces,* 87**,** 159-163.

KUMARI, A., KUMAR, V. & YADAV, S. 2012. Nanotechnology: a tool to enhance therapeutic values of natural plant products. *Trends Med Res,* 7**,** 34-42.

LACCOURREYE, O., WERNER, A., LACCOURREYE, L. & BONFILS, P. 2017. Benefits, pitfalls and risks of phytotherapy in clinical practice in otorhinolaryngology. *European annals of otorhinolaryngology, head and neck diseases,* 134**,** 95-99.

LANKATILLAKE, C., HUYNH, T. & DIAS, D. A. 2019. Understanding glycaemic control and current approaches for screening antidiabetic natural products from evidence-based medicinal plants. *Plant methods,* 15**,** 105.

LEBLANC, E. S., PATNODE, C. D., WEBBER, E. M., REDMOND, N., RUSHKIN, M. & O'CONNOR, E. A. 2018. Behavioral and pharmacotherapy weight loss interventions to prevent obesity-related morbidity and mortality in adults: updated evidence report and systematic review for the US Preventive Services Task Force. *Jama,* 320**,** 1172-1191.

LEKOUBOU, A., AWAH, P., FEZEU, L., SOBNGWI, E. & KENGNE, A. P. 2010. Hypertension, diabetes mellitus and task shifting in their management in sub-Saharan Africa. *International journal of environmental research and public health,* 7**,** 353-363.

LEON, B. M. & MADDOX, T. M. 2015. Diabetes and cardiovascular disease: Epidemiology, biological mechanisms, treatment recommendations and future research. *World journal of diabetes,* 6**,** 1246.

LIGGITT, D. & DINTZIS, S. M. 2018. 14 - Pancreas,. *In:* PIPER M. TREUTING, S. M. D., KATHLEEN S. MONTINE, (ed.) *Comparative Anatomy and Histology (Second Edition).* second edition ed. University of Washington, School of Medicine, Seattle, WA, United States: Academic Press.

LIM, J., YEAP, S. P., CHE, H. X. & LOW, S. C. 2013. Characterization of magnetic nanoparticle by dynamic light scattering. *Nanoscale research letters,* 8**,** 1-14.

LIN, J. S., O'CONNOR, E. A., EVANS, C. V., SENGER, C. A., ROWLAND, M. G. & GROOM, H. C. 2014. Behavioral counseling to promote a healthy lifestyle for cardiovascular disease prevention in persons with cardiovascular risk factors: an updated systematic evidence review for the US preventive services task force.

LINDSTRÖM, J., PELTONEN, M., TUOMILEHTO, J. & GROUP, F. D. P. S. 2005. Lifestyle strategies for weight control: experience from the Finnish Diabetes Prevention Study. *Proceedings of the nutrition society,* 64**,** 81-88.

MACDONALD, P. E., JOSEPH, J. W. & RORSMAN, P. 2005. Glucose-sensing mechanisms in pancreatic β-cells. *Philosophical Transactions of the Royal Society B: Biological Sciences,* 360**,** 2211-2225.

MADRAZO-IBARRA, A. & VAITLA, P. 2020. Histology, Nephron. *StatPearls [Internet]*.

MANN, E. & BELLIN, M. D. 2016. Secretion of insulin in response to diet and hormones. *Pancreapedia: The Exocrine Pancreas Knowledge Base*.

MARÍN-JUEZ, R., CAPILLA, E., CARVALHO-SIMOES, F., CAMPS, M. & PLANAS, J. V. 2014. Structural and functional evolution of glucose transporter 4 (GLUT4): a look at GLUT4 in fish. *Glucose Homeostasis,* 174.

MARIN, S., MIHAIL VLASCEANU, G., ELENA TIPLEA, R., RALUCA BUCUR, I., LEMNARU, M., MINODORA MARIN, M. & MIHAI GRUMEZESCU, A. 2015. Applications and toxicity of silver nanoparticles: a recent review. *Current topics in medicinal chemistry,* 15**,** 1596-1604.

MARQUIS, B. J., LOVE, S. A., BRAUN, K. L. & HAYNES, C. L. 2009. Analytical methods to assess nanoparticle toxicity. *Analyst,* 134**,** 425-439.

MCCARTHY, M. I. 2010. Genomics, type 2 diabetes, and obesity. *New England Journal of Medicine,* 363**,** 2339-2350.

MCTAGGART, J. S., CLARK, R. H. & ASHCROFT, F. M. 2010. SYMPOSIUM REVIEW: The role of the KATP channel in glucose homeostasis in health and disease: more than meets the islet. *The Journal of physiology,* 588**,** 3201-3209.

MIZUSHIMA, T. 2011. Drug discovery and development focusing on existing medicines: drug re-profiling strategy. *The Journal of Biochemistry,* 149**,** 499-505.

MLOZI, S. H., MMONGOYO, J. A. & CHACHA, M. 2020. The in vivo toxicity evaluation of leaf and root methanolic extracts of Tephrosia vogelii Hook. f using animal model. *Clinical Phytoscience,* 6**,** 1-9.

MOORE, T. L., RODRIGUEZ-LORENZO, L., HIRSCH, V., BALOG, S., URBAN, D., JUD, C., ROTHEN-RUTISHAUSER, B., LATTUADA, M. & PETRI-FINK, A. 2015. Nanoparticle colloidal stability in cell culture media and impact on cellular interactions. *Chemical Society Reviews,* 44**,** 6287-6305.

MÜLLER, T., FINAN, B., CLEMMENSEN, C., DIMARCHI, R. & TSCHÖP, M. 2017. The new biology and pharmacology of glucagon. *Physiological Reviews,* 97**,** 721-766.

MUNIYAPPA, R., TELLA, S. H., SORTUR, S., MSZAR, R., GREWAL, S., ABEL, B. S., AUH, S., CHANG, D. C., KRAKOFF, J. & SKARULIS, M. C. 2019. Predictive accuracy of surrogate indices for hepatic and skeletal muscle insulin sensitivity. *Journal of the Endocrine Society,* 3**,** 108-118.

MURTY, B., SHANKAR, P., RAJ, B., RATH, B. & MURDAY, J. 2013. Unique properties of nanomaterials. *Textbook of Nanoscience and Nanotechnology.* Springer.

MUTYAMBIZI, C., PAVLOVA, M., CHOLA, L., HONGORO, C. & GROOT, W. 2018. Cost of diabetes mellitus in Africa: a systematic review of existing literature. *Globalization and health,* 14**,** 3.

NASROLLAHZADEH, M., SAJJADI, M., SAJADI, S. M. & ISSAABADI, Z. 2019. Green nanotechnology. *Interface Science and Technology.* Elsevier.

NAVALE, A. M. & PARANJAPE, A. N. 2016. Glucose transporters: physiological and pathological roles. *Biophysical reviews,* 8**,** 5-9.

NIDDK. 2016. *National Institute of Diabetes and Digestive and Kidney Diseases: Diabetes overview* [Online]. Available: https://www.niddk.nih.gov/health-information/diabetes/overview/what-is-diabetes [Accessed].

NIDDK. 2018. *Insulin resistance and prediabetes* [Online]. USA. Available: https://www.niddk.nih.gov/health-information/diabetes/overview/what-is-diabetes/prediabetes-insulin-resistance [Accessed 06 June 2020].

OECD 2008. OECD guidelines for the testing of animals. *In:* OECD (ed.) *425.* OECD.

OKOSUN, I. S., OKOSUN, B., LYN, R. & AIRHIHENBUWA, C. 2020. Surrogate indexes of insulin resistance and risk of metabolic syndrome in non-Hispanic white, non-Hispanic black and Mexican American. *Diabetes & Metabolic Syndrome: Clinical Research & Reviews,* 14**,** 3-9.

OLOKOBA, A. B., OBATERU, O. A. & OLOKOBA, L. B. 2012. Type 2 diabetes mellitus: a review of current trends. *Oman medical journal,* 27**,** 269.

OLSON, A. L. 2012. Regulation of GLUT4 and insulin-dependent glucose flux. *ISRN molecular biology,* 2012.

OMORUYI, B. E., BRADLEY, G. & AFOLAYAN, A. J. 2012. Antioxidant and phytochemical properties of Carpobrotus edulis (L.) bolus leaf used for the management of common infections in HIV/AIDS patients in Eastern Cape Province. *BMC Complementary and Alternative Medicine,* 12**,** 1-9.

OMRAN, B. A., NASSAR, H. N., FATTHALLAH, N. A., HAMDY, A., EL-SHATOURY, E. H. & EL-GENDY, N. S. 2018. Waste upcycling of Citrus sinensis peels as a green route for the synthesis of silver nanoparticles. *Energy Sources, Part A: Recovery, Utilization, and Environmental Effects,* 40**,** 227-236.

ORWA C, MUTAU A, KINDT R, JAMNADASS R & S, A. 2009. *Tephrosia vogelii Hook f. Faaceae - Papillooideae* [Online]. Agroforestry Database. [Accessed 25 April 2021].

OYEDEMI, S., ADEWUSI, E., AIYEGORO, O. & AKINPELU, D. 2011. Antidiabetic and haematological effect of aqueous extract of stem bark of Afzelia africana (Smith) on streptozotocin–induced diabetic Wistar rats. *Asian Pacific journal of tropical biomedicine,* 1**,** 353-358.

PATEL, H. N., FREEMAN, A. M. & WILLIAMS, K. A. 2017. Diabetes: An Opportunity to Have a Lasting Impact on Health Through Lifestyle Modification. *The American journal of managed care,* 23.

PATNODE, C. D., EVANS, C. V., SENGER, C. A., REDMOND, N. & LIN, J. S. 2017. Behavioral counseling to promote a healthful diet and physical activity for cardiovascular disease prevention in adults without known cardiovascular disease risk factors: updated evidence report and systematic review for the US Preventive Services Task Force. *Jama,* 318**,** 175-193.

PHAN, H. T. & HAES, A. J. 2019. What does nanoparticle stability mean? *The Journal of Physical Chemistry C,* 123**,** 16495-16507.

PHILIP, D. 2008. Synthesis and spectroscopic characterization of gold nanoparticles. *Spectrochimica Acta Part A: Molecular and Biomolecular Spectroscopy,* 71**,** 80-85.

PITCHAIPILLAI, R. & PONNIAH, T. 2016. In vitro antidiabetic activity of ethanolic leaf extract of bruguiera Cylindrica L.–glucose uptake by yeast cells method. *International Biological and Biomedical Journal,* 2**,** 171-175.

PIZZORNO, J. 2016. Is the diabetes epidemic primarily due to toxins? *Integrative Medicine: A Clinician's Journal,* 15**,** 8.

PONNANIKAJAMIDEEN, M., RAJESHKUMAR, S., VANAJA, M. & ANNADURAI, G. 2019. In vivo type 2 diabetes and wound-healing effects of antioxidant gold nanoparticles synthesized using the insulin plant Chamaecostus cuspidatus in albino rats. *Canadian journal of diabetes,* 43**,** 82-89. e6.

QAID, M. M. & ABDELRAHMAN, M. M. 2016. Role of insulin and other related hormones in energy metabolism—A review. *Cogent Food & Agriculture,* 2**,** 1267691.

RAJARAJESHWARI, T., SHIVASHRI, C. & RAJASEKAR, P. 2014. Synthesis and characterization of biocompatible gymnemic acid–gold nanoparticles: a study on glucose uptake stimulatory effect in 3T3-L1 adipocytes. *RSC Advances,* 4**,** 63285-63295.

REHMAN, G., HAMAYUN, M., IQBAL, A., UL ISLAM, S., ARSHAD, S., ZAMAN, K., AHMAD, A., SHEHZAD, A., HUSSAIN, A. & LEE, I. 2018. In vitro antidiabetic effects and antioxidant potential of Cassia nemophila Pods. *BioMed research international,* 2018.

REIMONDEZ-TROITIÑO, S., CSABA, N., ALONSO, M. & DE LA FUENTE, M. 2015. Nanotherapies for the treatment of ocular diseases. *European Journal of Pharmaceutics and Biopharmaceutics,* 95**,** 279-293.

RENA, G., HARDIE, D. G. & PEARSON, E. R. 2017. The mechanisms of action of metformin. *Diabetologia,* 60**,** 1577-1585.

RICHTER, C. 2003. *Hottentot Fig (Carpobrotus edulis)* [Online]. Otto Richters and sons. Available: https://www.richters.com/show.cgi?page=QandA/Medicinal/20031016-4.html [Accessed 02 February 2021 2021].

RICHTER, E. A. & HARGREAVES, M. 2013. Exercise, GLUT4, and skeletal muscle glucose uptake. *Physiological reviews,* 93**,** 993-1017.

ROCHA, M., RODRIGUES, M., PEREIRA, C., PEREIRA, H., DA SILVA, M., DA ROSA NENG, N., NOGUEIRA, J., VARELA, J., BARREIRA, L. & CUSTÓDIO, L. 2017. Biochemical profile and in vitro neuroprotective properties of Carpobrotus edulis L., a medicinal and edible halophyte native to the coast of South Africa. *South African journal of botany,* 111**,** 222-231.

SAGHIR, F., HUSSAIN, K., TAHIR, M. N., RAZA, S. A., SHEHZADI, N., IFTIKHAR, S., SHAUKAT, A., NAHEED, S. & SIDDIQUE, S. 2020. Antidiabetic Screening, Activity-guided Isolation and Molecular Docking Studies of Flower Extracts of Pongamia pinnata (L.) Pierre. *Journal of Medicinal plants and By-product*.

SAIRAM, S. & UROOJ, A. 2012. Effect of Artocarpus altilis on carbohydrate hydrolyzing enzymes and glucose uptake by yeast cells: an ex-vivo study. *Journal of herbs, spices & medicinal plants,* 18**,** 140-151.

SALATA, O. V. 2004. Applications of nanoparticles in biology and medicine. *Journal of nanobiotechnology,* 2**,** 3.

SALMASI, A.-M. & DANCY, M. 2005. The glucose tolerance Test, but not HbA 1c, remains the gold standard in identifying unrecognized diabetes mellitus and impaired glucose tolerance in hypertensive subjects. *Angiology,* 56**,** 571-579.

SANGLE, N. 2012. *Anatomy & histology* [Online]. PathologyOutlines.com. Available: https://www.pathologyoutlines.com/topic/kidneyanatomy.html [Accessed 6 April 2021].

SANTOS, F. A., FROTA, J. T., ARRUDA, B. R., DE MELO, T. S., DE CASTRO BRITO, G. A., CHAVES, M. H. & RAO, V. S. 2012. Antihyperglycemic and hypolipidemic effects of α, β-amyrin, a triterpenoid mixture from Protium heptaphyllum in mice. *Lipids in health and disease,* 11**,** 1-8.

SARKER, P., RAHMAN, M. M., KHAN, F., MING, L. C., MOHAMED, I. N., ZHAO, C. & RASHID, M. A. 2019. Comprehensive Review on Phytochemicals, Pharmacological and Clinical Potentials of Gymnema sylvestre. *Frontiers in Pharmacology,* 10**,** 1223.

SENGANI, M. 2017. Identification of potential antioxidant indices by biogenic gold nanoparticles in hyperglycemic Wistar rats. *Environmental toxicology and pharmacology,* 50**,** 11-19.

SHAH, M., BADWAIK, V. D. & DAKSHINAMURTHY, R. 2014. Biological applications of gold nanoparticles. *Journal of Nanoscience and Nanotechnology,* 14**,** 344-362.

SHANKER, K., MOHAN, G. K., MAYASA, V. & PRAVALLIKA, L. 2017a. Antihyperglycemic and anti-hyperlipidemic effect of biologically synthesized silver nanoparticles and G. sylvestre

extract on streptozotocin induced diabetic rats-an in vivo approach. *Materials Letters,* 195**,** 240-244.

SHANKER, K., NARADALA, J., MOHAN, G. K., KUMAR, G. & PRAVALLIKA, P. 2017b. A sub-acute oral toxicity analysis and comparative in vivo anti-diabetic activity of zinc oxide, cerium oxide, silver nanoparticles, and Momordica charantia in streptozotocin-induced diabetic Wistar rats. *RSC advances,* 7**,** 37158-37167.

SHANMUGASUNDARAM, E., RAJESWARI, G., BASKARAN, K., KUMAR, B. R., SHANMUGASUNDARAM, K. R. & AHMATH, B. K. 1990. Use of Gymnema sylvestre leaf extract in the control of blood glucose in insulin-dependent diabetes mellitus. *Journal of ethnopharmacology,* 30**,** 281-294.

SHEN, J., OBIN, M. S. & ZHAO, L. 2013. The gut microbiota, obesity and insulin resistance. *Molecular aspects of medicine,* 34**,** 39-58.

SHENG, Z., CAO, J.-Y., PANG, Y.-C., XU, H.-C., CHEN, J.-W., YUAN, J.-H., WANG, R., ZHANG, C.-S., WANG, L.-X. & DONG, J. 2019. Effects of lifestyle modification and anti-diabetic medicine on prediabetes progress: a systematic review and meta-analysis. *Frontiers in endocrinology,* 10**,** 455.

SHWETHA, U., LATHA, M., RAJITH KUMAR, C., KIRAN, M. & BETAGERI, V. S. 2020. Facile synthesis of zinc oxide nanoparticles using novel Areca catechu leaves extract and their in vitro antidiabetic and anticancer studies. *Journal of Inorganic and Organometallic Polymers and Materials***,** 1-8.

SIBUYI, N. R. S., MOABELO, K. L., MEYER, M., ONANI, M. O., DUBE, A. & MADIEHE, A. M. 2019. Nanotechnology advances towards development of targeted-treatment for obesity. *Journal of Nanobiotechnology,* 17**,** 1-21.

SINGH, A. V., LAUX, P., LUCH, A., SUDRIK, C., WIEHR, S., WILD, A.-M., SANTOMAURO, G., BILL, J. & SITTI, M. 2019. Review of emerging concepts in nanotoxicology: Opportunities and challenges for safer nanomaterial design. *Toxicology mechanisms and methods,* 29**,** 378-387.

SMITS, H. P., SMITS, G. J., POSTMA, P. W., WALSH, M. C. & VAN DAM, K. 1996. High-affinity glucose uptake in Saccharomyces cerevisiae is not dependent on the presence of glucose-phosphorylating enzymes. *Yeast,* 12**,** 439-447.

STECK, A. K. & REWERS, M. J. 2011. Genetics of type 1 diabetes. *Clinical chemistry,* 57**,** 176-185.

STENBIT, A. E., TSAO, T.-S., LI, J., BURCELIN, R., GEENEN, D. L., FACTOR, S. M., HOUSEKNECHT, K., KATZ, E. B. & CHARRON, M. J. 1997. GLUT4 heterozygous knockout mice develop muscle insulin resistance and diabetes. *Nature medicine,* 3**,** 1096-1101.

SUN, Y. & XIA, Y. 2002. Shape-controlled synthesis of gold and silver nanoparticles. *science,* 298**,** 2176-2179.

SUTTIE, A. W. 2006. Histopathology of the spleen. *Toxicologic pathology,* 34**,** 466-503.

SZABLEWSKI, L. 2019. Introductory Chapter: Glucose Transporters. *Blood Glucose Levels.* IntechOpen.

TABORSKY JR, G. J. 2010. The physiology of glucagon. SAGE Publications. *Journal of Diabetes Science and Technology*, volume 4, issue 6, November 2010.

TAGI, V. M., GIANNINI, C. & CHIARELLI, F. 2019. Insulin resistance in children. *Frontiers in Endocrinology,* 10.

TAYLOR, R. 2013. Type 2 diabetes: etiology and reversibility. *Diabetes care,* 36**,** 1047-1055.

TCHUENTE, T. 2018. Acute and sub-chronic oral toxicity studies of the leaves aqueous extract of Clerodendrum umbellatum Poir. on mice. *AMERICAN JOURNAL OF PHYSIOLOGY,* 7**,** 75-85.

TEUSINK, B., DIDERICH, J. A., WESTERHOFF, H. V., VAN DAM, K. & WALSH, M. C. 1998. Intracellular glucose concentration in derepressed yeast cells consuming glucose is high enough to reduce the glucose transport rate by 50%. *Journal of bacteriology,* 180**,** 556-562.

THAKUR, R. S. & AGRAWAL, R. 2015. Application of nanotechnology in pharmaceutical formulation design and development. *Current Drug Therapy,* 10**,** 20-34.

THRASHER, J. 2017. Pharmacologic management of type 2 diabetes mellitus: available therapies. *The American journal of cardiology,* 120**,** S4-S16.

TODD, J. A. 2010. Etiology of type 1 diabetes. *Immunity,* 32**,** 457-467.

TODD, J. A., WALKER, N. M., COOPER, J. D., SMYTH, D. J., DOWNES, K., PLAGNOL, V., BAILEY, R., NEJENTSEV, S., FIELD, S. F. & PAYNE, F. 2007. Robust associations of four new chromosome regions from genome-wide analyses of type 1 diabetes. *Nature genetics,* 39**,** 857-864.

TOMKINS, M. & SMITH, D. 2020. Should we continue to use the 75-g OGTT to diagnose diabetes? : Springer.

TSENG, K.-H., HSIEH, C.-L., HUANG, J.-C. & TIEN, D.-C. 2015. The effect of NaCl/pH on colloidal nanogold produced by pulsed spark discharge. *Journal of Nanomaterials,* 2015.

TURNER, S., DIAKO, C., KRUGER, R., WONG, M., WOOD, W., RUTHERFURD-MARKWICK, K. & ALI, A. 2020. Consuming Gymnema sylvestre Reduces the Desire for High-Sugar Sweet Foods. *Nutrients,* 12**,** 1046.

UCSC. 2006. *IR tables* [Online]. Available: https://cpb-us-e1.wpmucdn.com/sites.ucsc.edu/dist/9/291/files/2015/11/IR-Table-1.pdf [Accessed 03 March 2021].

UMRANI, R. D. & PAKNIKAR, K. M. 2014. Zinc oxide nanoparticles show antidiabetic activity in streptozotocin-induced Type 1 and 2 diabetic rats. *Nanomedicine,* 9**,** 89-104.

VARGAS, E., PODDER, V. & SEPULVEDA, M. A. C. 2019. Physiology, Glucose Transporter Type 4 (GLUT4). *StatPearls [Internet].* StatPearls Publishing.

VECCHIO, I., TORNALI, C., BRAGAZZI, N. L. & MARTINI, M. 2018. The discovery of insulin: an important milestone in the history of medicine. *Frontiers in endocrinology,* 9**,** 613.

VEGA, J. R., GUGLIOTTA, L. M., GONZALEZ, V. D. & MEIRA, G. R. 2003. Latex particle size distribution by dynamic light scattering: novel data processing for multiangle measurements. *Journal of colloid and interface science,* 261**,** 74-81.

VIVES-PI, M. & PUJOL-AUTONELL, I. 2015. What potential is there for liposomal-based nanotherapy for the treatment of Type 1 diabetes? : Future Medicine.

WHITE, J. R. 2014. A brief history of the development of diabetes medications. *Diabetes Spectrum,* 27**,** 82-86.

WHO, W. H. O. 2009. Monographs on selected medicinal plants. Volume IV. Libros Digitales-World Health Organization (WHO).

WILCOX, G. 2005. Insulin and insulin resistance. *Clinical biochemist reviews,* 26**,** 19.

XU, P.-T., SONG, Z., ZHANG, W.-C., JIAO, B. & YU, Z.-B. 2015. Impaired translocation of GLUT4 results in insulin resistance of atrophic soleus muscle. *BioMed research international,* 2015.

YAKOOB, A. T., TAJUDDIN, N. B., HUSSAIN, M. I. M., MATHEW, S., GOVINDARAJU, A. & QADRI, I.

2016. Antioxidant and hypoglycemic activities of clausena anisata (Willd.) Hook F. ex benth. root mediated synthesized silver nanoparticles. *Pharmacognosy Journal,* 8

YEH, G. Y., EISENBERG, D. M., KAPTCHUK, T. J. & PHILLIPS, R. S. 2003. Systematic review of herbs and dietary supplements for glycemic control in diabetes. *Diabetes care,* 26**,** 1277-1294.

YU, E. Y., WONG, C. K., HO, S., WONG, S. Y. & LAM, C. L. 2015. Can HbA1c replace OGTT for the diagnosis of diabetes mellitus among Chinese patients with impaired fasting glucose? *Family practice,* 32**,** 631-638.

ZAFAR, M. & NAEEM-UL-HASSAN NAQVI, S. 2010. Efectos de la Diabetes Inducida por STZ en los Pesos Relativos de Riñón, Hígado y Páncreas en Ratas Albinas: un Estudio Comparativo. *International Journal of Morphology,* 28**,** 135-142.

ZHANG, N., DU, S. & MA, G. 2017. Current lifestyle factors that increase risk of T2DM in China. *European journal of clinical nutrition,* 71**,** 832-838.

ZIMMET, P., ALBERTI, K. & SHAW, J. 2001. Global and societal implications of the diabetes epidemic. *Nature,* 414**,** 782-787.

ZISMAN, A., PERONI, O. D., ABEL, E. D., MICHAEL, M. D., MAUVAIS-JARVIS, F., LOWELL, B. B., WOJTASZEWSKI, J. F., HIRSHMAN, M. F., VIRKAMAKI, A. & GOODYEAR, L. J. 2000. Targeted disruption of the glucose transporter 4 selectively in muscle causes insulin resistance and glucose intolerance. *Nature medicine,* 6**,** 924-928